DURBAN UNIVERSITY OF TECHNOLOGY
INYUVESI YASETHEKWINI YEZOBUCHWEPHESHE

INFINITE DILUTION ACTIVITY COEFFICIENT MEASUREMENTS OF DIFFERENT ORGANIC SOLUTES IN CYRENE AS A POTENTIAL GREEN SOLVENT FOR CHEMICAL SEPARATION PROCESSES

by

Melusi Danisa

This dissertation is submitted in the fulfilment of the requirements for the degree of Master of Engineering in Chemical Engineering to the Faculty of Engineering and the Built Environment at Durban University of Technology.

Supervisor: Dr. Peterson Thokozani Ngema
Co-Supervisors: Dr. Nkululeko Nkosi
Prof. Suresh Ramsuroop

28 February 2024

PREFACE

The work presented in this dissertation was performed in the Research Laboratory in the Department of Chemical Engineering at the Durban University of Technology. Dr. Peterson T. Ngema supervised the work and was co-supervised by Prof. Suresh Ramsuroop and Dr. Nkululeko Nkosi.

DECARATION

I, **Melusi Danisa (21334525),** the undersigned student, declare that

i. Except where otherwise indicated, the research reported in this report is my original work.

ii. This report does not contain other persons' data, pictures, graphs, or other information unless expressly acknowledged as being sourced from others.

iii. This report does not contain other person's writing unless expressly acknowledged as being sourced from other researchers. Where other written sources have been quoted. Then:

   a. Their words have been re-written, but the general information attributed to them has been referenced.

   b. Where their exact words have been used, their writing has been placed inside quotation marks and referenced.

iv. This dissertation does not contain text, graphics or tables copied and pasted from the internet unless expressly acknowledged, and the source is detailed in the dissertation and the reference sections.

v. The contents presented in this dissertation is original, except where the work of others is stated in the text. The results presented have not been previously submitted to any tertiary institution as part of a degree. I at this moment certify that the above statement is correct.

Signature of Candidate

As the candidates' supervisors, we have approved the submission of this dissertation.

.. . .

Supervisor (Dr. P.T Ngema) Co-supervisor (Dr N Nkosi) Co-supervisor (Prof. S Ramsuroop)

ABSTRACT

Biofuels are increasingly consumed globally. The search for eco-friendly solvents to replace conventional organic solvents derived from fossil fuels continues to grow. Biofuels derived from plant dry matter are abundantly available, which justifies researchers' ongoing interest in them. Researchers are exploring several options to facilitate the easy integration of this resource into existing systems.

The focus of this project as a replacement for volatile organic compounds VOCs, a bio-derived solvent (BDS), cyrene, classified as dihydrolevoglucosenone by evaluating its extractive efficiency in this study for various separation using pre-screening technique known as gas-liquid chromatography (GLC) instead of directly testing cyrene as a potential alternative to conventional solvents. In contrast to direct methods, GLC offers the advantage of assessing numerous separation problems in a shorter period than direct methods. Cyrene's intermolecular interaction strengths with 32 volatile organic compounds (i.e. alkanes, alkenes, alkynes, cycloalkanes, ketones, alcohols, aromatics, heterocyclics, nitrile, esters and water) were assessed using infinite dilution activity coefficients (IDAC) measured at T = (303.15 to 333.15) K and 101.3 kPa. Further analysis of IDAC data was performed to determine the chemical thermodynamic properties, i.e., partial excess molar properties ($\Delta H_1^{E,\infty}, T_{ref}\Delta S_i^{E,\infty}, \Delta G_i^{E,\infty}$) obtained at infinite dilution, to assess the cyrene and solute mixtures and quantify their non-ideal behaviour in real mixtures. Addition to this, Aspen Plus and COSMO-RS software were used to build thermodynamic models in conjunction with the experimental data to make predictions.

ACKNOWLEDGEMENTS

I wish to thank the following people for their contribution to my work:

- I want to express my utmost gratitude to Dr P.T Ngema, Prof S. Ramsuroop, and Dr N. Nkosi, the supervisor and co-supervisors, for their expert supervision and guidance during the research. Lastly, my mentor and postgraduate colleague, Banzi P. Mbatha (D.Eng. Candidate), are sincerely acknowledged for their support, wisdom, and motivation during this work.
- It would be remiss of me not to acknowledge the contributions made by my colleagues in the Chemical Engineering postgraduate office.
- The laboratory technicians at the Department of Chemical Engineering, in particular Jafar Bux, thank you for your assistance in the laboratory.
- I would like to thank NRF for their financial support.
- My family for their support, motivation, and encouragement during this time.

Table of Contents

LIST OF TABLES

LIST OF FIGURES

NOMENCLATURE

Symbols

A	Parameter (regressed) in the extended Antoine vapour pressure equation
B	Parameter (regressed) in the extended Antoine vapour pressure equation
B_{i1}	Second viral coefficient of the solute [$m^3.mol^{-1}$]
B_{i2}	Mixed viral coefficient of the solute [$m^3.mol^{-1}$]
C	Parameter (regressed) in the extended Antoine vapour pressure equation
C_L	Concentration of solute in liquid phase [$mol.m^{-3}$]
C_M	Concentration of solute in mobile phase [$mol.m^{-3}$]
$\hat{f}_i$	Fugacity component i in solution [kPa]
f_i	Fugacity of pure component i [kPa]
H^E	Partial molar excess enthalpies at infinite [$kJ.mol^{-1}$]
I_c	Critical ionisation potential [$kJ.mol^{-1}$]
J_2^3	Pressure correction term
$K_{j.s}^{\infty}$	Capacity at infinite dilution of solvent (s)
K_L	Partitioning coefficient
n	Number of carbon atoms
n_3	Number of moles of carbon in column
P	Total pressure [Pa]
p_1	Partial vapour pressure [Pa]
P_c	Critical pressure [Pa]
P_i	Inlet pressure [Pa]
$P_i^o \ or \ P_i^*$	Saturated vapour pressure [Pa]
P_o	Outlet (atmospheric) pressure [Pa]
p_w^o	Saturation vapour pressure of water [Pa
R	Universal gas constant [$J.mol^{-1}.K^{-1}$]
$S_{ij.s}^{\infty}$	Selectivity at infinite dilution of component (i) over component (j). in solvent
T	Absolute temperature [K]
T_c	Critical temperature [K]
T_f	Temperature of flow meter [K]
t_G	Retention time of inert chemical (helium) [s]

t_r	Retention time of solutes (s)
U	Flow rate $[m^3.s^{-1}]$
U_o	Corrected flow rate of helium gas $[m^3.s^{-1}]$
V	Volume $[m^3]$
V_c	Critical molar volume $[cm^3.mol^{-1}]$
V_G	Gas phase volume $[m^3]$
v_i	Liquid molar volume of pure solute $[cm^3.mol^{-1}]$
v_i^{∞}	Partial molar volume of solute $[cm^3.mol^{-1}]$
V_L	Liquid phase volume $[m^3]$
V_N	Net retention volume $[m^3]$
x_i	Mole fraction of component i in liquid phase
y_i	Mole fraction of component i in gas phase

Greek Letters

$\alpha_{ij.s}$	Relative volatility of species i over species j. in solvent (s)
α	Relative volatility/separation factor
γ_i	Activity coefficient of each species in a solution
γ_{13}^{∞}	Infinite dilution activity coefficient
μ_i	Chemical potential of species i
ρ	Density
ω_i	Acentric factor

Subscript

f	Bubble flow meter
G	Gas phase
J	Component
r	Reduce property
N	Net retention time
w	Water
o	Outlet

c	Critical property
ij	Interaction properties
L	Liquid phase
M	Mobile phase
sol	Solute property
i	Pure species

Superscript

L	Liquid phase
exp	Experimentally determined
M	Mobile phase
lit	Literature
o	Outlet
sat	Saturated value
∞	Infinite dilution value
v	Vapour phase
l	Liquid phase

Notation

Δ	Denotes variation

Abbreviations

GC	Gas chromatography
GLC	Gas-liquid chromatography
IGS	Inert gas striping
VLE	Vapour-liquid chromatography

NRTL	Non-Rando Two Liquid
UNIQUAC	Universal quasichemical
COSMO-RS	Conductor-like screening Model for Real Solvent
IDAC	Infinite dilution activity coefficient
EXP	Experimental
LIT	Literature
IL	Ionic Liquid
DES	Deep eutectic solvent
VOC	Volatile organic compound
RD	Relative deviation

CHAPTER ONE

INTRODUCTION

Chapter Overview

This chapter introduces a bio-derived solvent (BDS) from a renewable source, such as biomass, that can be used as a replacement for conventional solvents which are currently used in chemical and petrochemical industries.

1.1 Background

The use of volatile organic compounds (VOCs) in chemical and petrochemical industries has raised serious concerns, as these organic compounds poses risks to human health. They are ecologically unfriendly due to their volatility, and accounts to approximately 67% of the industrial emissions (Ram 2013). The commonly used volatile organic compounds in chemical industries are N-methyl-2-pyrolidone (NMP) and N-methyl-formamide (NMF), diethylene glycol (DEG), triethylene glycol (TEG) and glycerol also known as conventional solvents (Manyoni and Redhi 2022b). The solvents have been included in the European Union's Registration, Evaluation, Authorization and Restriction of Chemicals (REACH), which severely limits their use as industrial solvents due to its reproductive effect (Camp 2018). A replacement of these solvents is a priority based on the agenda for "green chemistry" (Tumba 2009; Perrone, Messa and Salomone 2023).

In this context, the replacement is characterized by low volatility, high chemical and physical stability for a potential separation (Brouwer and Schuur 2020; Jeřábek *et al.* 2023). A possible solution to this issue could require the use of a bio-derived solvent particularly cyrene, which is also known as dihydrolevoglucosenone (Camp 2018). It is a bicyclic, chiral, seven-membered heterocyclic cycloalkanone, which is a waste derived and fully biodegradable aprotic dipolar solvent, having a molecular formula $C_6H_8O_3$. Cyrene has been identified as a potential alternative to conventional solvents due to its biodegradability and low toxicity (Brouwer and Schuur 2019). As a result, it has minimal impact to the environment as well as humans. And more importantly, cyrene has been discovered as a solvent for many applications and has showed promising results in various fields such as the biomass pretreatment in the bio-refinery process and the extraction of hesperdin and rutin from natural productions (Camp 2018; Meng *et al.* 2020; Milescu 2021).

1.2 Problem statement

Distillation is a reliable technology when it comes to industrial separation processes, but these industrial separation processes uses a large amount of volatile organic compounds (VOCs) and the application of separation is not always as benign as desired. The conventional organic solvents are toxic, volatile, and also non-recyclable due to their inherent volatility, making them environmentally unfriendly. Although it is highly effective in many applications, this reliable technology can also be energy intensive and costly when it comes to mixtures that are difficult to separate by distillation due to pinch point or azeotrope or simple due to low relative volatility (Brouwer and Schuur 2020).

1.3 Scope of the study

In this contribution, this study focuses on the evaluation of dihydrolevoglucosenone, which is also known as "cyrene," an alternative to ionic liquids (ILs) and conventional organic solvents for extractive distillation on close-boiling point and azeotropic mixtures which have not yet being studied.

In this study, the experimental data for the computation of IDAC values were measured using the gas liquid chromatography (GLC) for different groups of organic solutes. This data is often used for check feasibility of separation processes for binary mixtures or limited miscibility (Mbatha 2021).

1.4 Aims and objectives

The aim for this study was as follow:

- To carry out preliminary assessment for the selected potential green solvent cyrene.
- To evaluate its separation ability in binary mixtures with azeotropic and close boiling points.

1.5 Objectives were as follows:

- To measure the new data at infinite dilution activity coefficients for the selected organic solutes using cyrene as a solvent at various temperatures.
- To generate new data since there is no published data on this study for the measurements of infinite dilution activity coefficient of cyrene-solute system.

- To calculate selectivity and capacity of cyrene performance against traditional solvents used in chemical industries.

1.6 Outline of thesis

The outline of the thesis is as follow:

- ***Chapter one***: Presents the introduction of the study. It also provides, aims, objectives, and outline of the research project and dissertation.
- ***Chapter two***: Presents the literature review of previous researchers for the evaluation of the thermodynamic functions related to infinite dilution activity coefficients.
- ***Chapter three***: Reviews fundamental principles of thermodynamics relevant to this study.
- ***Chapter four***: Outlines the experimental equipment and procedures used in this study
- ***Chapter five***: Presents the results and discussion of the infinite dilution activity coefficients for the test systems, experimental work and predicted models for the investigated cyrene solvent.
- ***Chapter six***: Presents conclusion and recommendations for future works.

CHAPTER TWO

Literature Review

Chapter Overview

This chapter provides an overview of the fundamental principles underlying green chemistry and its derivatives, with particular attention given to the physical properties of cyrene and its applications as a green solvent for separation processes. The experimental and predictive methods for the determination of infinite dilution activity coefficients are presented. There are various methods that can be used for the prediction of infinite dilution activity coefficients (IDACs). Some of these predictive methods are listed in this chapter. Moreover, this chapter also provides the use of gas-liquid chromatography (GLC), as a selected experimental method for the determination of infinite dilution activity coefficient, which has been widely used by other researchers.

In order to assist in assessing the significance of similar work and understand the impact of the present study, the following is reviewed in this chapter:

- Bio-derived alternative solvent in chemical industries (Brouwer and Schuur 2020)
- Generalities on the infinite dilution activity coefficients (IDACs) (Tumba 2009)

2.1 Types of solvents

2.1.1 Green solvents

Green solvents are environmentally friendly solvents, derived from renewable sources, without waiving to the process efficiency and selectivity (Perrone, Messa and Salomone 2023). Cyrene, for example, is a bio-derived solvent from the processing of agricultural crops such as the biomass-derived sugars from cellulose waste, as depicted in Figure 2-1 (Milescu *et al.* 2020). The use of green solvents in petrochemical industries is a key to most chemical processes, but not with severe implications for the environment. Green solvents were developed as more environmentally friendly and alternative to petrochemicals (Doble, Rollins and Kumar 2010). Currently, the solvent sector is dominated by petroleum-derived products. Bio-derived solvents are anticipated to experience a rapid expansion in the near future due to the significant issues

regarding human health, environmental conservation, safety, and energy usage. Green and sustainable chemistry is attracting a lot of interest (Milescu 2021).

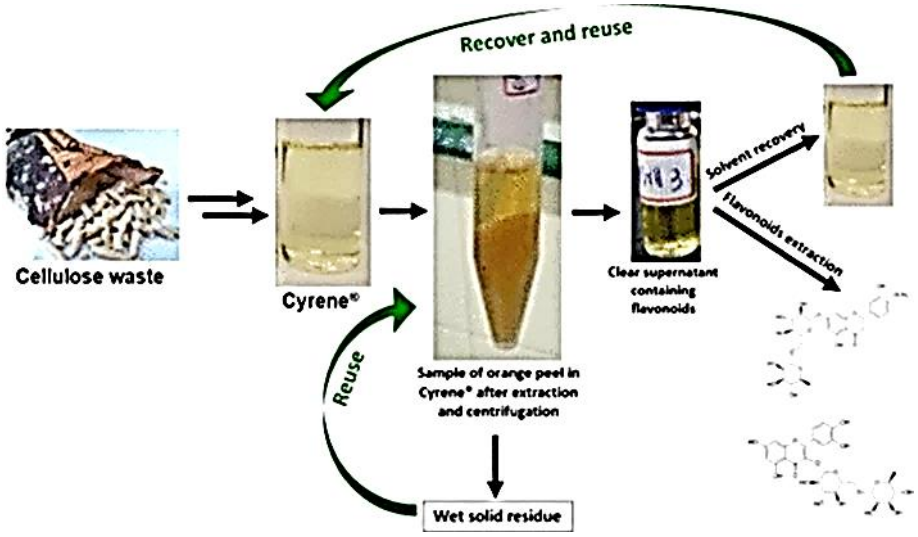

Figure 2- 1: Single-stage solid-liquid extraction of biomass derived sugars cellulose waste (Milescu *et al.* 2020).

2.1.2 Conventional solvents

Conventional solvents causes environmental health risks. These volatile organic compounds (VOCs) are carcinogens or reprotoxic, corrosive, flammable and exhibit acute toxicity (Milescu 2021). The European Union's Registration, Evaluation, Authorisation and Restriction of Chemicals (REACH) regulation has restricted the use of NMP due to its reproductive effect. They are associated with several serious problems associated with their use such as: its toxicity, non-green synthesis, and all contain nitrogen or sulphur content, so their incineration at the end of their usage generates nitrogen oxide (NOx) and sulphur oxide (SOx) (Milescu 2021).

2.2 Green Chemistry

In the early 1990's, the concept of green chemistry was developed to produce chemical products and processes that are much safer for a sustainable future (Abbott 1986; Alessi, Fermeglia and Kikic 1991). It has been considered as a new way of approaching things with the potential to advance sustainable developments (Wardencki, Curyło and Namieśnik 2005).

It is referred to as a proactive and inventive science that prioritizes pollution prevention and waste minimization. In simpler terms, it is safer, cheaper, cleaner, and smarter chemistry in a way that does not cause any harm to human health and the environment (Ali and Khan 2017). The term green solvent is commonly accepted because their production, use, and disposal are related to the twelve principles of green chemistry. Hence, Gu and Jerome suggested the twelve criteria that a green solvent needs to meet according to (Gu and Jerome 2013), as shown in Table 2-1.

Table 2-1: The Twelve Criteria of Gu and Jerome in selecting a "green" solvent (Anastas and Warner 1998; Gu and Jerome 2013)

Criteria	Reasons
Price	Green solvents have to be competitive not only in terms of price, but also in that their price should not be volatile over time in order to ensure the sustainability of the chemical process.
Grade	Technical-grade solvents are preferred in order to avoid energy-intensive purification processes required to obtain highly pure solvents.
Availability	A green solvent need to be available on a large scale, and the production capacity should not greatly fluctuate in order to ensure the constant availability of the solvent on the market.
Recyclability	In all chemical processes, a green solvent has to be fully recycled, of course, using eco-efficient procedures.
Synthesis	Green solvents should be prepared through an energy-saving process, and the synthetic reactions should have high atom economy.
Performance	To be eligible, a green solvent should exhibit similar and even superior performances (viscosity, polarity, density etc.) compared to currently employed solvents.
Flammability	For safety reasons, a green solvent should not be flammable during manipulation.

Stability	For use in a chemical process, a green solvent has to be thermally and (electro) chemically stable.
Storage	A green solvent should be easy to store and should fulfil all legislations to be safely transported either by road, train, boat or plane.
Renewability	The use of renewable raw materials for the production of green solvents should be favoured with respect to the carbon footprint.
Biodegradability	Green solvents should be biodegradable and not produce toxic metabolites.
Toxicity	Green solvents, whether used for personal and home care, paints, etc., must exhibit negligible toxicity to minimize all risks when manipulated by humans or released into the environment.

2.3 Cyrene as a green solvent

2.3.1 Definition and structure of cyrene

Cyrene is a clear, colourless, light-yellow liquid with a mild, smoky ketone-like odour. It is miscible with water and other organic solutes and has an initial boiling point of 227 ℃ at 1.007 hPa according to (Clark, Macquarrie and Sherwood 2013). The versatile bio-derived solvent has been reported for various applications, including being a medium of chemical reactions and membrane manufacture (Brouwer and Schuur 2020). Furthermore, cyrene was synthesized in a two-step process via the pyrolysis of cellulose to levoglucosenone, which is subsequently hydrogenated to dihydrolevoglucosenone (cyrene), respectively, as shown in Figure 2-2.

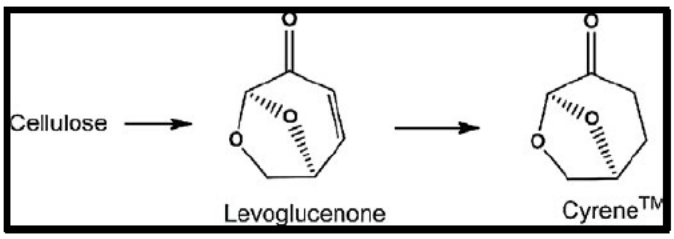

Figure 2- 2: Synthetic steps of bio-based solvent via pyrolysis of cellulose (Oklu, Matsinha and Makhubela 2019).

2.3.2 Brief history of cyrene as a green solvent

James Clark (2019) of the University of York and director, green chemistry centre of excellence, reported cyrene as a new potential green alternative to conventional solvents, namely, dimethylformamide (DMF) and n-methyl-2-pyrrolidone (NMP). According to the literature, cyrene could be considered an extension of the DMF and other dipolar aprotic solvents because the solvents features similar physical properties and characteristics while enabling medicinal chemists to execute a more sustainable chemical synthesis according to (Wilson *et al.* 2018).

This green solvent was also substituted for DMF in amide couplings, a fundamental reaction in drug discovery (Brouwer and Schuur 2020). Cyrene solvent was recognised as the bio-based chemical innovation of the year 2017 at the European Bio-Based Innovation Awards as reported by (Clark, Macquarrie and Sherwood 2013). It was synthesized in 1978 by (Qian *et al.* 2021) through the reduction of levoglucosenone, as demonstrated by the Weckhuysen group.

Many applications of cyrene have emerged since its recent rediscovery, including it as a solvent for various reactions such as fluorination, Menschutkins, Sonogashira, and Cacchi-type annulation, basic reaction, acyl substitution, Suzuki-Miyaura cross-coupling, amide synthesis, urea synthesis, MOF synthesis solid-phase synthesis, as well as a starting material for platform chemicals (Brouwer and Schuur 2020).

2.3.3 Classification and uses of solvents

Solvents are liquid used as a dissolving media for applications such as cleaning, extracting and purifying products, and the modification of materials according to (Milescu 2021). Almost half of the global solvents are used for paints and coating industry; other applications include pharmaceutical, cleaning products, chemical synthesis for polymers, and other chemical applications as reported by (Milescu 2021). Figure 2-3 shows the classification of solvents.

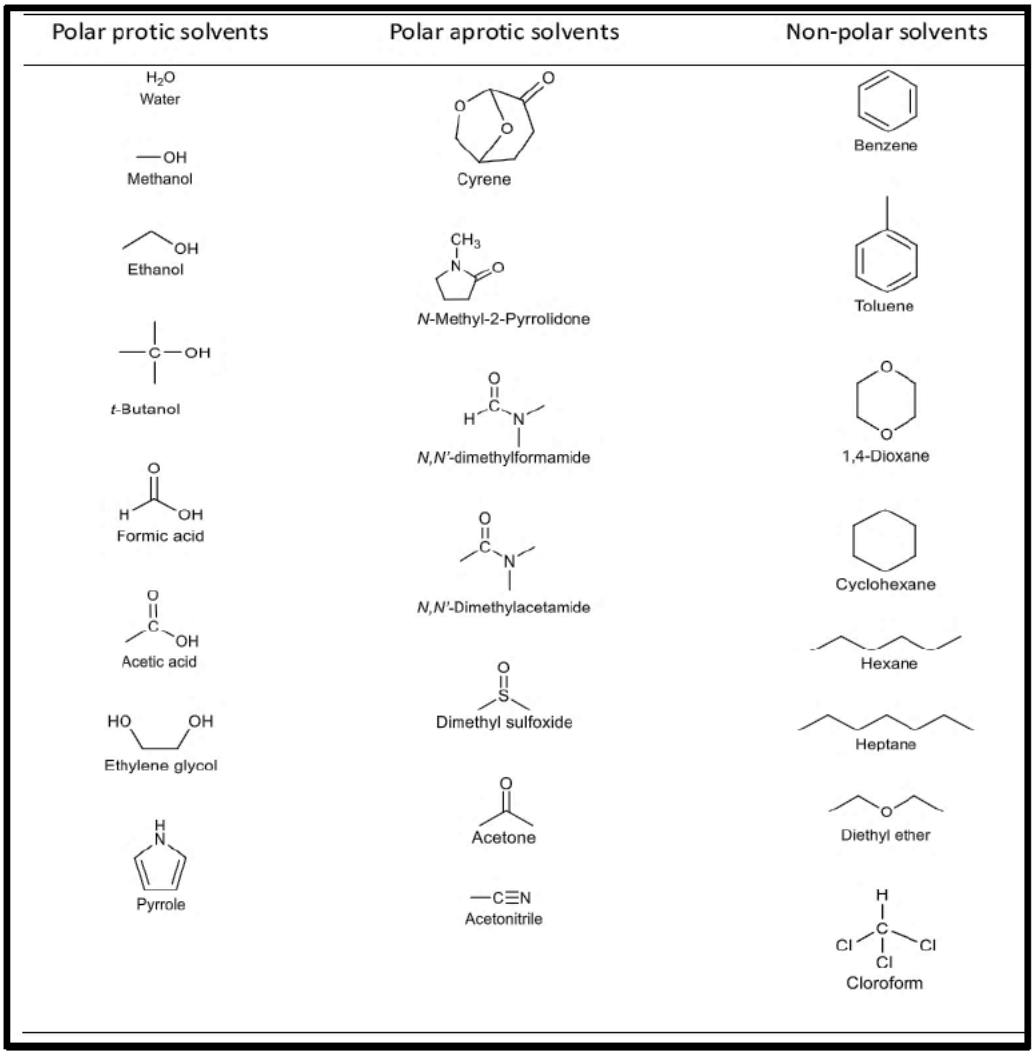

Figure 2- 3: Types of solvents based on their polarity (Milescu 2021).

2.3.4 Physical properties of cyrene against conventional solvents

Physiochemical and thermodynamic properties of substances are crucial because they help to define their constraints for the industrial applications. These properties includes density, viscosity, freezing point, boiling point and vapour pressure. The majority of organic solvents are hazardous and harmful to the environment, which is why it is important to know the characteristics of the chemical substances as reported by (Nkosi 2018). As a result, an attempt has been undertaken to find alternatives to organic compounds (OCs) that are more environmentally friendly and can be used in chemical processes. However, finding acceptable green solvents that can replace organic compounds (OCs) is still a challenge. There are requirements that must be met for a solvent to be deemed green in terms of the environmental regulations according to (Anastas and Kirchhoff 2002). Table 2-2 outlines the physical properties of cyrene compared to conventional solvents.

Table 2-2: Physical properties of cyrene in comparison with conventional aprotic solvents (Milescu 2021).

Solvent property	Cyrene	NMP	DMF
Molecular weight [g/mol]	128.13	99.13	73.09
Relative density [g/mL at 20°C]	1.25	1.028	0.948
Molar volume $[cm^3/mol]$	102.50	96.43	77.10
Boiling point [°C]	227	202	153
Melting/freezing point [°C]	<-19.99	-24	-60.99
Flash point [°C]	108	91	58
Surface tension [mN/m at 22°C]	72.5	40.4	N/A
Vapour pressure [hPa at 20-25°C]	0.28	0.39	3.6 – 5.16
Vapour density (Air =1)	N/A	3.42	2.52
Water miscibility at [20°C]	Miscible	Miscible	Miscible

2.3.5 Toxicity profile of cyrene

Table 2-3 presents the chemical safety report pertaining to cyrene, submitted to the European Chemicals Agency (ECHA). This report encompasses comprehensive details regarding the potential hazards posed to both the environment and human health (including the exposure and risk assessment) as reported by (Milescu 2021).

Table 2- 3: Hazards identification (Milescu 2021)

Signal word	**Warning**
Hazard statement(s)	
H319	Causes eye irritation
Precautionary statement(s)	
P264	Wash skin thoroughly after handling.
P280	Wear eye protection/face protection.
P305 + P351 +P338	If in eyes: Rinse cautiously with water for several minutes Remove contact lenses if present and easy to do. Continue rinsing
P337 + P313	If eye irritation persists: Get medical advice/ attention
Supplemental Hazard Statements	none

2.3.6 Life-cycle assessment for cyrene against NMP

When considering sustainability, it is crucial to take into account the concept of life cycle assessment (LCA) and its factors. The factors may include energy requirements, greenhouse gas emissions, ozone generation, and total organic carbon. The study of the life cycle was conducted to evaluate the impact of cyrene compared to NMP. The resulting environmental profile of cyrene, compared to that of NMP, showed a more favourable profile than the latter. As shown in Figure 2-4 shows a carbon footprint of cyrene production is much smaller than that of NMP (Milescu 2021).

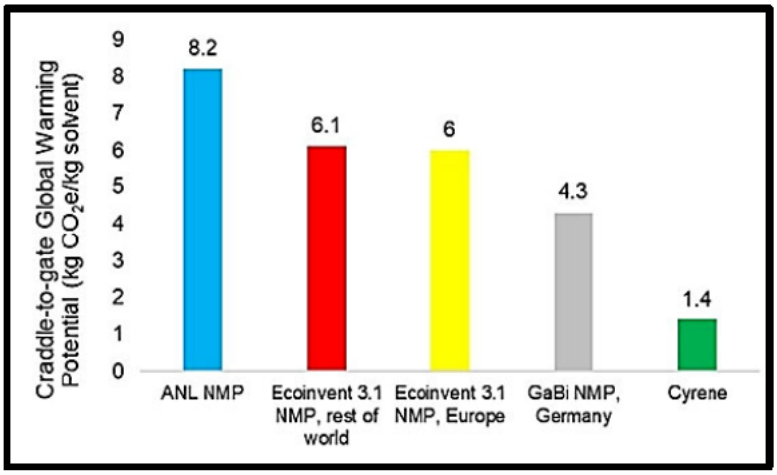

Figure 2-4: Life-cycle assessment for the carbon footprint of cyrene production in comparison with NMP (Milescu 2021).

2.3.7 Potential application of cyrene in the chemical industries

The cyrene solvent has been proposed as an alternative solvent to conventional solvents due to its low toxicity and biodegradable (Wilson *et al.* 2018). Table 2-4 presents an overview of the potential application of cyrene in the chemical industry. To date, cyrene has been studied in a wide range of applications related to chemical industry, and these includes the following:

- It is used as a dissolving medium for applications in cleaning, extracting, purifying products, and the modification of materials.
- Used for paints and coating industries, where solvent plays a major role in the total weight of the paint.
- Other applications include pharmaceutical, ink, personal care and household products, cleaning products, and chemical synthesis (for polymers and other chemicals).
- Also, cyrene can be used in the metal and wood industries, the food industry and medicinal applications.

This study focuses on the evaluation of cyrene as a potential solvent to replace conventional solvents in separation processes. The investigation of cyrene as an alternative is motivated by an in-depth study by (Brouwer and Schuur 2020). To date, there has not been enough data conducted on the investigation of cyrene for the close boiling point and azeotropic mixtures; hence, this study was undertaken to assess the feasibility of separation processes using cyrene as a potential solvent.

Table 2-4: Potential application of cyrene used in the chemical industry (Wilson *et al.* 2018).

Chemical industry	Application
Cross coupling	Both robust methods for the Sonogashira reaction have been developed by using cyrene.
Amide Bond formation	One of the most common reactions in the pharmaceutical industry is amide and bond formation.
Ureas	Enables an efficient, waste-minimizing method for synthesizing ureas from isocyanates and secondary amines.
Fluorination	Attributes to promote the fuorination reaction and was found to match the performance of NMP.
Graphene ink production	The highest-quality graphene ink is produced as an alternative to NMP.

2.4 Different types of distillation processes

The separation of close boiling point and azeotropic systems can be achieved by using a suitable solvent, which influences the activity coefficients and relative volatility. According to the study by (Ngema 2010), there are various methods for separating azeotropic mixtures in chemical and petrochemical industries, which are as follows:

- **Extractive distillation:** Closer to the distillates product, a high-boiling solvent is added to alter the relative volatility and separate the components. To recycle the solvent, a second column is added to separate the bottom product.
- **Reactive distillation:** The components of the azeotropic mixtures react favorably and reversibly with the separating agent. The reaction is then reversed to recover the original component, once the reaction product is separated from the non-reacting components.
- **Homogenous azeotropic distillation:** The liquid separating agent is completely miscible.

- **Heterogeneous azeotropic distillation:** Over a wide range of composition, the liquid separating agent, also known as the entrrainer or solvent, forms one or more azeotropes with other components in the mixture and causes two liquid phases to exit. For this type of distillation to work, immiscibility is the key.

Since this study focuses on one technique, namely extractive distillation, therefore, it is reviewed in this chapter.

2.4.1 Extractive distillation

In the separation of binary mixtures in an extractive distillation process, two columns are generally used: the first as an extractive column and the second as a solvent recovery column as reported by (Ngema 2010). Figure 2-4 below present the two columns. With this arrangement, component A and B in the binary feed are separated. The product is obtained as high-purity distillate in both the columns, and the solvent (S) is recovered in the second column as a bottom product as reported by (Ngema 2010). The solvent is not vaporized in the distillation process. A high-boiling point selective solvent is fed closer to the top of the distillation column.

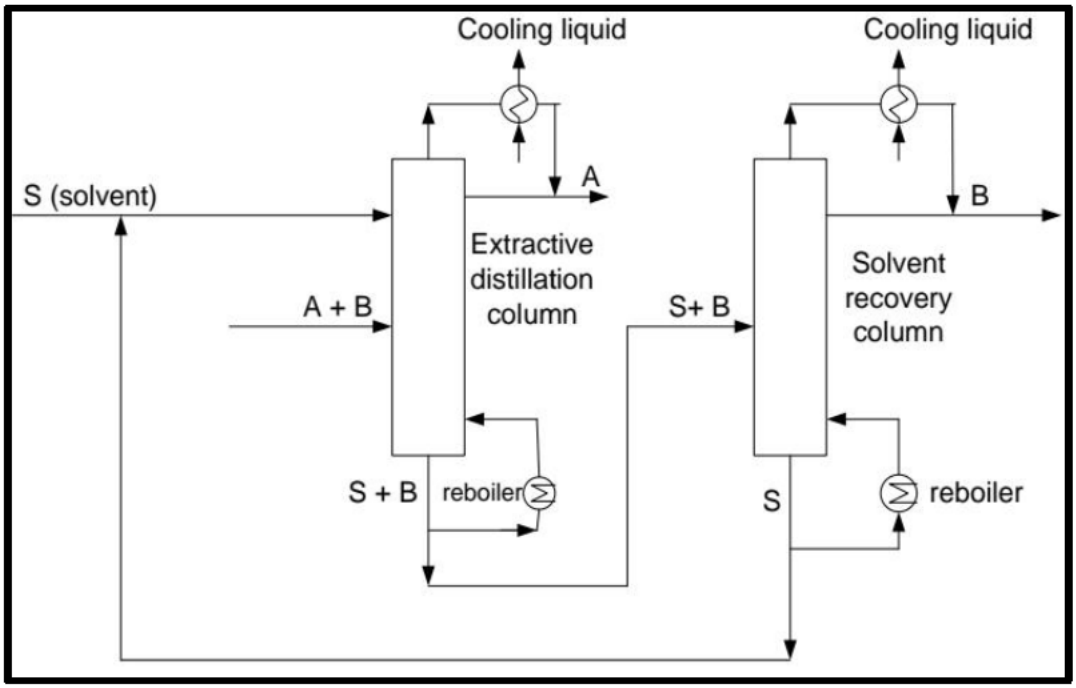

Figure 2-5: Extractive distillation with two column adapted from (Ngema 2010) A—carrier. B—solute and S—solvent

According to the study by (Ngema 2010), comparing azeotropic and extractive distillation, azeotropic distillation has the disadvantage that, in contrast to solvents used for extractive distillation, the solvent has to be vaporized first, which results in high energy consumption.

2.5 Infinite dilution Activity Coefficient (IDAC)

2.5.1 Definition

The activity coefficient is a factor used in thermodynamics to account for deviations from ideal behaviour in a mixture of chemical substances. Defined as a ratio of the activity (α_i) and the mole fraction (x_i). The activity coefficient (γ_i) of species in a solution is defined by the following equation:

$$\gamma_i = \frac{\hat{f}_i}{x_i f_i} \tag{2-1}$$

Whereby: $\hat{f}_i$ is the fugacity of component i in a solution

f_i Pure component fugacity

x_i Mole fraction of component i in a liquid phase

For an ideal solution $\gamma_i = 1$. Departure from ideal can be expressed in terms of activities from mole fractions are defined in the following equation.

$$\alpha_i = x_i \gamma_i \tag{2-2}$$

2.5.2 Important of IDACs

The infinite dilution activity coefficient is a significant characteristic that is crucial in chemical engineering and the environment. It is described as the activity coefficient limiting value when the concentration approaches zero according to (Seader, Henley and Roper 2016). It is used to account for the deviation of real solutions from ideal solutions because it reflects the extreme situation in which only solute-solvent interactions contribute to non-ideality, the activity

coefficient at infinite is particularly significant (Mbatha 2021). . This is graphically shown in Figure 2.2.

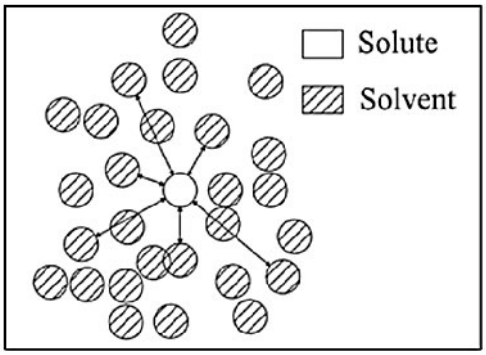

Figure 2-6: Graphical binary mixture of infinite dilution Adopted from (Singh 2017)

Infinite dilution activity coefficients provides accurate and helpful results in terms of phase equilibrium data for systems in the diluted region, in the chemical industry according to the study by (Seader, Henley and Roper 2016). Furthermore, IDAC data are helpful in designing different separation units for high-purity compounds. This is significant because high-purity chemicals require a good separation ability to remove the last traces of contaminants as reported by (Nkosi 2018).

The infinite dilution activity coefficient can guide in pre-selection of an alternative solvent for a particular separation process, and it can be used to design industrial separation processes. The description of the behaviour of mixtures in their dilute region is one of the most significant uses of the activity coefficients at infinite dilution, according to the study by (Nkosi 2018). Typical uses of the infinite dilution activity coefficient are as follows:

- Environmental pollution remediation is challenging, costly, and energy-intensive to get rid of any remaining impurities (Nkosi 2018).
- Industrial processes involving the production of high-purity products by raising the purity of chemicals at lower cost (Nkosi 2018).

The investigation is crucial to study the diluted region for both theoretical and practical purposes of infinite dilution activity coefficient (IDAC) values in chemical and environmental engineering according to (Sandler 1996).

- Predicting the existence of azeotropes (Seader, Henley and Roper 2016).

- Synthesis design and optimization of separation processes (Tumba 2009).
- Calculation of partition coefficient and Henry's law constants (Smith, Van Ness and Abbott 2001).
- Screening of solvent for solvent extraction and extractive distillation (Ricles, Sause and Green 1998).
- Prediction of retention volume in a gas chromatography (Doyle, Weir and de Loos 2005).
- Determination of excess molar enthalpies of solution (Smith, Van Ness and Abbott 2001).

2.6 Synthesis design and optimization of separation processes

According to (Fredenslund 2012), the knowledge of activity coefficients (γ^{∞}) at infinite dilution is of particular importance for the synthesis, design, and optimization of separation processes because the largest separation effort is required to remove the last traces of impurities. Furthermore, reliable (γ^{∞}) values are required to select selective solvents (entrainers) for separation processes such as extractive distillation, and so forth, or to check for separation problems such as azeotropic points and miscibility gaps. From the IDAC data, selectivity (${S_{ij.s}}^{\infty}$) and capacity (${k_{j.s}}^{\infty}$) of the solvent can be calculated. These two parameters play a vital role in selecting suitable solvents as entrainers in azeotropic extractive distillation as well as liquid-liquid extraction columns for the separation of any systems, including mixtures that are difficult to separate (azeotropes) or close-boiling point mixtures. Their respective IDAC values in each solvent are determined. Equation (2-1) is then used to compute the selectivity at infinite dilution (${S_{ij.s}}^{\infty}$) of each solvent with respect to (i/j) system.

$$ {S_{ij.s}}^{\infty} = \frac{{\gamma_i}^{\infty}}{{\gamma_{j.s}}^{\infty}} \tag{2-3} $$

and

$$ {k_{j.s}}^{\infty} = \frac{1}{{\gamma_i}^{\infty}} \tag{2-4} $$

Where $({S_{ij.s}}^{\infty})$, is the selectivity at infinite dilution of solvent (s) for a system consisting of (i) and (j), whereas $({\gamma_i}^{\infty})$ and $({\gamma_{j.s}}^{\infty})$ represents the limiting coefficient of (i) and (j) respectively, in the solvent (s), $({k_{j.s}}^{\infty})$, is the capacity at infinite dilution of solvent(s), which is used to determine the maximum amount of species (j) that can be dissolved in a solvent.

2.7 The predictions of existence of azeotropes

The use of activity coefficient data at infinite dilution can be used to observe the formation of azeotropes in binary mixtures according to (Tumba 2009). In the case of a mixture exhibiting a positive deviation from Raoult's law, the occurrence of azeotropes is characterised by a minimum temperature (pressure-maximum), but for mixtures that exhibit a negative deviation from Raoult's law ($\gamma_{13}^{\infty} < 1$), an azeotrope occurrence is characterised by pressure-minimum (temperature-maximum) as reported by (Nkosi 2018). In such situations, the equation (2-3) and (2-4) below are applicable.

$$(ln\gamma_{13}^{\infty}) > ln\left(\frac{{P_i}^{sat}}{{P_i}^{sat}}\right) > -(ln\gamma_{13}^{\infty}) \tag{2-4}$$

and

$$(ln\gamma_{13}^{\infty}) < ln\left(\frac{{P_i}^{sat}}{{P_i}^{sat}}\right) < -(ln\gamma_{13}^{\infty}) \tag{2-5}$$

Where (γ_{13}^{∞}) is the activity coefficient of component (i) and (j) and $({P_i}^{sat})$ is the saturation pressure for component (i) and (j).

2.8 The calculation of partition coefficients and Henry's law constant

Partitioning coefficients of solutes between a stationary and a mobile phase is the fundamental principle of all kinds of chromatographic methods. Therefore, activity coefficients at infinite dilution can be used to characterise any liquid system, for example, the ethanol-water partition coefficient $\left(K_{o/w}\right)$. Moreover, the partition coefficient can be used as a qualitative measure of the volatility of a substance. These parameters are closely related to Henry's law constant (H_{ij})

with the assumption that the vapour pressure behaves in an ideal gas according to (Berthod and Carda-Broch 2004). Equation (2-5) relates to Henry's law constant for activity coefficient at infinite dilution.

$$\gamma_{sol}{}^{\infty} = \frac{H_{ij}}{P_{sol}{}^{sat}} \tag{2-6}$$

and

$$H_{ij} = \gamma_{sol}{}^{\infty} P_{sol}{}^{sat} \tag{2-7}$$

Therefor:

$$K_{ow} = \frac{\gamma_{sol}{}^{\infty} P_{sol}{}^{sat} v_w{}^{L}}{RT} \tag{2-8}$$

Where P^{sat}, denotes saturation vapour pressure of pure liquid solute $v_w{}^{L}$ molar volume of pure water R, ideal gas constant and T is the absolute temperature.

2.9 Determination of excess molar enthalpies of solution

The Gibbs-Helmholtz equation depicts the effect of temperature dependence of the activity coefficient, which can be used to calculate the partial molar excess enthalpies at infinite.

$$\left[\frac{\partial (G^E/RT)}{\partial T}\right]_{p.x} = -\frac{H^E}{RT^2} \tag{2-10}$$

This leads to the following relation:

$$\left(\frac{\partial \ln \gamma_i}{\partial T}\right)_{p.x} = -\frac{{H_i}^E}{RT^2} \tag{2-11}$$

and

$$\left(\frac{\partial \ln {\gamma_i}^{\infty}}{\partial\left({}^{1}/_{T}\right)}\right)_{p.x} = -\frac{\Delta {H_i}^{E.\infty}}{R} \tag{2-12}$$

From the experimental data obtained, the partial excess enthalpy at infinite dilution for a given solute (i), the (R) and $({H_i}^{E.\infty})$ can be directly obtained from an equation of a straight line (slope) derived from Equation (2-5) and an ideal gas constant, T is the experimental temperature. Equation (2-6) is an approximation of experimental $({\gamma_i}^{\infty})$ values by the linear regression as reported by (Tumba 2009). According to the suggestion by (Heintz, Kulikov and Verevkin 2001), the use this equation to compute the standard deviation of measured values from the process of constructing a straight line that has the best fit to a series of data points.

$$\ln {\gamma_i}^{\infty} = a + b/T \tag{2-13}$$

2.10 Experimental and predictive methods for the determination of IDACs:

Infinite dilution activity coefficient can be measured either by direct or indirect methods. Direct extrapolation from already existing vapour-liquid equilibrium data is a component of indirect approaches (VLE). The direct method, which uses measurements in the diluted region, typically yield higher-quality results and more accurate outcomes than indirect techniques reported by (Nkosi 2018; Manyoni and Redhi 2022b).

2.10.1 The predictive methods

It is expensive and time consuming to measure the phase equilibrium data for multi-component systems. However, without any available experimental data, phase equilibrium data can now be predicted (Nkosi 2018). This is achievable through some well-founded thermodynamic

predictive models. The predictive thermodynamic models are very important in the separation processes according to (Lei, Li and Chen 2003) . They allow a rapid solvent selection at reduced cost as reported by (Novák, Matouš and Pick 1987). So assessing the data that is difficult to obtain experimentally and the development of process simulations as reported by (Wittig, Lohmann and Gmehling 2003). Some of these methods include:

- Group contribution method GCM.
- Conductor-like Screening Model for Real Solvents methods (COSMO-RS).
- Group contribution solvation model (GCS).
- Modified separation of cohesive energy density (MOSCED).
- Linear solvation relationship (LSR).
- Quantitative structure- property relationship (QSPR).

The group contribution method GCM and a conductor-like screening model for real solvent. COSMO-RS are the most successfully used predictive models by various researchers, and a brief description of the two models can be classified as follows:

2.10.1.1 Group contribution method (GCMs)

This technique is based on the group contribution method, which predicts that when groups are properly defined, the interaction energy of a systems is the sum of the interaction energies of its functional groups according to (Wittig, Lohmann and Gmehling 2003).

COSMO-RS

According to (Klamt 1995), the conductor-like screening model (COSMO-RS) is a quantum chemical prediction tool for thermophysical characteristics. The main objective of introducing this model was to determine a new approach for describing the dependence of IDAC on the mixture, temperature, and composition. This model is widely used for infinite dilution activity coefficient; it was developed by (Klamt 1995).

2.10.2 Experimental methods

There are quite a number of experimental methods that have been developed to determine activity coefficient at infinite dilution. These include the following:

- Gas-Liquid chromatography (Letcher 1980).
- Differential ebulliometer method (Gautreaux Jr and Coates 1955).
- Inert gas stripping method (Lerol *et al.* 1977).
- Differential static cell method (Paolo, Maurizio and Ireneo 1986).
- Dew point method (Trampe and Eckert 1993).
- Dilutor cell (Richon, Sorrentino and Voilley 1985).
- Headspace chromatography (Hussam and Carr 1985).
- Rayleigh distillation method (Dohnal and Horáková 1991).

Each of these techniques can only be used under specific conditions, as some of these methods generate poor results. For this study, a brief description of a gas-liquid chromatography GLC will be outlined.

2.10.2.1 Gas-Liquid Chromatography method (GLC)

Gas chromatography is a separation technique in which the components of a sample partition between two phases according to (Trampe and Eckert 1993).

- The stationary phase
- The mobile phase

According to the state of the stationary phase, gas chromatography can be classified as gas-solid chromatography (GSC), where the stationary phase is a solid, or gas-liquid chromatography (GLC), which uses a liquid as the stationary phase according to (Trampe and Eckert 1993). GLC, is to a great extent, more widely used than GSC. During the GC separation, the sample is vaporized and carried by the mobile gas phase (i.e. the carrier gas) through the column. Separation of the different components is achieved based on their relative vapour pressure and affinities for a substance towards the stationary phase, which can be described in chemical terms as an equilibrium constant called the distribution constant K_c, also known as

the partition coefficient, where $[A]_s$ is the concentration of compound A in the mobile phase according to (Trampe and Eckert 1993).

The identified elute is measured along with other experimental data, including its retention time, and other experimental parameters are used for computing the infinite dilution activity coefficient (IDAC) values of volatile organic solutes in a non-volatile or low volatility solvents. Table 2-5 summarizes the advantages and disadvantages of the Gas-liquid chromatography.

Table 2-5: The advantages and disadvantages of the Gas-Liquid Chromatography method (Trampe and Eckert 1993).

Advantages	**Disadvantages**
The method is fast, solutes can be injected at once.	Limited to thermally stable and volatile compounds.
Allows the separation of the components of complex mixtures in a reasonable time.	Most GC detectors are destructive except for mass spectrometer MS.
Mature technique with high sensitivity is available.	Method is suited for low volatility solvents.
Easy to operate it at any temperature within the capacity of the equipment.	It is limited to experimental temperature ranges.

According to a study done by (Letcher *et al.* 2005), the gas-liquid chromatography has been widely used to determine the activity coefficients at infinite dilution (γ_{13}^{∞}), where (1) refers to the solute and (3) to the solvent for all polar and non-polar solutes. The method was also supported by the previous work done by other researchers (Domańska *et al.* 2011; Prieto *et al.* 2017; Kabane *et al.* 2023).

(Williams-Wynn *et al.* 2013) determined activity coefficients at infinite dilution (γ_{13}^{∞}) for 25 hydrocarbon solutes included n-alkanes, alk-1-enes, alk-1-ynes, cycloalkanes, alkyl-benzenes and alkanols in diethylene glycol (DEG) and triethylene glycol (TEG) at temperatures ranging from (333.15 to 363,15) K using the gas-liquid chromatograph with pre-saturation of the carrier gas. This was taken further by calculating the selectivity and limiting capacity using the obtained infinite dilution activity coefficients (γ_{13}^{∞}). The partial excess molar enthalpies of chemical mixtures were obtained from experimental IDAC values. It appeared that the intermolecular interactions solute-solvent are dependent on the molecular structure of the solvent.

(Manyoni and Redhi 2022a) determined the activity coefficient for 32 organic solutes in the ionic-liquid (IL) 1,6-Hexanediol with the use of gas-liquid chromatography (GLC) at various temperatures (313.15 – 343.15) K and at atmospheric pressure. The partial molar excess enthalpies were determined using the Gibbs Helmholtz equation. In addition, the selectivity and capacity was also calculated for comparison between the experimental and literature data to verify if ionic liquids can be used as alternative solvents.

(Zhang *et al.* 2019) measured the activity coefficients at infinite dilution (γ_{13}^{∞}) for 33 organic solutes including n-alkanes, cycloalkanes, alk-1-enes, aromatics hydrocarbons, acetonitrile, acetone, tetrahydrofuran, ethyl acetate, 1,4-dioxane, chloro-methanes, alcohols in the ionic-liquid 1-hexyl-3-methylimidazolium chloride, [HMIM][Cl] were determined by gas liquid chromatography at temperatures range (313.15 – 363.15) K. Thermodynamic properties were derived the temperature dependence of the activity coefficients at infinite dilution (γ_{13}^{∞}). Furthermore, the selectivity and limiting capacity values, were obtained from the calculated (γ_{13}^{∞}) and were used to compare the literature values for the same separation problems used in the study.

(Domanska and Marciniak 2008) conducted experiments for activity coefficients at infinite dilution (γ_{13}^{∞}) for the 32 solutes; n-alkanes, alk-1-ynes, cycloalkanes, aromatic hydrocarbon, alcohols, tetrahydrofurane, tert-butyl methyl ether, and water in the ionic liquid 1-butyl-3-methylimidazolium,trifluoromethanesulfonate [BMIM][CF_3SO_3] by using the gas-liquid chromatography (GLC) from temperature range (298.15 – 368.15) K. The selectivity and capacity values were obtained from the calculated activity coefficient at infinite dilution (γ_{13}^{∞})

and the obtained values were used to compare with literature values of the same separation mixtures. Furthermore, partial excess molar enthalpies, were also computed using the experimental activity coefficient at infinite dilution using the Gibbs-Helmholtz equation.

(Mbatha *et al.* 2022) also conducted experimental measurement for infinite dilution activity coefficients (γ_{13}^{∞}) for various solutes which included alkanes, alkenes, alkynes, cycloalkanes, heterocyclic, alcohols, aromatics, ketones, esters, nitrile and water in a similar bio-derived solvent (BDS) 1-methy-4-(1-methylethenyl)-cyclohexene solvent, which is also known as D-Limonene using the gas-liquid chromatography at (303.15 – 333.15) K. The focus of using this bio-derived solvent was to assess the separation potential of the green solvent. This was supported by calculating the selectivity and limiting capacity of various chemical mixtures and compared with the work done in literature using the same separation mixtures. The obtained infinite dilution activity coefficient values (γ_{13}^{∞}) was used to calculate partial molar excess enthalpies at infinite dilution. For this study, it was observed that 1-methy-4-(1-methylethenyl)-cyclohexene was not suitable to be used as an alternative for separation processes.

2.11 Instrument Overview

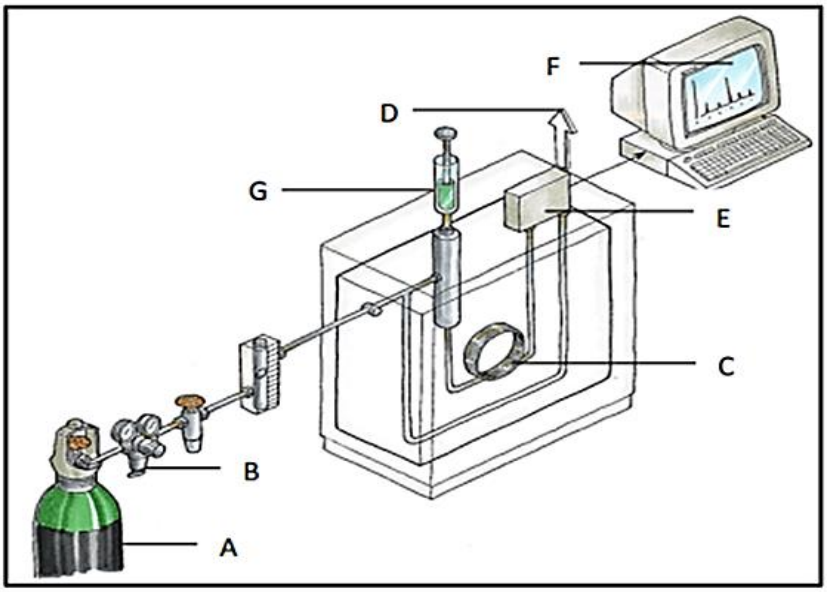

Figure 2- 7: Schematic diagram for a Gas-liquid Chromatography Adapted from (Nkosi 2018)

A – Helium (carrier gas); **B** – Carrier gas flow regulator valve; **C** – Packed column (oven); **D** – Effluent bubble flow metre (waste gases); **E** – Thermal conductivity detector (TCD); **F** – Retention time analysis (Chart recorder); **G** – Sample injection (solute).

2.11.1 Components of Gas Chromatography system

Carrier Gas

The role of the carrier gas is to carry the sample molecules along the column while they are not dissolved in or adsorbed on the stationary phase. The carrier gas is inert and does not interact with the sample and thus GC separation's selectivity can be attributed to the phase alone.

Injector

This is the place where the sample is volatilized and quantitatively introduced into the carrier gas stream. Usually a syringe is used for injecting the sample into the injection port. Samples can be injected manually or automatically with mechanical devices that are often placed on top of the gas chromatograph.

Column

The gas chromatographic column may be considered the heart of the GC system, where the separation of samples components takes place. We classify columns as either packed or capillary columns.

Detector

The detector senses a physicochemical property of the analyte and provides a response that is amplified and converted into an electronic signal to produce chromatogram.

2.12 Application of separation methods

2.12.1 The Differential Ebulliometer method

The utility of infinite-dilution activity coefficients for representing phase-equilibria behaviour has been recognized for some time according to (Gautreaux Jr and Coates 1955), showing that, when only binary limiting activity coefficients are used to determine the two parameters in the Wilson equation (1964), vapour-liquid equilibrium behaviour for many binary systems.

The correlation for activity coefficient ratio is given in the following data according to (Gautreaux Jr and Coates 1955).

- Isobaric (T-x_i). data
- Isobaric (T-y_i). data
- Isothermal (P-x_i). data
- Isothermal (P-y_i). data

Both isobaric P-x_i and isothermal T-x_i data can be measured using this technique. A predetermined criterion for the differential ebulliometry connects ebulliometers to the pressure manifold, ensuring each pressure in the ebulliometry is the same. Figure 2-5, represents a schematic diagram of the equipment as reported by (Richon, Sorrentino and Voilley 1985)

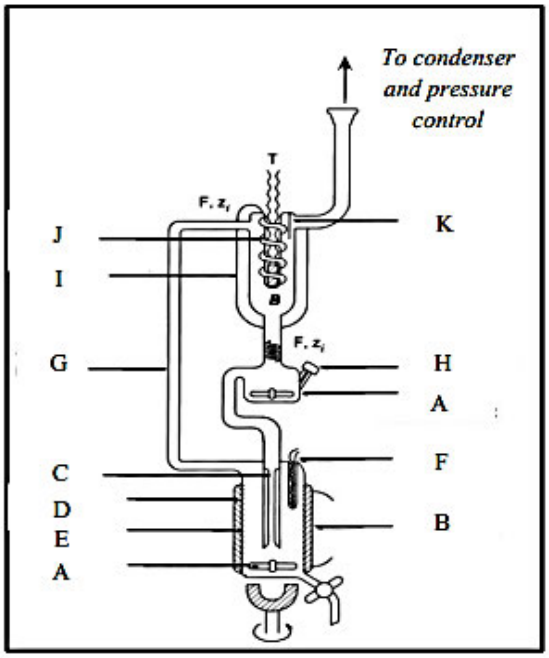

Figure 2- 8: Differential ebulliometer schematic diagram (Richon 2011).

A – Magnetic Stirring bar; **B** – Heating coil; **C** – Capillary; **D** – Reboiler; **E** – Fused ground glass; **F** – Temperature sensor (Pt 100); **G** – Cottrell pump; **H** – Sample septum (mixing spiral); **I** – vacuum jacket; **J** – Fussed glass spiral; **K** – Splash guard.

Table 2-6: Advantages and disadvantages of differential ebulliometer (Harris 2000).

Advantages	Disadvantages
It is capable of measuring multiple systems at once.	For an accurate measurement, it requires expertise.
It is used for systems with high relative volatility.	It is time consuming method.
	The equipment setup and maintenance are costly.

2.12.2 The inert gas stripping method (IGS)

When an inert gas flow is present in a mixture at a certain isotherm and inside a cell, a component that is very weak is taken out of the mixture. At regular intervals, the amount of departing gas is monitored, and an exponential decline in solute concentration over time should be seen. This phenomenon has a connection to the activity coefficient at infinite dilution, which may be predicted. This method can be applied to volatile solutes in solvents that are either non-volatile or volatile but have a high relative volatilities as reported by (Tumba 2009). The continuous gas extraction technique, or the dilutor cell, is another name for this approach. The set-up used in this work, which is similar to that described by (Tumba 2009), is depicted in a simplified flow diagram in Figure 2-6.

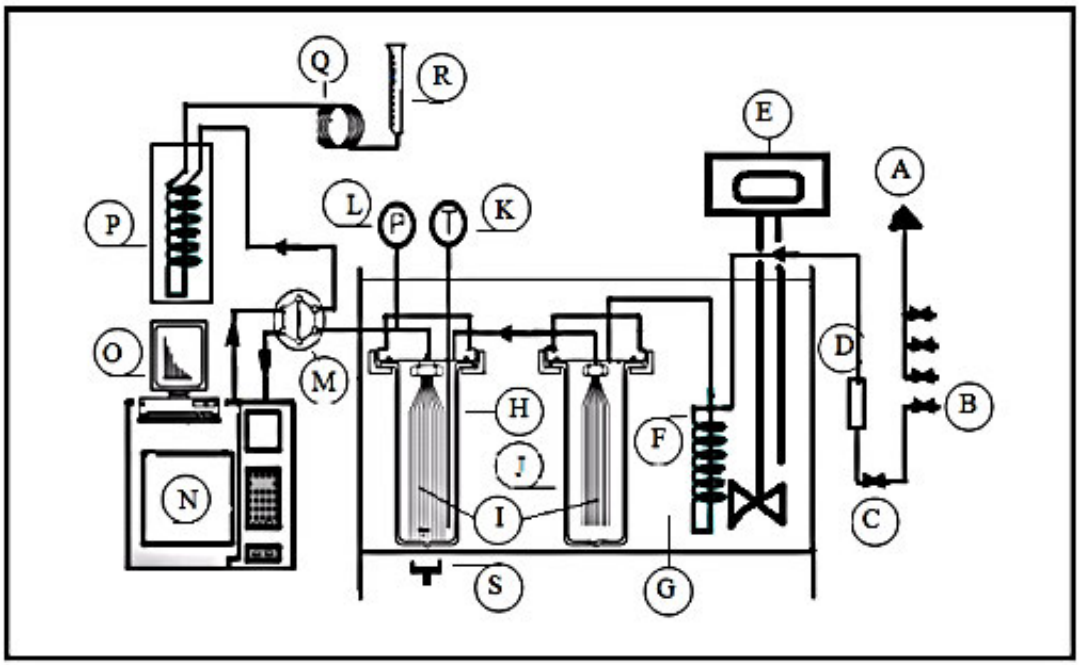

Figure 2-9: Flow diagram of the experimental set up for the inert gas stripping method Adapted from (Tumba 2009)

A-Helium. Nitrogen and air supply for the GC; **B**- Nitrogen line; **C**-Valve; **D**- flow regulator; **E**-Immersion temperature controller; **F**-Coil tube (Heat exchanger); **G**-Transparent acrylic bath; **H**- Dilutor cell; **I**-Capillaries; **J**-Presaturation cell; **K**-Platinum resistance thermometer; **L**-Pressure transducer; **M**-Sampling valve; **N**-GC apparatus; **O**-PC monitor; **P**-Cold trap; **Q**- Coil tube (Heat exchanger); **R**-Soap bubble flow-meter; **S**-Magnetic stirrer.

Table 2-7: The advantages and disadvantages of a gas stripping method (Tumba 2009).

Advantages	**Disadvantages**
Systems with solvents having a high volatility can be measured.	It is challenging to measure systems with low volatility solutes
It is possible to measure mixtures of different solvents.	There is a need for solute purification.
It is possible to study mixtures of various solutes simultaneously.	In order to get better results, there must be good contact between the gas and the liquid.

Only peak area ratios are utilised in calculation. GC calibration is not necessary.

2.12.3 The differential static cell method

The static head method is used for the determination of the vapour pressure at equilibrium for mixtures of known composition. A study by (Paolo, Maurizio and Ireneo 1986) used the static cell of (Gibbs and Van Ness 1972) to measure isothermal T-xi data. The equation, which was proposed by (Gautreaux Jr and Coates 1955), can be used to compute values for the activity coefficient at infinite dilution. The static cell consist of two cells, one cell as the reference cell, which contains pure solvent and the other cell contains a mixture of solvent-solute as reported by (Mbatha 2021). A small, piece quantity of degassed solute is then introduced and the pressure difference at equilibrium is observed (Soni 2003). According to (Raal and Muhlbauer 1998) the accuracy is limited to the quantity of solute used. Figure 2-10 shows the illustration of the static cell apparatus, adapted from (Mbatha 2021).

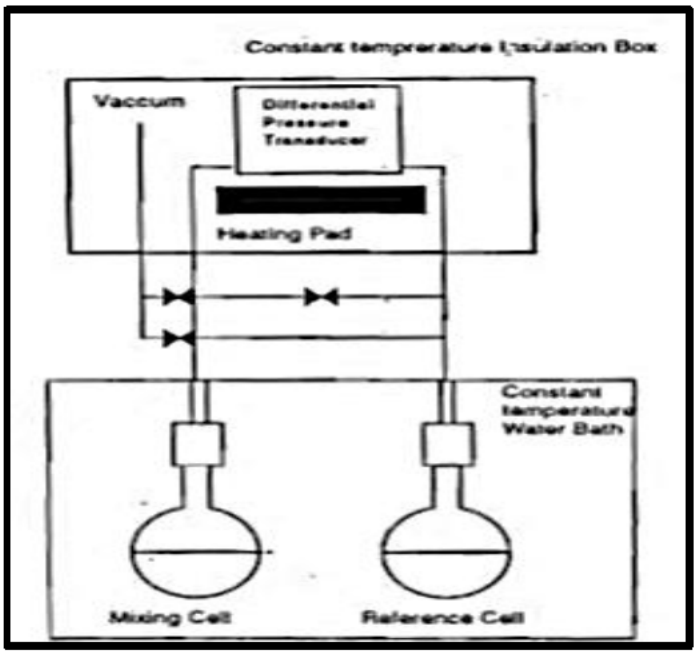

Figure 2-10: Schematic diagram of differential the static cell method (Mbatha 2021)

Table 2-8: The advantages and disadvantages of the differential static cell (Moollan 1995)

Advantage	Disadvantage
Capable of measuring systems with high volatility or partial miscibility.	It requires high-purity, degassed solvents, and it is time consuming.
Solvents with high boiling point can be measured.	Vapour hold-up must be accounted for.
Pressure is measured directly so as to reduce errors.	

2.12.4 The dilutor cell method

(Lerol *et al.* 1977) presented the dilutor cell apparatus and procedure for measuring infinite dilution activity coefficients using the principle of exponential dilution. The glass cell, which is constructed from pyrex, contains the dilute mixture and is kept in a water jacket for an isothermal operation. A tube allows the gas to enter the dilutor cell. The tube ends near the bottom of the cell in a fine-porosity fritted disk to produce a fine stream of bubbles. Provision is made by introducing a small amount of solute using a syringe of approximately $10\mu l$ through a septum as reported by (Soni 2003). The central feature is the dilutor flask, as illustrated in Figure 2-11.

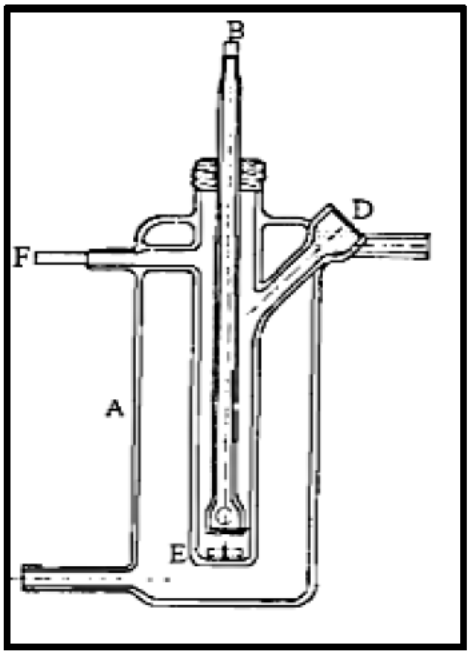

Figure 2-11: Dilutor cell adapted from (Soni 2003)

A- Water jacket; B-Gas inlet; C- Fritted disk gas dispersion device; D-Provision for solute inject to cell; E- magnetic stirrer bar; F- Gas outlet

The dilutor cell was developed to improve the mass transfer between the solvent-solute interactions. Mass transfer considerations led to the development of a dilutor cell by (Richon, Sorrentino and Voilley 1985). The sensitivity of the method to bubble size is needed to find an appropriate bubble rise height, which leads to an increase in the length of the cell according to (Soni 2003). Different types of the dilutor cell are outlined in detail by (Soni 2003). Figure 2-12 shows another type of dilutor cell method.

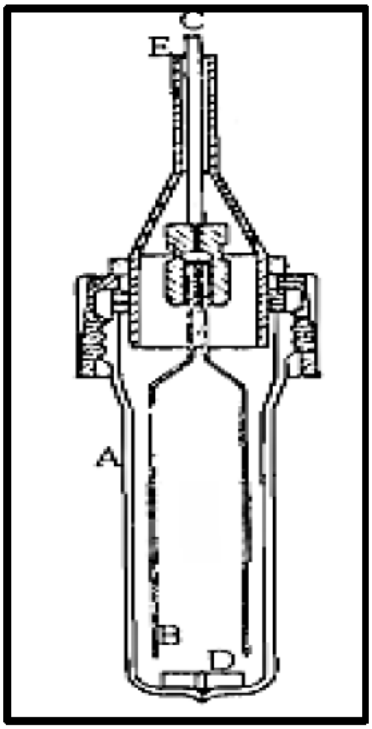

Figure 2-12: Dilutor cell (Richon, Sorrentino and Voilley 1985)

A - Water jacket; B - Capillaries to act as gas dispersion device; C - Gas inlet; D. Magnetic stirrer bar; E - Gas outlet

(Richon, Sorrentino and Voilley 1985) proposed a cell design that can be used for the limiting activity coefficients in mixtures that exhibit properties of high viscosity. The equipment has been specifically designed to handle mixtures with viscosities of up to 1000 cP, which is far higher than the 50 cP of the conventional method. The inert gas is used in the dilutor flask, as shown in Figure 2-13.The cell is equipped with an Archimedes screw to circulate the liquid; in addition, (Richon, Sorrentino and Voilley 1985) provide an analysis of mass transfer factors pertaining to the design of the cell.

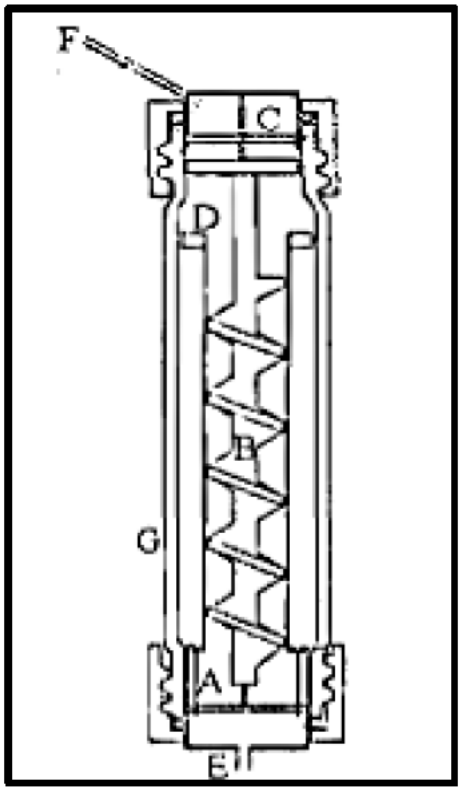

Figure 2-13: Dilutor cell design of viscous and foaming mixtures (Richon, Sorrentino and Voilley 1985)

A - Capillary dispersion device; B - Archimedes screw; C - Foam breaking device; D - BIaded screw; E - Gas inlet; F - Gas outlet; G - Water jacket

2.12.5 The dew point method

According to (Trampe and Eckert 1993), the dew point method was developed to determine the infinite dilution activity coefficient at the dilute vapour phase. This method is applicable to systems with low solute volatility. Since there is a change of temperature of the dew point of the vapour solvent, this method operates the same as the differential ebulliometer when a dilute amount of solvent is added according to (Soni 2003).

This method revolves around a general D2 chilled mirror model, as shown in Figure 2-14 and Figure 2-15, where it was used for measuring humidity of vapour samples as reported by (Trampe and Eckert 1993). The advantages and disadvantages for this method is listed in Table 2-9 (Fowlis and Scott 1963) and (Trampe and Eckert 1993).

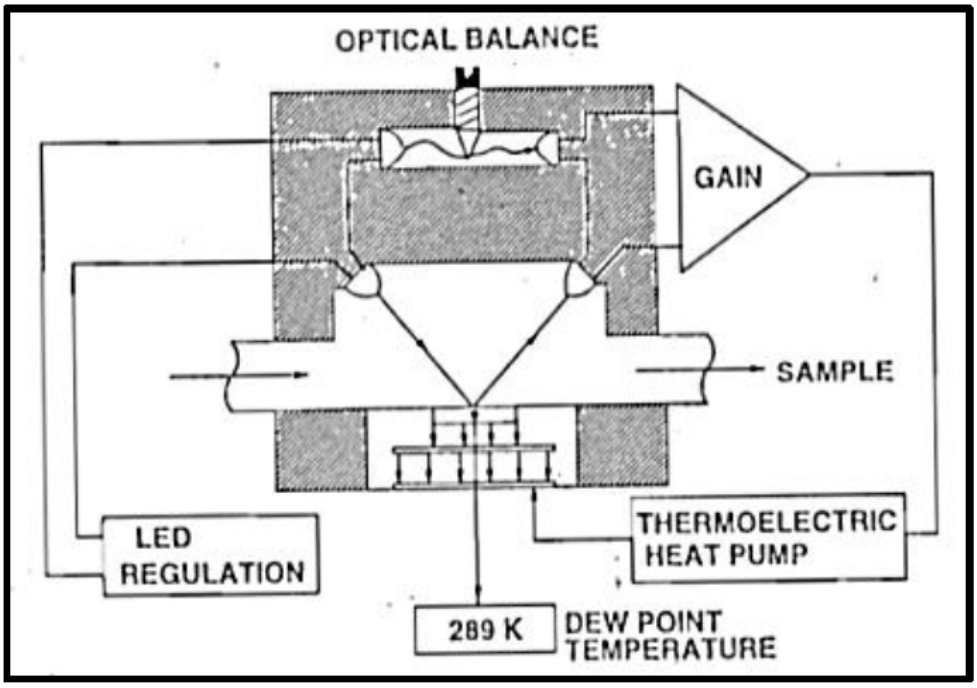

Figure 2-14: Schematic diagram of the dew point sensor (Trampe and Eckert 1993).

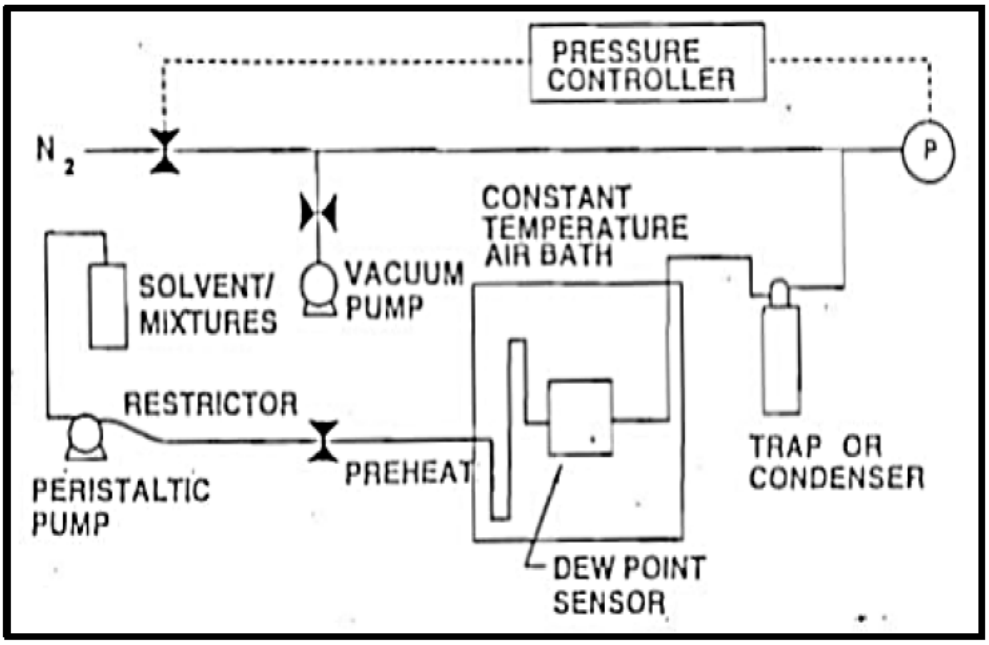

Figure 2-15: The experimental set-up for measuring activity coefficient at infinite dilution (Trampe and Eckert 1993).

Table 2-9: The advantages and disadvantages of Dew point method (Trampe and Eckert 1993).

Advantages	Disadvantages
Only applicable to systems with low volatility.	High purity of solvent is required.

2.12.6 Headspace chromatography

The headspace technique in a gas chromatography GC enables the observation of the gas phase within the chromatography vial located above the sample. It is defines as the gaseous state that exists above a sample's liquid or solid phase as reported by (Mbatha 2021). The sample is subjected to control heating above an oven until the vapour phase reaches equilibrium with the sample phase. This method analyses volatile components, while non-volatile components remain in the same sample vial. This method is considered the cleanest form of GC analysis since the most of the non-volatile are retained in the sample vial according to (Sithersingh 2018). Figure 2-16 represents the headspace chromatography, which does not make pressure measurements, therefore, it confirms the thermodynamic consistency using the area test according to (Redlich and Kister 1948).

According to (Sithersingh 2018), this technique can be conducted in different ways, as listed below.

- Dynamic headspace extraction (DHE)
- Multiple headspace extraction (MHE)
- Static headspace extraction (SHE)
- Solid phase micro extraction (SPME)

The use of the headspace chromatography has grown rapidly due to its ability to investigate the volatile organic compounds (VOCs) as reported by (Mbatha 2021). The advantages and disadvantages are listed in Table 2-10.

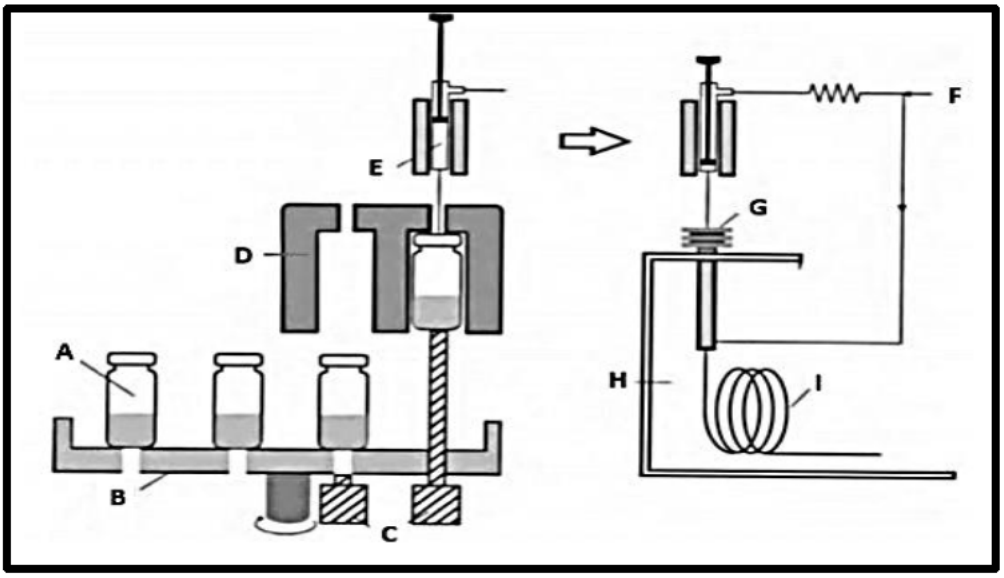

Figure 2-16: Schematic diagram of a headspace chromatography (Kolb and Ettre 2006).

A – Vial; B – Carousel; C – cylinder; D – Heaster; E – Syringe; F – Carrier gas; G – Injector; H – Chromatography; I – Column

Table 2-10: Advantages and disadvantages of headspace chromatography (Sarafraz-Yazdi and Amiri 2010).

Advantages	**Disadvantages**
It is not a time-consuming method.	Low sensitivity and accuracy
It can extract water-soluble and volatile analytes.	
It is cost effective and easy to use.	
Perfect cleaning of samples of complex composition.	

CHAPTER THREE

THERMODYNAMICS FUNDAMENTALS

Chapter Overview:

The objectives of this chapter was to briefly explain the underlying thermodynamic principles needed to develop a theoretical comprehension of the data for the infinite dilution activity coefficients obtained from measurements. This study was concerned with the development of equations related to the gas-liquid chromatography (GLC) method.

3.1 Thermophysical Properties

It is very important to understand thermophysical properties of liquid mixtures when looking for solvents that works better for certain applications, or changing certain physicochemical properties of materials that would improve industrial processes. Therefore, these properties can be to assess the intermolecular interactions within a liquid mixture (Dohrn and Pfohl 2002).

3.1.1 Equations for computation of IDAC

The measurements of activity coefficients at infinite dilution was obtained by applying the principles of thermodynamics to the experimental data. According to (Conder and Young 1979), Equation (3-1) defined the solute partition distribution coefficient K_L between two phases as follows:

$$K_L = \frac{q}{c} = \frac{C_L}{C_M} \tag{3-1}$$

Where:

$$C_L = \frac{x_1 n_3}{V_L} \tag{3-2}$$

and

$$C_M = \frac{y_1 n_2}{V_G} \tag{3-3}$$

Where (C_M) and (c) is the concentration of solute in the mobile phase, (C_L) and (q) is a concentration of solute in the liquid phase. When the solute appears as a vapour or liquid at equilibrium; (x_i) and (y_i) represents the mole fractions of solute in the liquid and vapour phase (V_L) and (V_G) represents the volume of liquid and vapor phase (n_2) and $(n_3)$is the number of moles of carrier gas in a liquid and vapour phase.

When the solute is in equilibrium, the chemical potential in both the liquid and mobile phase is assumed to be equal.

$$\mu_i^L = \mu_i^M \tag{3-4}$$

and

$$\mu_i{}^{id} = \mu_i^o + RT \ln \alpha_i \tag{3-5}$$

Where (α_i) is the activity, (T) is the system temperature, which is a constant in the above equation and $(\mu_i{}^o)$, is the chemical potential of (i) in the real solution $(\mu_i{}^{id})$, is the chemical potential that (i) would have had if the solution had been perfect according to (Whitehead 1996)

Substituting the (α_i) by concentration and substituting it into Equation (3- 4) and (3-5) yields the following equation:

$$\mu_i^{O.L} + RT \ln C_L = \mu_i^{O.M} + RT \ln C_M \tag{3-6}$$

Where the partition coefficient K_L and $\Delta\mu_i^O$ are constants.

This leads to:

$$\ln \frac{C_L}{C_M} = \frac{\mu_i^{o.M} - \mu_i^{o.L}}{RT} \quad (3\text{-}7)$$

and

$$K_L = \frac{C_L}{C_M} exp\left(\frac{\Delta\mu_i^o}{RT}\right) \quad (3\text{-}8)$$

The net retention volume (V_N), is directly proportional to the partition coefficient (K_L) and the volume of the liquid-phase (V_L) as shown below:

$$V_L = K_L V_L \quad (3\text{-}9)$$

Where, (K_L) can be used to determine the column pressure according to (Lobien and Prausnitz 1982).

Equation (3-9) was derived from Equation (3-1) by means of substitution for C_L and C_M.

$$K_L = \frac{x_i n_3 V_G}{y_i n_2 V_L} \quad (3\text{-}10)$$

Where, (x_i) and (y_i) are mole fractions of the solute in the liquid and gas phase, (n_3) and (n_2) are the number of moles for the solvent in the liquid and gas phase, (V_G) and (V_L) are the volume of gas and liquid phase.

Taking into considerations that the vapour phase (V_G) is an ideal gas, it then yields the following equation:

$$V_G = \frac{n_2 RT}{P} \quad (3\text{-}11)$$

Equation (3-12) was simplified from Equation (3-13) using the modified Raoult's law.

$$K_L = \frac{n_3 RT}{\gamma_{13}^{\infty} P_i^* V_L} \tag{3-12}$$

the modified Rault's law is given as follow:

$$yP = xy_{13}^{\infty} P_i^* \tag{3-13}$$

Where, (P) is the solute pressure and (P_i^*) is the saturated vapor pressure.

For thermodynamic properties, (Laub and Pecsok 1978) proposed that Equation (3-9) can be used to attain the distribution coefficient, (K_L) at low pressure in the column. This relates the net retention volume, (V_N) to the volume of stationary phase (V_L) and partition coefficient (K_L).

The expression of Equation (3-12), as proposed by (Porter, Deal and Stross 1956), can be modified into Equation (3-14) as shown below.

$$\gamma_{13}^{\infty} = \frac{n_3 RT}{V_L K_L P_i^*} \tag{3-14}$$

This expression can be rearranged in terms on the net retention volume.

$$\gamma_{13}^{\infty} = \frac{n_3 RT}{V_N P_i^*} \tag{3-15}$$

(Everett 1965; Cruickshank, Windsor and Young 1966) further developed Equation (3-16) to attain the derived equation for solute-solute and solute-carrier gas imperfection and also account for the pressure drop within the column which can be used to compute the infinite dilution activity coefficients for greater accuracy through the solute retention (Heintz, Kulikov and Verevkin 2001):

$$\ln \gamma_{13}^{\infty} = \left(\frac{n_3 RT}{V_N P_i^*}\right) - \frac{(B_{11} - v_1^*)P_i^*}{RT} + \frac{(2B_{12} - v_i^{\infty})J_2^3 P_o}{RT} \qquad (3\text{-}16)$$

Where (P_o) is the outlet column pressure, which is equal to the atmospheric pressure; (P_1) is the inlet pressure of the column; (P_i^*) is the solute saturation pressure at varying temperature (T), obtained through Antoine Equation as reported by (Poling, Prausnitz and O'connell 2001). (B_{i1}) is the second virial coefficient of the solute; (B_{i2}) is the mixed second virial coefficient of the solute(i) with a carrier gas(2); (v_i) is the liquid molar volume of pure solute; $(J_2^3 P_o)$ is the mean column pressure; (v_1^*) is the molar volume of the solute; and (v_i^{∞}) is the partial molar volume of solute at infinite dilution; (R) is the universal gas constant; (T) is the column temperature, and (V_N) represents the net retention volume of solute obtained in the Equation (3-17) according to (Letcher 1980).

$$V_N = (J_2^3)^{-1} U_O (t_r - t_G) \qquad (3\text{-}17)$$

Where, (J_2^3) is the pressure correction term; (t_r) is the retention time for solutes; (t_G) is the retention for the un-retained gas and, (U_O) is the corrected outlet column volumetric flow rate of the carrier gas, that is measured with a soap bubble flow meter.

Equation (3-18) for the determination of pressure correction factor was discovered by (Everett 1965) as follows:

$$J_2^3 = \left(\frac{2}{3}\right)\left[\frac{\left(\frac{P_i}{P_o}\right)^3 - 1}{\left(\frac{P_i}{P_o}\right)^2 - 1}\right] \qquad (3\text{-}18)$$

Where, (P_i) denotes the column inlet pressure computed from the column pressure drop, displayed by the gas chromatography (GC) equipment. The column volumetric flow rate from bubble flow is computed using the following Equation (3-19).

$$U_O = U\left(1 - \frac{P_w}{P_o}\right)\frac{T}{T_f} \tag{3-19}$$

Where, (T_f) is the flow meter temperature; (P_w) is the water vapor pressure at temperature (T_f); and (U) is the volumetric flow rate of the measured carrier gas by soap bubble flow meter at the column outlet. The vapour pressure of water and the solutes involved in the two methods developed by (Laub and Pecsok 1978), was correlated using the Antoine equation that was proposed by (Poling, Prausnitz and O'connell 2001).

The vapour pressure values (P_w), were calculated by using Equation (3-20), using the Antoine constants as follow:

$$log_{10}P = A - \frac{B}{C + T} \tag{3-20}$$

The constants used in the Antoine equation were obtained from different literature sources. all available in appendix A1 (Poling, Prausnitz and O'connell 2001).

3.1.2 Estimation of viral coefficients

Using the equation proposed by (Hudson and McCoubrey 1960) the second viral coefficients of pure solutes (B_{i1}) were calculated using the following equation:

$$B/V_c = 0.43 - 0.886\left(\frac{T_c}{T}\right) - 0.694\left(\frac{T_c}{T}\right)^2 - 0.0375(n-1)\left(\frac{T_c}{T}\right)^{4.5} \tag{3-21}$$

Where, (V_c) is the critical volume; (T_c) is the critical temperature and, (n) is the number of carbon atoms. These critical parameters were computed using the mixing rule of (Hudson and McCoubrey 1960).

$$T_c = 128(T_{C11}.T_{C22})^{0.5}(I_{C11}.I_{C22})^{0.5}\left(V_{C11}.V_{C22}/I_{C12}\right) \tag{3-22}$$

Whereby.

$$I_{C12} = (I_{C11} + I_{C22})^{0.5}\left(V_{C11}^{1/3} + V_{C12}^{1/3}\right)^{6} \quad (3\text{-}23)$$

and

$$V_{C12} = \frac{1}{8}\left(V_{C11}^{1/3} + V_{C12}^{1/3}\right)^{3} \quad (3\text{-}24)$$

and

$$n_{12} = \frac{n_1 + n_2}{2} \quad (3\text{-}25)$$

The saturated molar volume, denoted as (v_i^*), were obtained using the modified Rackett equation proposed by (Poling, Prausnitz and O'connell 2001), which is outlined as follows, as mentioned by (Rackett 1970):

$$v_i^* = V_c(0.29056 - 0.08775\omega)\left(1 - \frac{T}{T_c}\right)^{\frac{2}{7}} \quad (3\text{-}25)$$

Where, (ω) is the acentric factor of the solute obtained from various sources of literature, all available in appendix A (Table A-3)

In this study, it was assumed that the infinite dilution molar volume (V_i^{∞}) of the solute, is equal to the standard molar volume (v_i^*), for the purpose of calculations.

Evaluating the second viral coefficients from experimental data poses significant challenges due to their inherent temperature dependence. According to (Poling, Prausnitz and O'connell 2001), the second viral coefficient of pure solute, (B_{11}), is considered the most reliable correlation for determining the second viral coefficient according to (Tsonopoulos, Dymond and Szafranski 1989), and is given by the following Equation (3-26):

$$\frac{B_{viral}P_c}{RT_c} = f^{(0)}(T_r) + \omega f^{(1)}(T_r) + a_1 f^{(2)}(T_r) + b_t f^{(3)}(T_r) \quad (3\text{-}26)$$

Where

$$f^{(0)} = 0.1445 - \frac{0.330}{T_r} - \frac{0.1385}{{T_r}^2} - \frac{0.0121}{{T_r}^3} - \frac{0.000607}{{T_r}^8} \quad (3\text{-}27)$$

$$f^{(1)} = 0.0637 + \frac{0.331}{{T_r}^2} - \frac{0.423}{{T_r}^3} - \frac{0.008}{{T_r}^8} \quad (3\text{-}28)$$

$$f^{(2)} = \frac{1}{{T_r}^6} \quad (3\text{-}29)$$

$$f^{(3)} = -\frac{1}{{T_r}^8} \quad (3\text{-}30)$$

$$T_r = \frac{T}{T_c} \quad (3\text{-}31)$$

Where, (B) is a viral coefficient; (P_c) signifies the critical pressure; (T_c) denotes the critical temperature, and (T_r) represents the reduced temperature. The values of variables (a) and (b) according to (Singh 2017), were used from the study conducted by (Tsonopoulos, Dymond and Szafranski 1989). The simplified equation proposed by (Smith, Van Ness and Abbott 2001), based on the (Tsonopoulos, Dymond and Szafranski 1989) model, is applicable to non-polar alkanes, alkenes, alkynes and aromatics. In this equation, the values of variables (a_t and b_t are set to zero) given by the Equation (3-32):

$$\frac{B_{viral}P_c}{RT_c} = f^{(0)}\left(\frac{T}{T_c}\right) + \omega f^{(1)} \tag{3-32}$$

Re-arranging equation (3-32) yields the following:

$$B_{ii} = B^o + \omega_i B^1 = \left[0.083 - \frac{0.422}{T_r{}^{1.6}}\right] + \omega_i \left[0.139 - \frac{0.172}{T_r{}^{4.2}}\right] \tag{3-33}$$

According to (Poling, Prausnitz and O'connell 2001), the second viral coefficients obtained using the simplified equation proposed by (Smith, Van Ness and Abbott 2001) are valid only for values $T_r > 0.6$ and $\omega < 0.4$.

The same equation was used for calculating second viral coefficients, where (T_c, ω, a_t andb_t) were taken from different literature sources, available in appendix A (Table A-3).

$$(T_c)_{12} = \sqrt{(T_c)_1 (T_c)_2 (1 - k_{12})} \tag{3-34}$$

$$(P_c)_{12} = 4(T_c)_{12}\left[\frac{\left(\frac{P_c V_c}{T_c}\right)_1 + \left(\frac{P_c V_c}{T_c}\right)_2}{\left[\left(V_c{}^{1/3}\right)_1 + \left(V_c{}^{1/3}\right)_2\right]^3}\right] \tag{3-35}$$

$$\omega_{12} = \frac{(\omega)_1 + (\omega)_2}{2} \tag{3-36}$$

Where, (k_{12}) is the empirical binary interaction variable according to (Holste *et al.* 1982).

For polar components (a_t and b_t) are given by:

$$(a_t)_{12} = \frac{(a_t)_1 + (a_t)_2}{2} \tag{3-36}$$

and

$$(b_t)_{12} = \frac{(b_t)_1 + (b_t)_2}{2} \tag{3-37}$$

3.1.3 Calculation of uncertainty

The uncertainty associated with all calculated values was determined using the law of propagation of uncertainties. This method takes into account the intrinsic uncertainties of measuring instruments, such as accuracy and repeatability. Additionally, it considers additional factors that contribute to the repeatability of measurements according to (Singh 2017). This can be found in the work of (Taylor and Kuyatt 1994), to which the reader is directed for additional insight. The equation can be expressed as follows:

$$u(\theta) = \sqrt{\sum_{i=1}^{y} \left[\frac{\partial \theta}{\partial x_i} u(x_i)\right]^2} \tag{3-39}$$

Where, (θ) represents the calculated variable (γ_{13}^{∞}) for this study, (y) is the number of independent variables and (x_i) is an independent variable used for computing (θ). Taking into consideration the repeatability of type (A) distributions of (q) repetitions, the error (u_r) is given by the standard deviation in the work of (Singh 2017) using the following equation:

$$u_r(\theta) = \sigma = \sqrt{\frac{1}{n-1} \sum_{j=1}^{q} \left(\theta_j - \bar{\theta}\right)^2} \tag{3-40}$$

Where, (θ_j) is (j^{th}) repetition, and $(\bar{\theta})$ is the mean value of (θ), for this work (γ_{13}^{∞}).

CHAPTER FOUR

EXPERIMENTAL APPARATUS AND PROCEDURE

Chapter overview:

This chapter outlines the experimental set-up and procedures used for the present study. The preparation and packing of the column for the measurements of infinite dilution activity coefficient (IDAC) data using the gas-liquid chromatography (GLC) was considered. The uncertainties of the experimental parameters were taken into consideration and reported in this study (Gao *et al.* 1992).

4.1 Materials

4.1.1 Purity of chemicals

The list of all chemicals used in this study were purchased from different suppliers together with their CAS number (see appendix A) Table A-1. They contain high purity within acceptable limits without any further purity. The chemical used are sammarised in Table 4-1 below. They were analytical graded with purities ranging from (97.00 to 99.99) % mass. Additionally the moisture content of the investigated solvent was measured using a Metrohm 702 SM Titrino Meter (Karl Fischer). Taking into consideration the repeatability, the mass percent water content was found to be 0.23 wt% (1.3259g), 0.01 wt% (0.9530g) and 0.11 wt% (1.0273g) in cyrene.

Table 4-1: Summary of chemical used

Chemicals		
n-hexane	ethanol	acetonitrile
n-heptane	methanol	thiophene
n-octane	propan-1-ol	pyridine
n-nonane	propan-2-ol	water
cyclopentane	benzene	methylacetate
cyclohexane	toluene	ethylacetate
cycloheptane	ethylbenzene	cyrene
cyclooctane	m-xylene	dichloromethane
hex-1-ene	o-xylene	helium
hept-1-ene	p-xylene	hexadecane
dec-1-ene	acetone	
hex-1-yne	butan-2-one	
oct-1-yne	pentan-2-one	

4.1.2 List of laboratory safety

- Laboratory PPE
- Chemical storage
- Safety goggles
- First aid kit
- Safety gloves
- Chemical spill kit
- Fire safety
- Chemical spill kit

4.1.3 List of equipment used in this study

- Shimadzu GC-2014 gas-chromatograph, with a thermal conductivity detector (TCD)
- A 51056 Heidolph vacuum pump
- 1 m long, 4.1 mm inner diameter (ID) stainless steel column
- Thermometer
- Laboratory barometer
- Soup bubble flow meter
- AR2140 analytical mass balance
- Helium gas cylinder
- Oven
- DMA 4100 M density meter
- Anton Paar Oscillation U-tube DSA 5000 M
- Anto Paar refractometer
- Round bottom flask
- Glass vial
- Syringe

4.2 Infinite dilution activity coefficient measurements from GLC

4.2.1 Experimental set-up

The experimental set-up for this study involves a Shimadzu GC-2014, as shown in Figure 4-1, to determine activity coefficients at infinite dilution. The (GLC) is equipped with a thermal conductivity detector (TCD), which is located at the exit side of the column. Its function is to detect the vaporized organic gases exiting the column, which is displayed on the computer in a form graphs to determine the retention time of each organic solutes using the (GC) software. This experimental setup is similar to the one used by (Nkosi 2018; Mbatha 2021; Manyoni and Redhi 2022b).

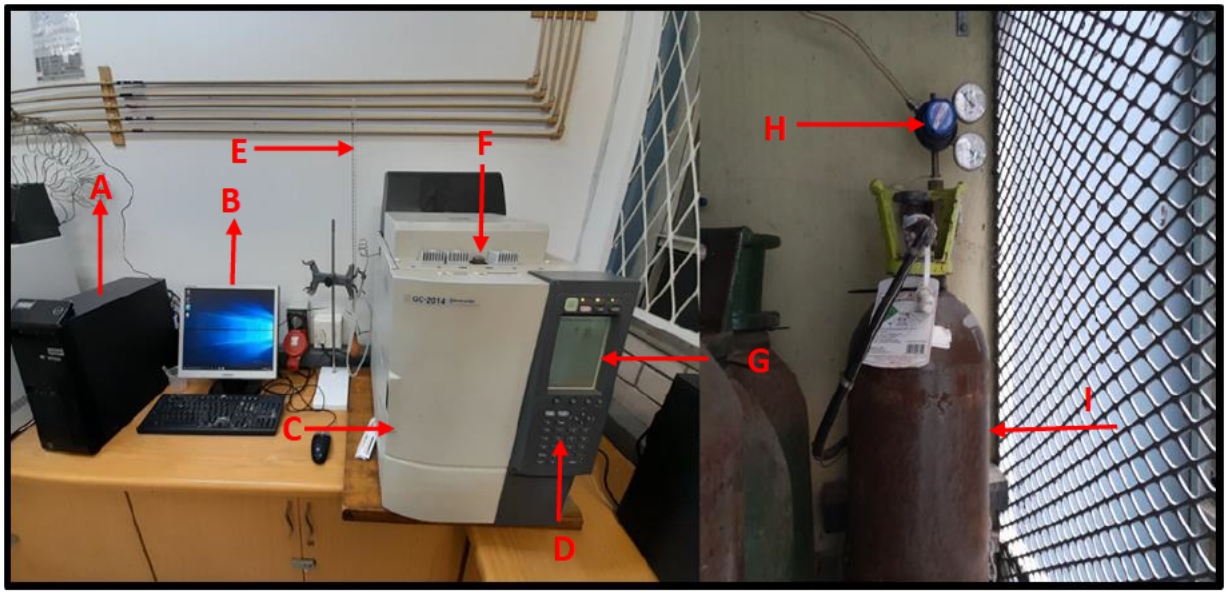

Figure 4-1: Experimental set-up for Gas-liquid chromatograph

A – computer; B – PC monitor; C – Column oven; D – Operation panel; E – Bubble flow meter; F – Manual injector; G – GC screen monitor; H – Pressure regulator; I – Helium (carrier gas).

4.2.2 Calibration method

In this study, the calibration method for the gas-liquid chromatography assisted on validation of the experimental configuration as well as the accuracy of the equipment before the actual measurements were conducted. The reagents used for the calibration are as follows:

- n-hexane
- hexadecane
- cyclohexane
- benzene
- calibrated temperature probe
- stainless steel column

First the column oven temperature set for at least 4 points, from 30℃ to 300℃. After about 10 minutes, the observed temperatures were recorded from a calibrated temperature probe. The column oven temperature was ensured that it corresponds with a set temperature. The injector port and detector temperatures must be equal to the set temperatures. The carrier gas flow rate be within (15-20) $ml.min^{-1}$. A standard mixture, by weighing approximately 50 mg of hexadecane in a 50 ml volumetric flask containing approximately 30 ml of n-hexane and finally makeup a volume of 50 ml with n-hexane. Inject ($1.0\ \mu L$) of standard solution of different concentration and record the retention times. This would give accurate results when the actual experimental measurements are conducted.

4.2.3 Experimental procedure

The main equipment used for measurements was the gas chromatograph (GC). Two 1 m long. 4.1 mm diameter stainless steel column were washed with hot water thereafter rinsed with cold water and flushed with acetone. After the drying process both columns were prepared with different loadings to monitor adsorption effect during experimental works. Each column was weighed before and after packing and installed it in the oven for conditioning for at least 8 hours at temperature of 353.1 K. This allowed enough time for the support material to undergo the drying process to stabilize pressure, temperature of the column and to remove any impurities in the column. The mass of the column was weighed multiple times using a mass balance to monitor any changes of mass. If there are no further changes of mass of the packed column, it was assumed that there is no loss of solvent in the packed column.

For all experiment undertaken, the gas chromatography (GC) detector and temperature injector port were set at temperature 250.15 K. Infinite dilution activity coefficient measurements of various organic solutes, were conducted at different temperatures ranging from (303.13-333.15) K. Each solute was injected in small quantities of (0.2- 0.3μL), due to sensitivity of the (GC), one solute was injected at a time per run and the output signal from TCD was recorded for the calculation of infinite dilution activity coefficients using Equation (3-16). The flow transmitter built into the (GC) was not calibrated accurately, hence compromising the reliability of the results obtained. The flow rate of the inert carrier gas was measured by means of soap bubble flow meter.

4.2.4 Determination of inlet and outlet pressure

The outlet pressure was measured at atmospheric pressure, as the end of the column was exposed to the atmosphere. The measurements were obtained using an LCD digital air pressure meter (SCT-108.001.37) with an uncertainty $\pm 10\ Pa$ as shown in Figure 4-2 and with the list of LCD digital barometer specifications in Table 4-2. The inlet pressure was calculated using the pressure drop through the packed column, depending on the inlet gas flow set by the (GC) operator. Inlet pressure is calculated as follows:

$$P_i = P_o + \Delta P \tag{5-1}$$

Where, (P_i) the inlet pressure, and (P_o) the outlet pressure.

Figure 4-2: LCD digital pressure meter SCT-108.001.37

Table 4-2: Specifications of LCD digital pressure meter SCT-108.001.37

Atmospheric pressure	Type absolute pressure range: 300~ 1100 mb(HPA); 8.85 INHG ~ 32.45 INHG Resolution: 1 MB/HPA; 0.01 INHG Sensing time: 15 minutes
Altitude	Altitude range: -700m~+900m. -2296ft~+29520ft

	Resolution: 0.1m for -500.0m to 999.9m; otherwise 1m
	Sensing time: 2 seconds
Temperature	Temperature range: -10℃ ~+60℃ or +14℉~ +140℉
	Resolution: 0.1℃ or 0.1℉
	Sensing time: 1 minute
Power	2 × 3 volts
Ambient temperature for plastic case	0℃ ~+50℃ or +14℉~ +122℉

Taken from instruction manual for LCD digital pressure meter

4.2.5 Flow rate measurements

The flow rate of the gas at the exit of the column was measured using a soap bubble flow meter. A 50-ml calibrated burette was placed at the column outlet, and a soap bubble was formed over the gas flow stream by means of a rubber teat. The gas flow was maintained at a range of (15-20) $ml.min^{-1}$ with an accuracy of ($\pm$ 0.50%). A stop watch was used to record the time it took for the bubble to exit the burette. It was crucial to maintain air during the flow rate measurements to prevent air from entering the meter. This precaution is necessary due to the higher diffusion rate of light gases such as helium through soap films compared to air, which can lead to inaccurate readings.

4.2.6 Determination of the solvent number of moles (n_3)

a) Preparation of the stationary phase

An analytical, calibrated mass balance in Figure 4-3, with a precision of $\pm$ 0.0001 g, was used to weigh a round bottom flask. A Chromosorb® W-HP 80/100 was used as a solid support material; this was then added to the round bottom flask and weighed. The amount of solvent was then added to the solid support material within the flask and then weighed on the basis of the required percentage loading to give approximately 27 – 33% by mass of the solvent as illustrated in Figure 4-3.

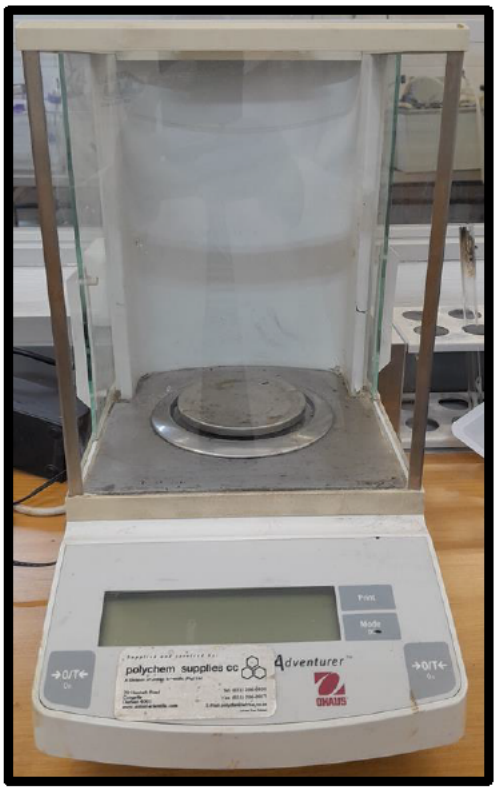

Figure 4-3: AR2140 analytical mass balance

b) Coating solid support with a solvent

To ensure a uniform coating of the solvent over the solid support material, dichloromethane was added in a mixture of solid and solvent to a round bottom flask, as illustrated in Figure 4-4. This was to allow the solvent to be evenly distributed over the solid support and the total mass to be weighed. The round bottom flask was sealed with a hallow rubber stopper, with a small pipe connected at the top of the flask to remove dichloromethane.

Figure 4-4: A 250 ml round bottom flask

c) Removal of dichloromethane

A round bottom flask was attached to the Heidolph pump 5106, as shown in Figure 4-5, to remove the dichloromethane in a solution by applying suction to create vacuum. Small traces of dichloromethane were removed by placing the round bottom flask in the incubator (oven) until all dichloromethane evaporated and lastly, the coated solid support was completely dried. The flask was weighed and compared to the original mass prior to adding of dichloromethane.

Figure 4-5: A 51056 Heidolph vacuum pump

d) Packing of the column

The packed column was plugged with an inert glass wool, acted as a stopper at the end of the column. It was then clamped vertically using a stand, and a funnel attached to the open end with a rubber tube. The previously dried-coated solid support was then poured into the funnel, flowing to an empty column. The column was tapped using a steel rod to ensure a uniform and tightly packed stationery phase. When the solid support was not filling up anymore, it was assumed that the column was fully packed. A new mass was weighed and recorded, since the packed column mass includes the mass of an inert glass wool plugged into the end of the column. Finally, the packed column was then rolled into a round shape using a steel bar, as shown below in Figure 4-6. The packed column was then ready to be installed into the (GC) for conditioning.

Figure 4-6: Round shaped and an installed column into a GC oven

4.2.6 Determination of retention times (t_r and t_g)

The solute and un-retained gas (helium) retention times (t_r) were determined and checked using a stopwatch. The peak retention times (t'_R) were determined on the chart by multiplying the chart speed by the distance from solute injection to the point where the tangents to the solute peak intercept and the gas hold-up time (t_G) was determined by injecting ($0.1\mu L$) of helium gas (Letcher 1980). With respect to retention times (t_r and t_G) the estimated uncertainty was ± 0.5 seconds. Figure 4-7 illustrates the chromatogram retention time using the peak properties.

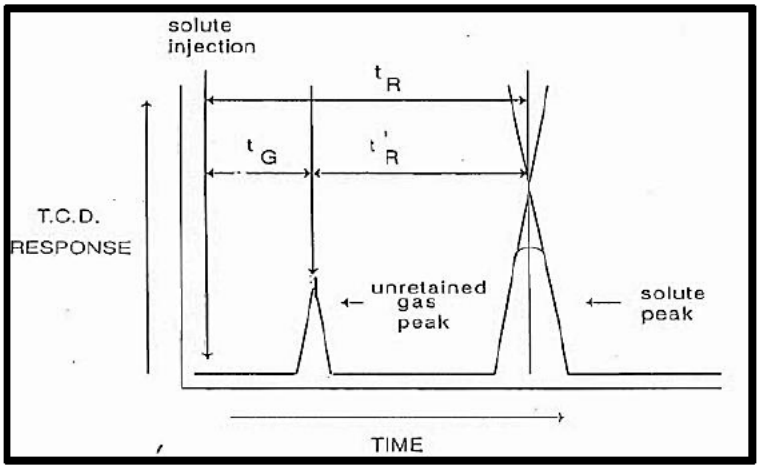

[a] *un-retained gas retention time (t_r), peak retention time (t'_r) and hold-up time (t_g)*

Figure 4-7: Illustrates the chromatogram retention time using the peak properties (Singh 2017)

4.3 Experimental apparatus and method used in this work

In this study, the refractive index (n) was measured using the Anton Paar Refractometer, the density (ρ) using the DMA 4100 M density meter, in the temperature range (298.15 to 333.15) K, with an accuracy of $\pm$ 0.001 K at P = (101.3 ± 2) kPa. The Anton Paar Refractometer was connected to the DMA 4100 M, as shown in Figure 4-8, for the refractive index measurements display. A vibrating U-shaped tube was kept inside a cavity of a metallic block with a peltier device that allows temperature and stability for the measurements of density.

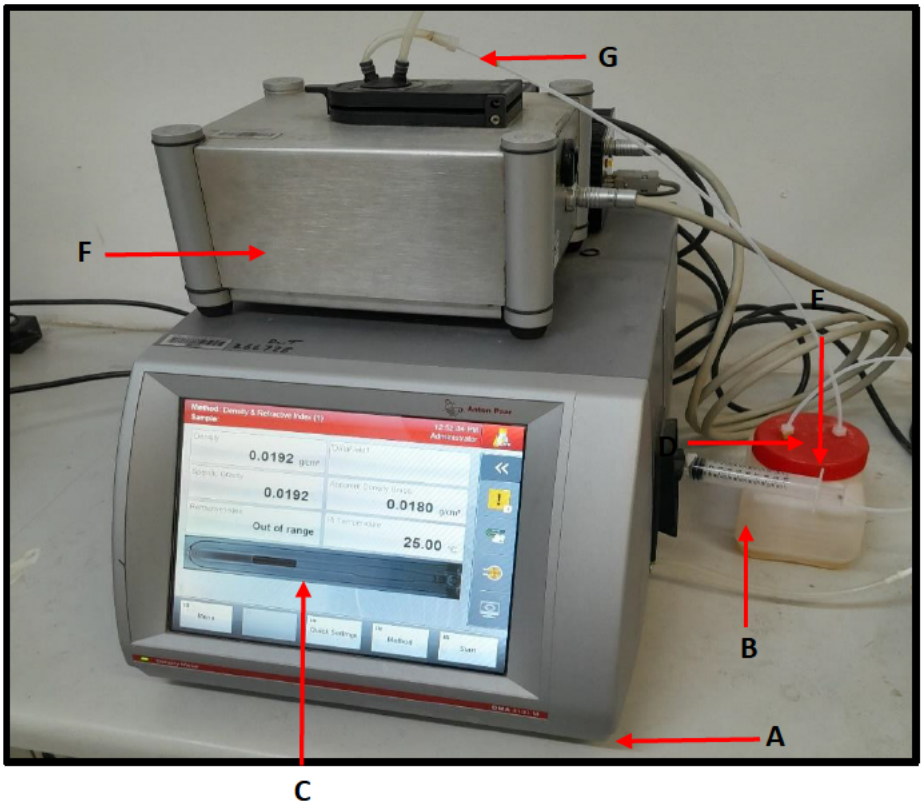

Figure 4-8: Experimental set-up for Anton Paar refractometer and DMA 4100 M density meter.

A- DMA 4100 M density meter; B- Syringe feeding to inlet line; C-DMA measurements display; D-Waste line (DMA 4100); E- Waste container; F- Anton Paar refractometer; GWaste line (Refractometer).

4.3.1 Refractive index

The glass prism of the refractometer was wiped with a lint-free cloth and non-water base sample of organic chemicals like acetone to eliminate any impurities surrounding the prism glass. To obtain accurate results of the equipment, a water calibration was conducted at 298.15 K, as presented in Table 4-3. Small droplets of the sample were dosed into the refractometer using a 10 ml syringe to achieve a thin film across the prism, and the lid was closed for measurements. The instruments operated simultaneously and set the desired temperatures on the DMA 4100 M. This instrument was allowed to stabilize for some time before recording the data. In addition, measurements were done three times to account for repeatability. Its relative deviation (R.D) was found to be -0.16%, thus the equipment is more accurate and reliable.

Table 4-3: Calibration of the refractometer using ultra-distilled water at 298.15 K.

T/K	RI (η)		R.D%
	Lit. [a]	Exp.	
298.15	1.4732	1.4708	-0.16

[a] *(Heintz, Kulikov and Verevkin 2001)*

4.3.2 Density meter

The Anton Paar DMA 4100 M densimeter, with a U-shaped tube, was used to measure the density of cyrene. The instrument inlet was flushed with acetone before experiment were conducted, removing any contaminants within the pipe and the instrument itself. For density measurements, ultra-distilled water was used for calibration of the equipment at a temperature of 298.15 K, as shown in Table 4-4, to ensure that the equipment produced an accurate result, the sample was dosed on the inlet of the instrument and allowed to flow through the pipe. If there was a formation of bubbles in the U-tube pipe, cyrene was dosed again to remove bubbles, and this was observed through the screen of the instrument. A temperatures range of (293.15 to 333.15) K were used for the measurements, The density results were displayed on the LED screen of the instrument and this was repeated three times to validate in respect of its accuracy. The relative deviation was found to be acceptable with a value of -2.24%, thus the equipment is more accurate.

Table 4-4: Calibration of density meter using ultra-distilled water at 298.15 K.

T/K	Density ($g.cm^{-3}$)		R.D%
	Lit. [b]	Exp.	
298.15	1.250[b]	1.222	-2.24

[b]*(Sigma Aldrich.2020)*

4.3.3 Viscometer

The viscosity for cyrene were measured using the Anton Paar Oscillation U-tube DSA 5000 M, as shown below in Figure 4-9. The cell was connected to one end of the U-tube so that the same liquid can pass without any losses, and the same metallic can control temperature. Ethanol was used to clean the cell and acetone for drying using the Xsample 452 module. For the viscosity measurements, ultra-distilled water was used to calibrate the instrument at a temperature of 298.15 K to ensure that the equipment produces accurate results. The vial was filled with a sample and placed into the Xsample 452. To avoid bubbles, more cyrene was filled inside the U-tube pipe until all the bubbles disappeared. The desired temperature was set on the instrument and allowed it to stabilize for some time before measurements were displayed on the LED screen of the equipment. The relative deviation was found to be 0.77% as shown in Table 4-5, and is within acceptable limits, since it is less than 4%, thus the equipment is reliable.

Table 4-5: Calibration for Anton Paar Oscillation U-tube DSA 5000 using double distilled water at 298.15 K.[c]

T/K	Viscocity (mPa.s)		R.D%
	Lit. [c]	Exp.	
298.15	11.62[c]	11.71	0.77

[c]*(Milescu 2021)*

4.3.4 Sound and velocity analyser

The sample is injected into the sound measuring cell, which is enclosed by an ultrasonic transmitter on one side and a receiver on the opposite site. The transmitter emits sound waves of a known duration into the sample. The velocity of sound, denoted as (u), can be computed by using the period of sound waves and the distance between the transmitter and receiver. According to (Singh 2017), the speed of sound can also be calculated using the equation below:

$$Pu = \frac{l \times (1 + 1.6 \times 10^{-5} \Delta T)}{\frac{P_s}{512} - A \times f_3} \quad (5\text{-}2)$$

Where, (l) is the length or distance of the sound wave, (ΔT) is the temperature change, and (P_s) is the oscillation duration of received sound waves. (A) is apparatus constant for sound velocity, and (f_3) is the correction term for temperature.

Figure 4 -9: Anton Paar Oscillation U-tube (DSA 5000 M) viscosity and speed of sound analyser adapted from (Singh 2017).

CHAPTER FIVE

RESULTS AND DISCUSSIONS

Chapter overview

This chapter outlines an overview of the experimental results and discussions pertaining to the n-hexadecane test system. This was done in order to validate the reliability of the experimental configuration, as well as the accuracy of the experimental procedures used for the present study. The relevance of cyrene as a separating agent was assessed and compared with the work done by other researchers on ionic-liquids (IL), and conventional solvents such as NMP and sulfolane for the separation of azeotropic and close boiling point mixtures. The common industrial challenges associated with separation problems were selected to investigate the potential of cyrene by determining its selectivity and limiting capacity at infinite dilution.

The obtained experimental data for cyrene includes the measurements of its density (ρ), viscosity (μ), and refractive index (η). In addition, the thermodynamic data obtained included the measurements of activity coefficients at infinite dilution (γ_{13}^{∞}), partial molar properties $\left(\Delta G_1^{E,\infty}, \Delta H_1^{E,\infty}, and\ \Delta S_1^{E,\infty}\right)$, as well as selectivity $\left(S_{ij}^{\infty}\right)$and capacities $\left(k_j^{\infty}\right)$ for the industrial separation problems. Furthermore, the systems that were examined for a potential separation, includes a mixture of; n-hexane/benzene, n-hexane/hexene, n-octane/benzene, acetone/ethanol, cyclohexane/ethanol, and n-octane/pyridine, were selected to compare the extraction potential under the investigation of cyrene.

5.1 Chemicals used for this study

The chemicals used in this study are sourced from different suppliers, as shown in Appendix A (Table A-1). All the chemicals used contain high purity within acceptable limits without any further refinement.

All the properties used in this study were sourced from the textbooks: The CRC Handbook of Chemistry and Physics ,95th Edition, and Properties of Gases and Liquids, 5th Edition (Poling, Prausnitz and O'connell 2001). These properties are critical temperature, critical pressure, acentric factor, and critical volume. The properties contribute to the calculation of IDACs, which rely on pure components for the calculation of second virial coefficients, i.e.,

(B_{11} and B_{12}) as indicated in Chapter Two, Equation (3-26), according to (McGlashan and Potter 1962).

Table 5-1 presents the properties measurements of cyrene at temperature of 298 15 K. The purity of cyrene solvent was evaluated by comparing three measured properties with the values reported in the literature. These properties are density, viscosity and refractive index. Appendix A (Table A-4) contains further information regarding the measurements within the temperature range of 293.15 K to 333.15 K.

Table 5-1: Dynamic viscosity (η), density (ρ) and refractive index (RI) at different temperatures for Cyrene in the Present Work and Literature at P = (101.3 ± 2) kPa .[a]

T/K	RI		ρ/g.cm^{-3}		μ/mPa.s	
	Lit. [b]	Exp.[a]	Lit. [c]	Exp.[a]	Lit. [c]	Exp.[a]
298.15	1.4712	1.4714	1.2473	1.2474	11.50	11.70

[a] *This work ,*[b]*(Jeřábek et al. 2023),* [c]*(Baird et al. 2019)*

For the cyrene solvent, the properties measurement for viscosity were found to strongly agree with that of literature data, leading to a 0.83% relative deviation (Ziemblińska-Bernart, Bielecki and Wasiak 2019).

The densities of cyrene were measured using the Anton Paar density and velocity meter, model DSA 500M digital vibrating tube densitometer, with an uncertainty of ± 0.0001 g/cm^3 and the refractive index was measured using the Atago refractometer model RX-7000α with an uncertainty of ± 0.0001 g/cm^3. The apparatus was confirmed by measuring the density, and the refractive index of the distilled water. The sample was injected into the apparatus without producing any air bubbles; this was done at least two times to test the efficiency of the approach.

5.2 Experimental data

5.2.1 Infinite dilution activity coefficients data in n-hexadecane test system

The infinite dilution activity coefficient of the test system for hexane, benzene and cyclohexane was measured at temperature of 313.15 K. This was an initial step before experiments were conducted in order to verify the reliability and accuracy of the data obtained from the gas-liquid

chromatography (GLC), more like calibration of the equipment. This was compared with other published data in literature see Table 5-2 below.

Table 5-2: The experimental activity coefficients measured at infinite dilution ($\boldsymbol{\gamma_i^{\infty}}$) for selected organic solutes (1) in hexadecane (3) measured against literature data at 313.15 K. Solute standard states are hypothetical liquids at zero pressure.[a]

Solutes	γ_{13}^{∞}		
	Exp.	Lit.	%A.R.D
benzene	1.042	0.995[b],1.005[c]	3.68
n-hexane	0.904	0.883[b], 0.890[d], 0.903, 0.910[e]	0.11
cyclohexane	0.794	0.765[f], 0.778[b], 0.795[c]	-0.13

[a] Standard uncertainties *u* are *u*(*p*) = 2.0 kPa, *u*and *u*(*T*) = 0.05 K, of reported values. Relative standard uncertainty $u_r(\gamma_{13}^{\infty})$ = 1.4 %, of reported values. [b](Chien *et al.* 1981), [c](Castells *et al.* 1990), [d](Snyder and Thomas 1968), [e](Hicks and Young 1968), [f](Letcher and Jerman 1976)

The relative deviation was calculated using Equation (5-1) and was found to deviate within 3.68 % from the literature data with reference to benzene. This has verified the GLC method, and provided accurate and reliable results.

$$R.D = \frac{\gamma_{13}^{\infty.exp} - \gamma_{13}^{\infty.lit}}{\gamma_{13}^{\infty.lit}} \times 100\% \qquad (5\text{-}1)$$

5.2.2 Analysis of infinite dilution activity coefficients of cyrene

Two column loadings (27% and 33%) were prepared for the measurements of activity coefficients at infinite dilution at four distinct temperatures ranging from (303.15 – 333.15) K. The experimental IDAC data for the cyrene system are provided in Tables 5-3 to 5-5, and Figures 5-1 to 5-10. As known, lower activity coefficients at infinite dilution is an indication of a strong interaction between solvent and solute, whereas higher activity coefficients at infinite dilution is an indication of a weak interaction between solvent and solute. It was very useful to plot the IDAC values as the natural logarithmic ($\ln \gamma_{13}^{\infty}$) against the inverse absolute temperature (1000 *T*/K) with respect to their functional group as a function of the carbon chain length.

The separation capability in terms of activity coefficients at infinite dilution per functional group was determined in the following hierarchy for the system investigated:

- Alk-1-anes > alk-1-enes > alk-1-yne > cycloalkanes > alkylbenzenes > alkanols > esters > heterocyclic compounds (i.e., pyridine and thiophene) > nitrile > ketones, for [cyrene] system.

5.2.3 Measurements of infinite dilution activity coefficients for the new system

The measurements of activity coefficients at infinite dilution (γ_i^{∞}) of 32 organic solutes for the new system using cyrene as a solvent was conducted at temperature range of (303.15 – 333.15)K. Since two colums of different loadings of 8.853 mmol and 9.752 mmol, were prepared, they were averaged as shown in Table 5-5. The results of the two loadings are tabulated as Table 5-3 and Table 5-4. To ensure reproducibility, the data was tested for consistency and potential adsorption effects using two column loadings. In addition, to ensure accuracy of the measured data, a repeatability of runs were taken into consideration, as this would give a clear insight of the measured values (Gautreaux Jr and Coates 1955; Deenadayalu, Letcher and Reddy 2005; Bahadur *et al.* 2014).

It was observed that the activity coefficients at infinite dilution (γ_i^{∞}) increased with increasing of the alkyl chain length and decreased with increasing temperature, meaning as you add more heat into the system there are a greater chances of achieving the separation for a better solubility. It is worth noting that a chemical structure of solutes plays an important role in terms of solvent - solute interaction, since different groups were used to assess the behaviour of activity coefficients. The n-alkane groups exhibited higher activity coefficients indicating that the interaction between the solute-solvent was weaker than that of other solutes, this is because alkane groups are single bonded hydrocarbons, so it became easier for the solvent to break the bonds of an alkane to form new bonds resulting into a much higher activity coefficients (Manyoni and Redhi 2022b). Lower activity coefficients were observed for all polar solutes namely, aromatics, alcohols, ketones, esters, nitrile and water. This indicates a strong intermolecular forces, which are van der Waals forces acting between polar molecules such as hydrogen bonds (Nkosi 2018). For the solutes having the same carbon number (i.e. C_6), benzene, cyclohexane, n-hexane, hex-1-ene and cyclohexene, the presence of a double bond and a cyclic structure have a delocalized pi (π) bonds, which results into high electronegativity (Li *et al.* 2022). Ketones were observed to have the lowest activity coefficients at infinite dilution (γ_i^{∞}), this is due to its functional group, which consists of a carbonyl group in which the carbon atom is double bonded to an oxygen atom (c=o), resulting into much stronger interaction leading to low activity coefficients (γ_i^{∞}).

Table 5-3: The experimental activity coefficients measured at infinite dilution for selected organic solutes (1) and water in the cyrene solvent (3) at different temperatures, with solvent loading n_3 = 8.853 mmol (27.135 wt.%).[a] Solute standard states are hypothetical liquids at zero pressure.

	T/K			
Solute	303.15	313.15	323.15	333.15
n-hexane	33.64	30.22	27.84	25.23
n-heptane	42.38	36.71	34.27	31.20
n-octane	49.58	46.59	40.16	36.99
n-nonane	57.17	50.80	47.11	43.27
hex-1-ene	30.51	25.10	20.41	17.08
hept-1-ene	32.95	30.01	28.18	26.49
dec-1-ene	69.17	59.96	54.13	50.23
hex-1-yne	25.17	17.82	13.30	9.84
oct-1-yne	33.62	27.88	23.81	19.84
cyclopentane	13.08	11.20	8.93	7.981
cyclohexane	18.12	16.46	15.34	14.57
cycloheptane	20.43	18.47	17.16	16.37
cyclooctane	23.96	20.79	18.82	17.34
benzene	6.236	5.640	5.329	5.027
toluene	7.100	6.316	5.991	5.396
ethylbenzene	9.667	8.376	7.304	6.577
m-xylene	8.786	7.484	6.500	5.767
o-xylene	12.788	10.552	8.865	6.950
p-xylene	8.985	7.778	6.705	6.105
acetone	1.683	1.611	1.574	1.495
butan-2-one	1.972	1.853	1.689	1.521
pentan-2-one	2.231	2.020	1.868	1.764
methanol	4.015	3.515	3.216	2.974
ethanol	6.108	5.125	4.873	4.630
propan-1-ol	7.730	6.839	5.966	5.426
propan-2-ol	7.979	7.199	6.352	6.209
methyl acetate	4.217	4.166	3.892	3.578
ethyl acetate	5.413	5.046	4.921	4.880
pyridine	2.091	1.426	1.159	0.873
thiophene	4.343	4.117	3.744	3.331
acetonitrile	3.524	3.323	3.073	2.750
water	8.782	7.322	6.388	5.918

[a] Standard uncertainties u (0.68 level of confidence) are $u(p)$ = 2.0 kPa and $u(T)$ = 0.05 K of reported values. Relative standard uncertainty $u_r(\gamma_{13}^{\infty})$ = ± 1.4 % of reported values.

Table 5-4: The experimental activity coefficients measured at infinite dilution for selected organic solutes (1) and water in the Cyrene solvent (3) at different temperatures, with solvent loading n3 = 9.752 mmol (33.033 wt.%).[a] Solute standard states are hypothetical liquids at zero pressure.

	T/K			
Solute	303.15	313.15	323.15	333.15
n-hexane	33.64	30.67	28.17	25.89
n-heptane	42.84	37.65	34.36	31.27
n-octane	50.15	43.94	41.23	36.94
n-nonane	58.31	50.93	47.20	43.39
hex-1-ene	29.10	24.28	20.09	16.04
hept-1-ene	30.46	27.34	24.47	20.44
dec-1-ene	69.50	60.49	55.99	50.67
hex-1-yne	24.69	16.91	12.49	9.53
oct-1-yne	33.05	27.10	22.38	18.08
cyclopentane	13.02	11.06	9.30	7.55
cyclohexane	17.54	16.27	14.90	14.09
cycloheptane	20.23	18.27	16.92	16.06
cyclooctane	22.97	20.58	18.54	17.11
benzene	5.844	5.534	5.295	4.955
toluene	6.572	5.884	5.352	4.806
ethylbenzene	9.550	8.019	7.038	6.527
m-xylene	8.851	7.852	6.620	5.842
o-xylene	13.10	10.60	8.899	7.210
p-xylene	9.192	7.933	6.866	5.940
acetone	1.772	1.660	1.575	1.519
butan-2-one	2.040	1.889	1.708	1.671
pentan-2-one	1.986	1.901	1.820	1.712
methanol	3.542	3.172	2.773	2.299
ethanol	5.862	5.282	4.538	3.729
propan-1-ol	6.966	6.273	5.678	5.260
propan-2-ol	7.120	6.946	6.734	6.233
methyl acetate	4.036	3.618	3.362	3.242
ethyl acetate	5.235	4.832	4.394	4.067
pyridine	2.543	1.792	1.306	0.998
thiophene	4.235	3.907	3.637	3.473
acetonitrile	2.997	2.655	2.487	2.407
water	8.828	7.515	6.640	5.532

[a] Standard uncertainties u (0.68 level of confidence) are $u(p)$ = 2.0 kPa and $u(T)$ = 0.05 K of reported values. Relative standard uncertainty $u_r(\gamma_{13}^{\infty}) = \pm$ 1.4 % of reported values.

Table 5-5: The experimental average activity coefficients measured at infinite dilution (γ_i^∞) for selected organic solutes (1) and water in the cyrene solvent (3) at different temperatures.[a] Solute standard states are hypothetical liquids at zero pressure.

	T/K			
Solute	303.15	313.15	323.15	333.15
n-hexane	33.64	30.44	28.01	25.56
n-heptane	42.61	37.18	34.31	31.23
n-octane	49.86	45.27	40.69	36.96
n-nonane	57.74	50.87	47.15	43.33
hex-1-ene	29.80	24.69	20.25	16.56
hept-1-ene	31.70	28.68	26.33	23.46
dec-1-ene	69.34	60.23	55.06	50.45
hex-1-yne	24.93	17.36	12.89	9.68
oct-1-yne	33.33	27.49	23.10	18.96
cyclopentane	13.05	11.13	9.11	7.77
cyclohexane	17.83	16.36	15.12	14.33
cycloheptane	20.33	18.37	17.04	16.21
cyclooctane	23.47	20.69	18.68	17.22
benzene	6.040	5.587	5.312	4.991
toluene	6.836	6.100	5.672	5.101
ethylbenzene	9.609	8.197	7.171	6.552
m-xylene	8.818	7.668	6.560	5.805
o-xylene	12.94	10.58	8.882	7.080
p-xylene	9.089	7.856	6.786	6.022
acetone	1.728	1.635	1.575	1.507
butan-2-one	2.006	1.871	1.699	1.596
pentan-2-one	2.108	1.961	1.844	1.738
methanol	5.985	5.204	4.705	4.179
ethanol	3.778	3.344	2.995	2.636
propan-1-ol	7.348	6.556	5.822	5.343
propan-2-ol	7.549	7.072	6.543	6.221
methyl acetate	5.324	4.939	4.658	4.473
ethyl acetate	8.818	7.668	6.560	5.805
pyridine	2.317	1.609	1.232	0.936
thiophene	4.289	4.012	3.690	3.402
acetonitrile	3.260	2.989	2.780	2.578
water	8.805	7.418	6.514	5.725

[a] Standard uncertainties u (0.68 level of confidence) are $u(p)$ = 2.0 kPa and $u(T)$ = 0.05 K of reported values. Relative standard uncertainty $u_r(\gamma_{13}^\infty) = \pm 1.4$ % of reported values.

5.3 Partial molar properties

The thermodynamics partial molar excess enthalpy ($\Delta H_1^{E,\infty}, T_{ref}\,\Delta S_i^{E,\infty}, \Delta G_i^{E,\infty}$) at infinite dilution were calculated to give a better understanding in terms of intermolecular interactions. The enthalpy values were calculated using the Gibbs-Helmholtz Equation (2-12) at the reference temperature (T_{ref}) of 313.15 K as depicted in Table 5-6. Positive enthalpy values are observed for all solutes, it indicates an endothermic dissolution, meaning that the energy released from the solute-solvent bond formation is higher than the energy required to break the formation of solute-solvent bonds. High enthalpy values were obtained for alcohols and heterocyclic (pyridine). This implies that more energy is required to break the bonds in the solvent-solute interaction. A negative entropy values for n-alkanes (n-hexane, n-heptane, n-octane and n-nonane), ketone (pentan-2-one) and heterocyclic (thiophene) are observed. This indicates that a solute molecule is restructuring itself in the voids of the solvent (Kabane *et al.*), while positive entropy values for the rest of the solutes shows that the hydrogen bonds are breaking to allow the solvent to interact for a new bond formation. The Gibbs free energy is the change in enthalpy and entropy during the dissolution process, it reflects different solute-solvent interaction (Li *et al.* 2022). Positive Gibbs free energy values are observed for all the solutes, indicating a non-spontaneous process and requires more input of energy to occur (Kabane *et al.*). Furthermore, $\Delta G_1^{E,\infty}$, shows an increasing trend as the alkyl chain length increases.

Table 5-6: Coefficients *a* and *b* of Eq. (4), limiting partial molar excess enthalpies ($\Delta H_i^{E,\infty}$), entropies ($T_{ref}\Delta S_i^{E,\infty}$), and Gibbs free energies ($\Delta G_i^{E,\infty}$) for organic solutes in cyrene solvent at a reference temperature T = 313.15 K and p = (101.3 ± 2) kPa.[a]

Solute	*a*	*b*	$\Delta H_i^{E,\infty}$	$T_{ref}\Delta S_i^{E,\infty}$	$\Delta G_i^{E,\infty}$	R^2
		K	kJ.mol^{-1}	kJ.mol^{-1}	kJ.mol^{-1}	
n-hexane	0.92	0.49	7.62	-1.27	8.89	0.999
n-heptane	1.02	0.36	8.51	-0.90	9.41	0.991
n-octane	1.01	0.57	8.43	-1.50	9.93	0.999
n-nonane	0.95	0.92	7.89	-2.34	10.2	0.991
hex-1-ene	1.77	-3.27	14.7	8.47	6.27	0.997
hept-1-ene	0.74	0.42	6.18	-1.10	7.28	0.994
dec-1-ene	0.76	0.48	6.35	-1.23	7.58	0.985
hex-1-yne	1.04	-0.29	8.67	0.78	7.89	0.995
oct-1-yne	1.98	-3.12	16.5	8.10	8.35	0.998
cyclopentane	1.00	0.17	8.29	-0.45	8.74	0.994
cyclohexane	1.06	0.74	8.79	-1.88	10.7	0.991
cycloheptane	3.17	-7.25	26.3	18.91	7.43	0.999
cyclooctane	1.88	-2.70	15.7	7.03	8.63	0.998
benzene	1.19	-2.14	9.90	5.60	4.29	0.998
toluene	1.20	-2.63	9.98	6.84	3.14	0.998
ethylbenzene	0.67	-0.17	5.53	0.64	4.90	0.996
m-xylene	1.09	-1.59	9.03	3.94	5.09	0.998
o-xylene	0.63	-0.28	5.24	0.76	4.48	0.995
p-xylene	0.96	-1.25	7.99	3.28	4.71	0.994
acetone	1.30	-2.03	10.8	5.32	5.48	0.992
butan-2-one	0.45	-0.95	3.76	2.48	1.28	0.997
pentan-2-one	0.79	-1.91	6.57	4.94	1.63	0.994
methanol	0.65	-1.39	5.38	3.63	1.75	1.000
ethanol	0.65	-0.81	5.44	1.91	3.54	0.998
propan-1-ol	0.97	-1.60	8.09	3.94	4.16	0.999
propan-2-ol	1.42	-2.52	11.8	6.54	5.30	0.999
methyl acetate	2.00	-4.03	16.6	10.5	6.14	0.995
ethyl acetate	1.40	-2.40	11.6	6.24	5.37	0.999
thiophene	0.78	-1.41	6.52	3.67	2.85	1.000
pyridine	0.79	-1.13	6.53	2.91	3.62	0.995
acetonitrile	3.02	-9.14	25.1	23.9	1.24	0.997
water	1.44	-2.57	12.0	6.73	5.22	0.998

[a]Standard uncertainties u are u(P) = ± 2.0 kPa. u(γ_{13}^{∞}) = ± 1.4 %. u(T) =0.05 K. u($\Delta H_1^{E,\infty}$) = ± 1.7 % of reported values.

5.4 Predicted activity coefficients at infinite dilution on various models for the selected solutes.

This work focused on the measurement of experimental infinite dilution activity coefficients (γ_{13}^{∞}) and the development of predicted models for the extractive distillation column. The development of these predictive model would facilitate the utilisation of advanced process simulations. The design and optimization of many industrial processes depend on the accurate prediction of thermodynamic properties of compounds in a solution. Thermodynamic models including the conductor-like screening model for realistic solvation/segment activity coefficient (COSMO-RS/SAC), Soave-Redlich-Kwong Equation of State (SRK-EOS), Peng-Robinson, Lee Plock-EOS, and perturbed chain statistical associating fluid theory (PC-SAFT) were used to correlate experimental infinite dilution activity coefficients IDAC (γ_{13}^{∞}). When compared to experimental values, the predictions made using these models underperforms. The results showed that their IDAC values were significantly lower than those obtained during the experiments. The reason for this is that cyrene is a novel bio-derived solvent, which has led to some discrepancies in the software systems. For the SRK-EOS model in Table 5-8, acetone, butan-2-one, pentan-2-one, and water, were found to be slightly closer to the experimental values. On the other hand, Table 5-9 shows that the COSMO-RS predictions only agreed with ethanol. Table 5-7 presents the results of a comparison between the data obtained from the experiments and the SRK-EOS and COSMO-RS that were predicted. The relative deviation of acetone was found to deviate within 0.88 % of the SRK-EOS model, this indicated that the experimental value correlates with that of the model. In addition, the predictive model only incorporates the fitting of the solutes that were comparable with the experimental IDAC values, as depicted in Figure 5-1. The results that were predicted from PC-SAFT, Peng-Robinson, Lee Plock-EOS and COSMO-SAC were not sufficient for comparison of the activity coefficients at infinite dilution and are presented in Appendix C (Table C-1 to Table C-4).

Table 5-7: A comparison of experimental activity coefficients at infinite dilution (γ_{13}^{∞}), SRK model from Aspen , and COSMO-RS from Amsterdam modelling suite software (AMS) at *T*= 303.15 K.

		ln (γ_{13}^{∞})			R.D%
Solutes	Solvent	Experimental	SRK (Aspen)	COSMO-RS (AMS)	
acetone	cyrene	1.728	1.713	0.993	0.88
butan-2-one	cyrene	2.006	2.050	1.155	-2.15
pentan-2-one	cyrene	2.108	2.893	1.346	-27.1
water	cyrene	8.805	7.409	-	18.8
ethanol	cyrene	3.778	-	3.609	4.68

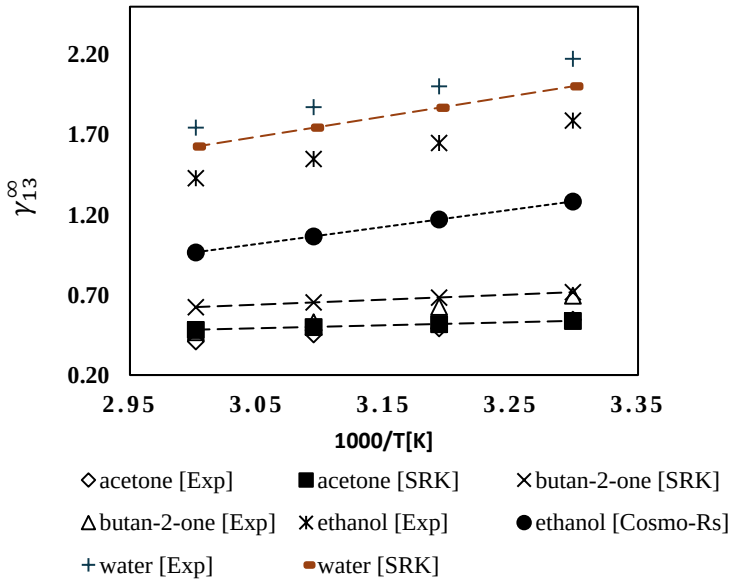

Figure 5-1: The plots of ln (γ_{13}^{∞}) values for selected organic solutes (1) in cyrene (3) for the comparison of experimental, SRK, and COSMO-RS model at varying temperatures of (303.15 to 333.15) K.

Table 5-8: Predicted activity coefficients at infinite dilution for various organic solutes at T = (303.15, 313.15, 323.15 and 333.15) K using Aspen Plus for SRK model.

	T/K			
Solute	303.15	313.15	323.15	333.15
n-hexane	9.582	8.517	7.639	6.907
n-heptane	14.28	12.32	10.75	9.47
n-octane	22.81	19.04	16.10	13.78
n-nonane	37.04	29.86	24.46	20.32
hex-1-ene	7.245	6.546	5.960	5.466
hept-1-ene	9.692	8.561	7.632	6.862
dec-1-ene	39.51	31.60	25.69	21.19
hex-1-yne	3.600	3.387	3.201	3.039
oct-1-yne	7.482	6.683	6.019	5.461
cyclopentane	2.204	2.120	2.037	1.973
cyclohexane	2.664	2.515	2.385	2.272
cycloheptane	-	-	-	-
cyclooctane	3.366	3.086	2.850	2.648
benzene	1.573	1.533	1.497	1.465
toluene	2.139	2.040	1.953	1.875
ethylbenzene	2.952	2.750	2.576	2.426
m-xylene	3.017	2.810	2.631	2.477
acetone	1.713	1.680	1.650	1.620
butan-2-one	2.049	1.981	1.921	1.867
pentan-2-one	2.893	2.732	2.591	2.467
methanol	1.053	1.042	1.032	1.024
ethanol	1.004	1.006	1.009	1.012
propan-1-ol	1.064	1.068	1.072	1.076
propan-2-ol	1.197	1.203	1.210	1.217
methyl acetate	1.632	1.606	1.583	1.560
ethyl acetate	2.559	2.454	2.362	2.280
pyridine	1.116	1.107	1.099	1.091
thiophene	1.202	1.188	1.177	1.166
acetonitrile	1.404	1.385	1.369	1.354
water	7.409	6.480	5.718	5.086

Table 5-9: Predicted activity coefficients at infinite dilution for various organic solutes at T = (303.15, 313.15, 323.15 and 333.15) K using Amsterdam Modelling Suite for COSMO-RS model.

	T/K			
Solute	303.15	313.15	323.15	333.15
n-hexane	7.743	7.300	6.891	6.514
n-heptane	9.820	9.193	8.618	8.092
n-octane	13.25	12.29	11.42	10.63
n-nonane	16.63	15.32	14.13	13.07
hex-1-ene	3.789	3.664	3.543	3.428
hept-1-ene	4.975	4.772	4.580	4.398
dec-1-ene	10.78	10.11	9.481	8.904
hex-1-yne	1.598	1.593	1.587	1.579
oct-1-yne	2.488	2.453	2.415	2.377
cyclopentane	4.810	4.597	4.398	4.212
cyclohexane	6.391	6.052	5.738	5.448
cycloheptane	7.927	7.457	7.025	6.629
cyclooctane	9.238	8.655	8.121	7.633
benzene	1.405	1.408	1.410	1.409
toluene	1.839	1.827	1.813	1.798
ethylbenzene	2.343	2.311	2.278	2.244
m-xylene	2.475	2.435	2.395	2.355
acetone	0.993	0.991	0.989	0.988
butan-2-one	1.155	1.149	1.143	1.137
pentan-2-one	1.346	1.334	1.321	1.310
methanol	3.104	2.835	2.600	2.395
ethanol	3.609	3.227	2.903	2.628
propan-1-ol	3.582	3.213	2.901	2.635
propan-2-ol	3.667	3.274	2.942	2.662
methyl acetate	1.048	1.046	1.044	1.042
ethyl acetate	1.226	1.218	1.211	1.204
pyridine	1.103	1.104	1.104	1.103
thiophene	0.989	1.007	1.023	1.038
acetonitrile	1.074	1.071	1.069	1.066
water	17.83	15.87	14.11	12.55

5.5 The effect of a molecular structure on activity coefficients at infinite dilution

A molecular structure of solutes influences the strength and nature of its interaction with the solvent structure, this then determines how much a molecule deviates from ideal behaviour in a solution for factors like polarity, size, charge distribution, ion strength, temperature and the presence of its functional group, all this plays an important role for determining the activity coefficient at infinite dilution.

In the present study, the effect of molecular structure for various organic solutes were observed. The alkanes, alkenes, alkynes and cycloalkanes interacted very little with cyrene solvent. This is supported by high IDAC values, which indicates that the London forces were too weak to overcome the solute-solvent interaction. Furthermore lower values were obtained for mostly polar solutes which are associated with stronger molecular interaction.

5.5.1 Alkanes:

These compounds are non-polar in nature. They are saturated hydrocarbons consisting of a single bonds. Alkanes are commonly known as aliphatic hydrocarbons due to their physical properties and long carbon chains. They interact with cyrene solvent through small-range van der Waals forces, which are weaker than the induced dipole-dipole interaction that is found in other systems. Due to the presence of a single bond, they exhibit a significantly lower reactivity in comparison the double and triple bonded hydrocarbons.

Figure 5-1 depicts the trend of activity coefficients at infinite dilution (γ_{ij}^{∞}) for the experimental and predicted values for the alkane group in relation to the alkyl chain length. The IDAC values for the alkanes increased with the increase in the carbon chain length of the organic solute, resulting in the occurrence of London dispersion forces, which are caused by the electrons moving farther away from the nucleus. The solute intermolecular forces gets weaker, which makes it easy for the solvent to break up the existing forces to form new bonds with much lesser time. Hence, the electron cloud of the solvent will easily overcome the smaller electron cloud of the solute, resulting in a weaker interaction. As a result, high activity coefficient values were observed, indicating a low level of solubility. It was also observed that as the temperature increases, the solubility also increases, indicating that the system requires more energy to enhance its solubility. The predicted activity coefficients were much lower than

that of the experimental data. Additionally, the intermolecular forces are broken down easily as the temperature rises.

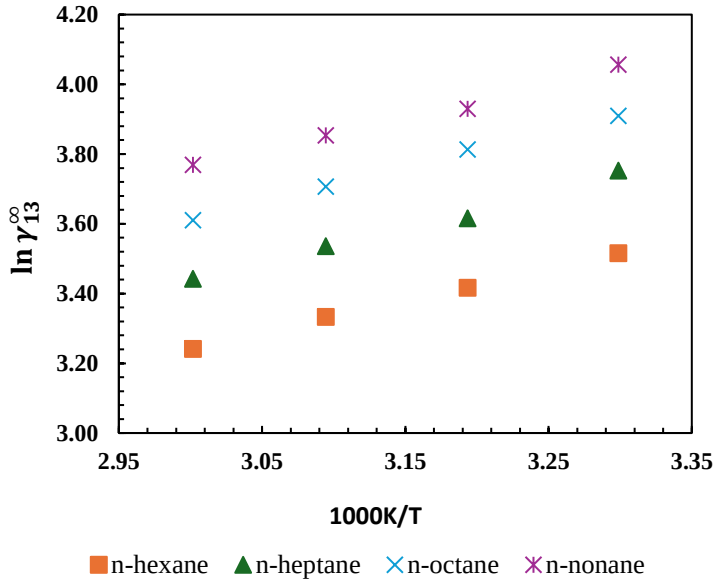

Figure 5-2: The plots of ln (γ_{13}^{∞}) values for selected alkanes (1) in cyrene (3), investigated at 101.3 ± 2 kPa and varying temperatures of (303.15 to 333.15) K.

5.5.2 Cycloalkanes:

Cycloalkanes are cyclic hydrocarbon structure they behave similarly to alkanes. Carbon and hydrogen atoms form a single carbon-carbon bond, making them saturated. They are classified as non-polar hydrocarbon molecules due to the low electronegativity values between carbon and hydrogen atoms. Cycloalkanes differ from alkanes solely in that they have a higher boiling point despite having the same amount of carbon atoms.

Figure 5-2 is the plot of experimental and predicted data showing a positive trend of the infinite dilution activity (γ_i^{∞}) coefficient values with respect to the increase in the carbon chain length. It was also observed that the activity coefficient values decreased with an increase in temperature. This is because cycloalkanes with larger surface area have stronger intermolecular interactions due to the ring shape, making it difficult to break the existing bonds to form new bonds. The predicted activity coefficient values were found to be much lower than the experimental values.

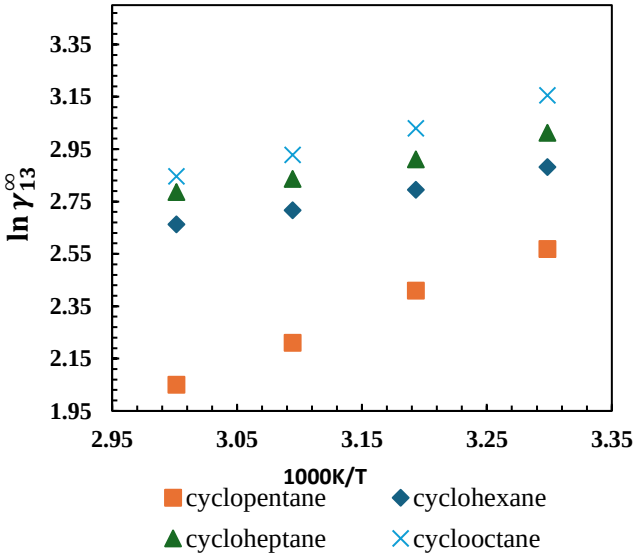

Figure 5-3: The plots of ln (γ_{13}^{∞}) values for selected cycloalkanes (1) in cyrene (3), investigated at 101.3 ± 2 kPa and varying temperatures of (303.15 to 333.15) K.

5.5.3 Alkenes:

The alkenes group are double-bonded hydrocarbon atoms, which makes them olefinic because they are unsaturated in nature. They have a similar structure to that of alkanes, and exclusively contain symmetrical carbon-hydrogen bonds. Alkenes are non-polar compounds with carbon and hydrogen atoms, allowing only London dispersion forces to operate in interactions.

Figure 5-3 shows the trend of increasing activity coefficients at infinite dilution (γ_i^{∞}) with alkyl chain length for an alkene group. As the non-polar solute increases in molecular size, its surface area also increases. As a result, the London dispersion forces between solute-solute molecules becomes stronger. Alkenes had a lower activity coefficients than the alkanes because of the forces necessary to break double-bonded hydrocarbon. The solute-solute intermolecular forces in the alkane group are considerably stronger compared to alkenes due to the loose packing of alkene molecules. This leads to a decrease in the effectiveness of the surface area between the solute-solute bonds for functional London dispersion forces. The behaviour of the alkene group in the cyrene solvent is attributed to a geometric configuration, and the Pi (π) electrons in alkenes exhibit greater polarization compared to those in alkanes, resulting in the formation of strong carbon-carbon bonds. This is further supported by their high activity coefficients values when compared with alkenes. Additionally, a much lower activity coefficients were observed for the predicted values as compared to the experimental values.

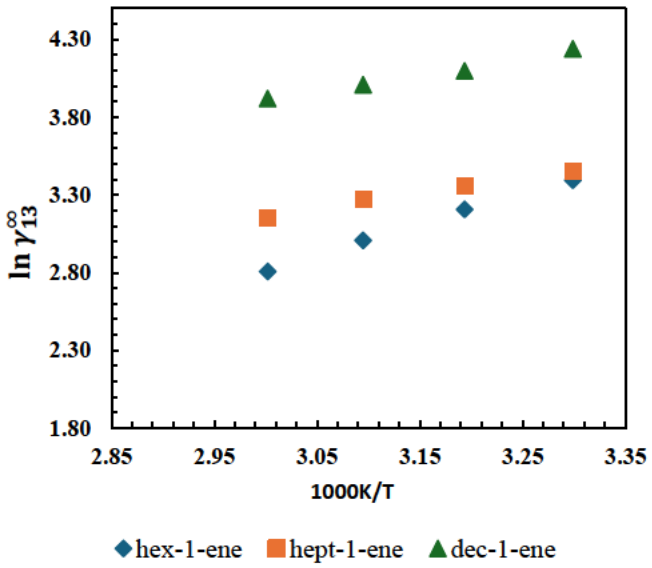

Figure 5-4: The plots of ln (γ_{13}^{∞}) values for selected alkenes (1) in cyrene (3), investigated at 101.3 ± 2 kPa and varying temperatures of (303.15 to 333.15) K.

5.5.4 Alkynes:

Alkynes have molecular structures that are similar to those of alkanes and alkenes. They are linear in molecular structure. Thus enhancing the strength of the London dispersion forces. The presence of triple bonds in these hydrocarbons contributes to their non-polar unsaturated hydrocarbons, and is primarily dominated by London dispersion forces. Figure 5-4 shows the experimental and predicted activity coefficients of the two alkynes; (hexyne and octyne). A much lower activity coefficients values are observed for the alkyne group as compared to that of the single bond and double bonded hydrocarbons. This led to a significant polarization of the triple bonds between carbon-carbon atoms. Alkynes exhibit greater polarization compared to alkanes and alkenes due to the presence of two pi (π) bonds that are not localized around carbon-carbon atoms, this results in the formation of a triple bonds. The solute-solute interaction for the triple bond exhibit greater strength as compared to double bonds. The pi (π) electrons are readily available to being attracted by molecules other than sigma bonds, which are located within the space of the atom. This leads to a strong interaction between the solute and solvent, resulting in a much lower values of activity coefficients. It was also observed that the activity coefficient values of the predicted were much lower than that of the experimental data, however they increased with the increase in the carbon chain length and decreased with increasing the temperature.

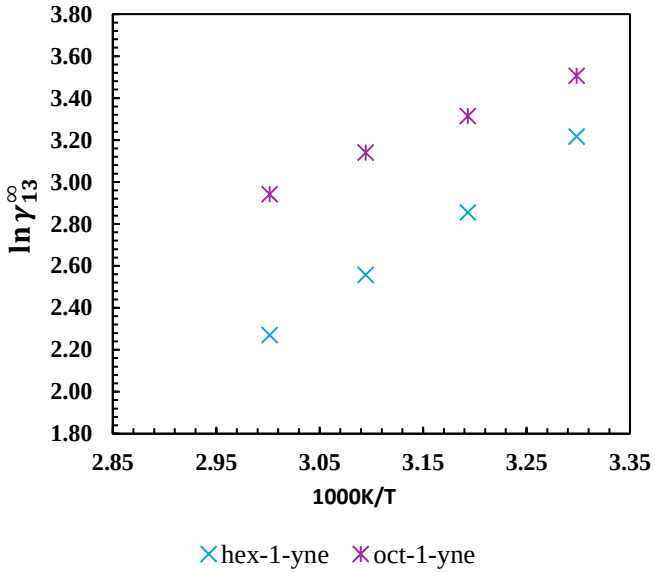

Figure 5-5: The plots of ln (γ_{13}^{∞}) values for selected alkynes (1) in cyrene (3), investigated at 101.3 ± 2 kPa and varying temperatures of (303.15 to 333.15) K.

5.5.5 Ketones:

Ketones are organic molecules that are characterized by the presence of a carboxyl functional group, which consists of a carbon atom bonded to an oxygen atom. The molecular structure contains a carbonyl groups (C=O) on both sides, which does not contain a hydrogen bonded to an electronegative oxygen atom. Ketones exhibit a significant electronegativity difference between the carbon and oxygen atom. Consequently, dipole-dipole forces will operate between the molecules, leading to an increase in the solute-solvent interaction. Dipole-dipole forces are significantly stronger than London forces. Because cyrene is a dipolar aprotic solvent and ketones are polar in nature, these will have a strong interaction. Figure 5-5 shows the experimental and predicted data for the activity coefficients at infinite dilution (γ_i^{∞}). It was observed that the experimental (γ_i^{∞}) values was comparable with that of the predicted for the acetone and butan-2-one solutes, but for the penta-2-one the activity coefficient of the predicted was much higher than that of the experimental value.

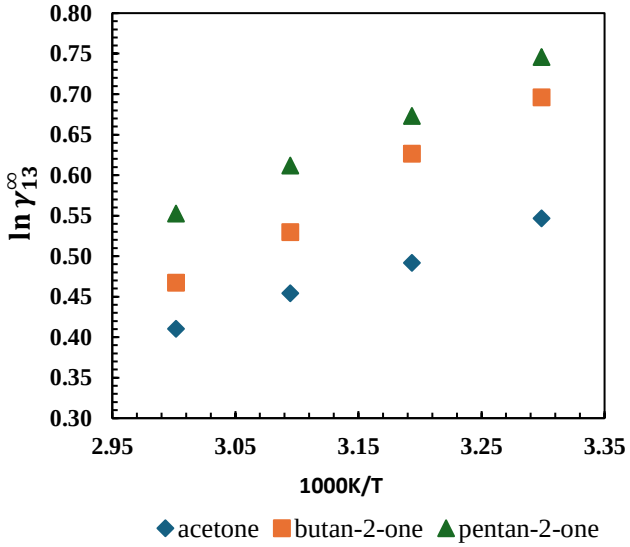

Figure 5-6: The plots of ln (γ_{13}^{∞}) values for selected ketones (1) in cyrene (3), investigated at 101.3 ± 2 kPa and varying temperatures of (303.15 to 333.15) K

5.5.6 Esters:

Esters are characterized as polar in nature. They have a strong electronegativity that is exhibited by the oxygen and carbon atoms. The presence of an alkyl group on both sides of the oxygen atom enables the oxygen atom to bond with hydrogen atom. Thus, the molecules will exhibit dipole-dipole interactions. Figure 5-6 shows a positive correlation between the alkyl chain length and activity coefficients, indicating that as the carbon chain length increases, the activity coefficients also increased, on the other hand, there was a negative correlation between temperature and activity coefficients, meaning that as the temperature rose, the activity coefficients decreased. This phenomenon occurs due to the increased impact of dipole-dipole intermolecular forces as the chain length of carbon atoms grows. Therefore, the number of electrons also increases. Esters showed relatively low activity coefficients when compared to alcohols with an equal number of carbons atoms. This is due to the formation dipole-dipole forces, which is supported with low activity coefficients, and indicate a strong contact also between the solute and solvent. The experimental (γ_i^{∞}) values are not comparable with the predicted values, however, medium range values were observed.

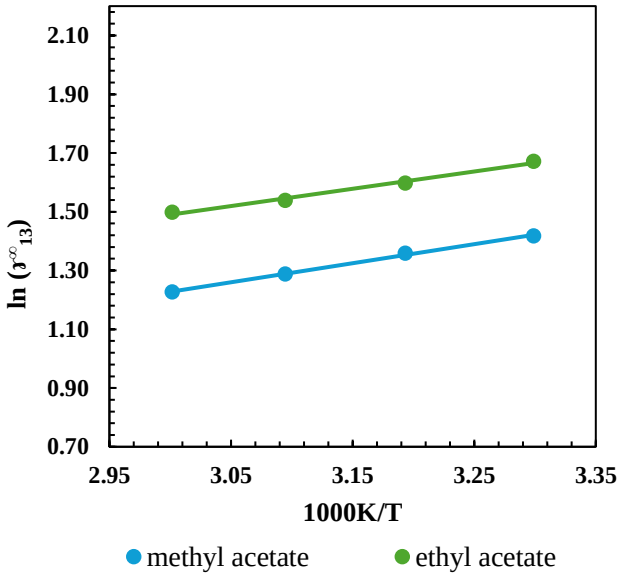

Figure 5-7: The plots of ln (γ^{∞}_{13}) values for esters (1) in cyrene (3), investigated at 101.3 ± 2 kPa and varying temperatures of (303.15 to 333.15) K.

5.5.7 Heterocyclic:

A heterocyclic compound, often known as a ring structure, is a cyclic compound in which the ring consists of atoms from at least two different elements. It consists of a single carbon atom bonded with another element, such as nitrogen, oxygen, or sulphur. The thiophene molecule is composed of a pentagonal ring consisting of four carbon atoms and one sulphur atom, while the pyridine molecule consists of a hexagonal ring of five carbon atoms and one nitrogen atom. The presence of a double bonds between two carbon atoms classifies these two organic solutes as unsaturated hydrocarbons. Figure 5-7 depicts the trend of the activity coefficients at infinite dilution $ln\gamma_{ij}^{\infty}(T)$ for the experimental and predicted values. It was observed that the activity coefficients increases as the alkyl chain length increases and decreased as the temperature is increased. Lower activity coefficients of the predicted values as compared to the experimental data were observed. When comparing thiophene to pyridine, it is observed that thiophene has a higher electronegativity than pyridine. This is because thiophene contains a sulphur atom, which contributes to its increase strength due to the London forces of solute-solute interactions. As a result, this led to an increase in energy required to break these cohesive forces between the solute molecules to form new bonds prior to the formation of intermolecular bonds with the solvent. The low activity coefficient values of both thiophene and pyridine indicate a strong intermolecular forces between the solute and solvent.

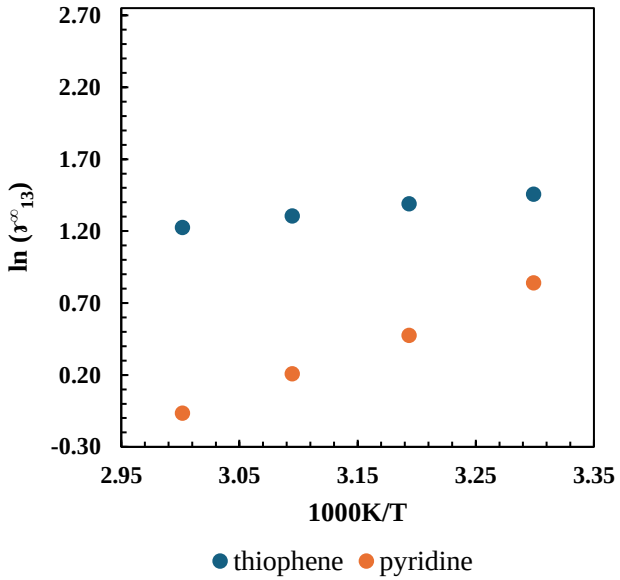

Figure 5-8: The plots of ln (γ^{∞}_{13}) values for heterocyclic (1) in cyrene (3), investigated at 101.3 ± 2 kPa and varying temperatures of (303.15 to 333.15) K.

5.5.8 Alcohols:

Alcohols are characterised by the presence of a hydroxyl (-OH) functional group. These molecules are classified as polar due to the significant difference in electronegativity between the oxygen and hydrogen atoms in the hydroxyl group. As a result, they actively engage in hydrogen bonding. Figure 5-8 shows that the activity coefficients of alcohols increasing with the increasing alkyl chain length. The presence of high intermolecular interactions between solute molecules are a result of an increase of the carbon chain length, leading to the electron being moved far away from the nucleus. Consequently, this leads to the formation of strong hydrogen bonds among the solute molecules, and more energy is required to break the solute-solute bonds to form new bonds with the solvent. In this study, it was observed that the activity coefficient values increased with an increase in chain length, but decreased with an increase in temperature. The predicted activity coefficient values were found to be much lower, since the deviation between the predictions of the SRK-EOS model data are relatively large as compared to those of the experimental values.

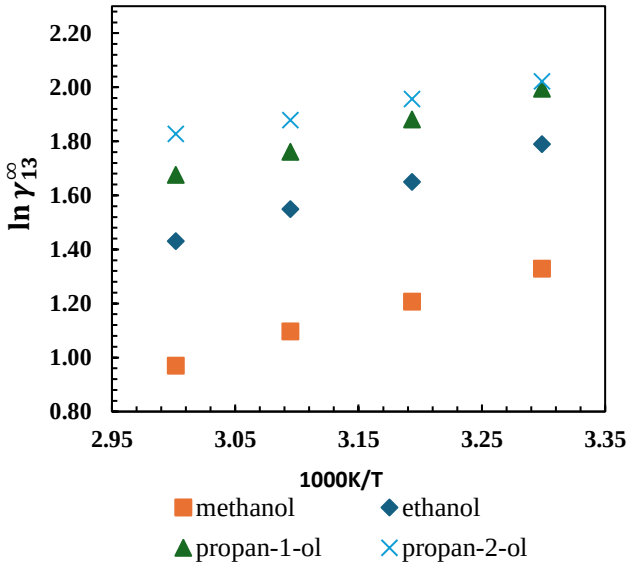

Figure 5-9: The plots of ln (γ_{13}^{∞}) values for selected alcohol (1) in cyrene (3), investigated at 101.3 ± 2 kPa and varying temperatures of (303.15 to 333.15) K.

5.5.9 Aromatics:

Aromatics refers to a group of substances that includes alkylbenzenes and heterocyclic compounds. Their chemical structure is cyclic and non-polar molecule, similar to that of cycloalkanes. Nevertheless, the ring consists of six unsaturated hydrogen atoms. The compound possesses pi(π) electrons, which forms an electron cloud with considerable density above and below the aromatic ring. Figure 5-9 shows the predictions of the SRK for $ln\gamma_{ij}^{\infty}(T)$ over the experimental values in a form of a plot. As shown on the plot in Figure 5-9 the predictions of the SRK model are not matching the experimental values. However, $ln\gamma_{ij}^{\infty}(T)$ are giving medium range values as compared to other models. A clear correlation between temperature and activity coefficients, showing a decrease of activity coefficients as temperature increases and an increasing activity coefficient with increasing of the alkyl chain length.

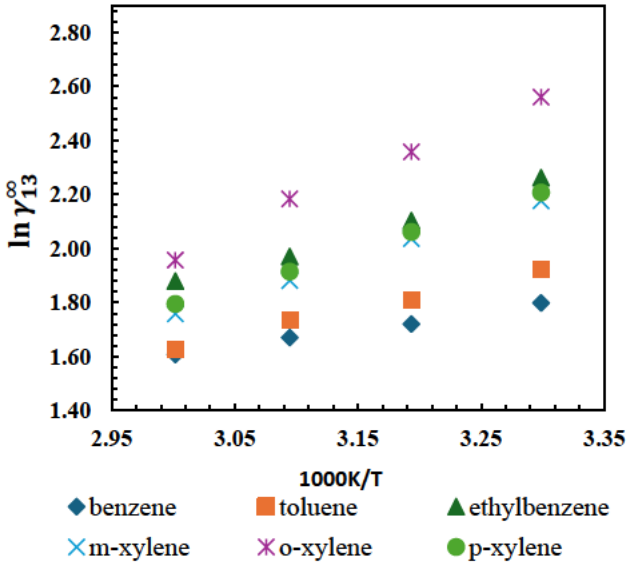

Figure 5-10: The plots of ln (γ_{13}^{∞}) values for selected aromatic (1) in cyrene (3), investigated at 101.3 ± 2 kPa and varying temperatures of (303.15 to 333.15) K.

5.5.10 Water:

Water is a polar compound composed of two hydrogen atoms and one oxygen atom. This molecule exhibit a strong polarity due to high electronegativity of the hydroxyl oxygen atoms. The presence of an oxygen atom, which is bonded to a hydrogen atom, actively contributes to being a hydrogen bond donor HBD. Therefore, due to the dipolar nature of cyrene as an aprotic solvent, this created a strong interaction between the solute and solvent. More energy is required to break the bond as the hydrogen bond that exists between the solute-solute molecules creates a strong force of attraction which becomes challenging for the new solute-solvent bond to be formed. Figure 5-10, shows the activity coefficients at infinite dilution $ln\gamma_{ij}^{\infty}$ values for both acetonitrile and water in the cyrene solvent. The trend indicates that when the temperature increases, the activity coefficients of both solutes decreases and increases with increasing the alkyl chain length. As can be seen in Figure 5-10, the predicted $ln\gamma_{ij}^{\infty}(T)$ for water using the SRK-EOS model is comparable with the experimental values. However, for the acetonitrile a lower $ln\gamma_{ij}^{\infty}$ of the predicted is observed.

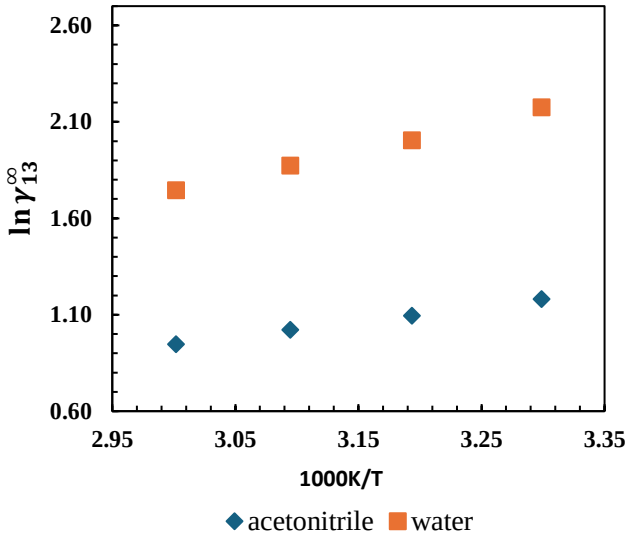

Figure 5-11: The plots of ln (γ_{13}^{∞}) values for selected acetonitrile and water (1) in cyrene (3), investigated at 101.3 ± 2 kPa and varying temperatures of (303.15 to 333.15) K.

5.6 Partition coefficients (K_L)

Table 5-11 presents the gas-liquid partial activity coefficients (K_L), for organic solutes in the cyrene solvent. Partition coefficients describe how a solute is distributed between two immiscible solvents. As a result, it was calculated to check how likely these organic solutes can dissolve in a cyrene solvent. The highest value at T= 313.15 K was observed for acetonitrile K_L = 329.0, and the lowest was observed for n-hexane K_L = 10.16. It was also observed that the K_L values decreased with decrease in temperature and increased with an increase in the carbon chain length.

Table 5-11: The experimental (gas–liquid) partition coefficients K_L for the organic solutes and water (1) in cyrene (3) at different temperatures and P = (101.3 ± 2) kPa.[a]

Solute	T/K			
	303.15	313.15	323.15	333.15
n-hexane	12.29	10.16	8.42	7.21
n-heptane	23.58	19.20	15.18	12.52
n-octane	45.29	33.67	27.30	21.67
n-nonane	87.52	65.85	48.53	37.40
hex-1-ene	13.85	13.77	13.68	13.64
hept-1-ene	25.79	25.64	25.48	25.40
dec-1-ene	64.98	64.59	64.20	63.97
hex-1-yne	146.9	146.0	145.1	144.6
oct-1-yne	11.31	11.24	11.18	11.14
cyclopentane	23.44	23.30	23.16	23.08
cyclohexane	146.5	145.6	144.7	144.2
cycloheptane	141.9	141.0	140.2	139.7
cyclooctane	62.10	61.73	61.36	61.14
benzene	69.32	68.91	68.49	68.25
toluene	59.50	59.14	58.79	58.58
ethylbenzene	113.6	112.9	112.2	111.8
m-xylene	85.90	85.38	84.87	84.57
o-xylene	62.62	62.25	61.87	61.66
p-xylene	112.9	112.2	111.5	111.1
acetone	187.2	186.0	184.9	184.3
butan-2-one	74.91	74.46	74.01	73.75
pentan-2-one	123.4	122.6	121.9	121.5
methanol	53.19	52.87	52.55	52.37
ethanol	40.40	40.15	39.91	39.77
propan-1-ol	59.43	59.07	58.72	58.51
propan-2-ol	215.7	214.4	213.1	212.4
methyl acetate	205.0	203.8	202.5	201.8
ethyl acetate	210.8	209.6	208.3	207.6
thiophene	85.67	85.16	84.64	84.64
pyridine	80.16	79.68	79.20	78.92
acetonitrile	331.0	329.0	327.0	325.9
water	91.06	90.51	89.97	89.65

[a] Standard uncertainties u (0.68 level of confidence) are $u(P)$ = 2.0 kPa and $u(T)$ = 0.05 K of reported values. Relative standard uncertainty $u_r(\gamma_{13}^{\infty})$ = ± 1.4 % and $u_r(K_L)$ = 30 %.

5.7 Selectivity and capacities

The infinite dilution activity coefficients plays an important role for the evaluation of separation potential on chemical mixtures. They give a clear insigth on separation of chemical mixtures for industrial application. The comparison on selectivity and limiting capacity from experimental activity coefficient data were obtained in Table 5-12 to Table 5-17 using Equation (2-4) and (2-5). These were calculated at T=313.15 K, and were compared to the previous work done by other researchers. The investigated separation problems are as follows: n-hexane (i)/benzene (j), n-hexane (i)/hex-1-ene (j), n-octane (i)/benzene (j), n-acetone (i)/ethanol (j), cyclohexane (i)/ethanol (j) and n-octtane (i)/pyridine (j),. For a mixture of acetone (i)/ethanol (j) it was observed that cyrene was having a higher selectivity as compared to other separation problems with selectivity ($S_{ij}^{\infty} = 37.4$), this implies that the investigated solvent is capable to separate aliphatics/aromatics mixture. However, it was also observed that the limiting capacity for these chemical mixtures in a cyrene solvent were very low, this implies that more of the solvent is required into the system to achieve a separation.

According to the data obtained from literature for comparison, ionic-liquid (IL) $4C_1NCl$ + 1,6 Hdiol for a mixture of acetone (i)/ethanol (j) was the best performing solvent having a selectivity of ($S_{ij}^{\infty} = 556$). The best capacity value was noted for ethanol, for (IL) $4C_1NCl$ + 1,6 Hdiol ($k_{ij}^{\infty} = 4.72$). Furthermore, it was worth noting that some of the separation problems for some ionic-liquids (IL) were having low selectivity and capacity values, this implies that they are not suitable to separate those chemical mixtures respectively.

5.7.1 Selectivity and limiting capacity of cyrene for n-hexane (i) and benzene (j)

Table 5-12, presents the selectivity of cyrene for n-hexane (i) over benzene (j) at T=313.15 K. The selectivity and capacity for cyrene in the mixture of n-hexane (i) and benzene (j) separation problem was compared with other solvents used by other researchers as shown in Table 5-12. The separation problem was satisfactory since its selectivity was above a unit. It was observed that cyrene outperforms limonene, [DDA][BF4] and NMA in terms of its selectivity value. This indicates that cyrene has a potential to separate the selected mixture. However, a lower capacity value is obtained, which implies that more solvent is required to achieve the desired separation. In addition, more energy will be used to pump the solvent into the system which is cost effective

Table 5-12: A comparison of the Selectivity ($\mathbf{S_{ij}^{\infty}}$) and Capacity ($\mathbf{k_j^{\infty}}$)at Infinite for hexane/benzene at the Temperature of T = 313.15 K and p = (101.3 ± 2) kPa.

	Selectivity $\mathbf{S_{iJ.s}^{\infty}}$	**Capacity $\mathbf{k_{J.s}^{\infty}}$**
Solvent (i)	**hexane(i)/benzene(j)**	**benzene(j)**
Cyrene[a]	5.534	0.183
Sulfolane[b]	18.262[†]	0.424[†]
Limonene[c]	0.811	0.008
NMP[d]	13.786[†]	0.714[†]
[DDA][BF_4][e]	5.258[†]	1.978[†]
NMA[f]	2.30[†]	1.132[†]

[a]This work; [b.](Möllmann and Gmehling 1997); [c](Mbatha 2021); [d](Krummen, Wasserscheid and Gmehling 2002);[e](Ziemblińska-Bernart, Bielecki and Wasiak 2019);[i]interpolated value.

5.7.2 Selectivity and limiting capacity of cyrene for n-hexane (i) and n-hex-1-ene (j)

Table 5-13, presents the selectivity and limiting capacity of cyrene for n-hexane (i) and n-hex-1-ene (j) mixture. The separation problem was compared with ionic-liquids (ILs), and green solvents at temperature of 313.15 K. The selectivity of this binary mixture was reliable, since it was above a unit. However, the only issue was with the limiting capacity, which was very low, which indicated that more of the solvent would need to be pumped into the system for an effective separation to occur, which would require more energy for the solvent to be pumped into the system.

Table 5-13: A comparison of the selectivity and capacity of solvents for n-hexane (***i***) and hex-1-ene (***j***) separation mixture at the temperature of 313.15 K and p = (101.3 ± 2) kPa.

	Selectivity $S_{iJ.s}^{\infty}$	**Capacity $k_{J.s}^{\infty}$**
Solvent	**n-hexane(i)/n-hex-1-ene(j)**	**n-hex-1-ene(j)**
Cyrene[a]	1.230	0.042
4C_1NCl + Gly: [1:2].[b]	3.040	0.002
4C1NCl + 1,6 Hdiol: [1:2].[b]	1.340	0.067
NMP + 3% (w/w) water.[c]	1.970[†]	0.102[†]
[EMIM][SCN].[d]	2.930[†]	0.011[†]
[ChCl + 1,5-PDO][e]	2.320	0.430
Ethaline[f]	2.230	0.004
Limonene.[g]	1.220	0.013

[a]This work. [b](Nkosi 2018). [c](Krummen, Wasserscheid and Gmehling 2002). [d](Domanska and Marciniak 2008).[e](Li et al. 2022),[f](Lindokuhle and Redhi 2023), [g](Mbatha 2021). [f]interpolated value.

5.7.3 Selectivity and limiting capacity of cyrene for n-octane (i) and benzene (j)

Table 5-14, presents the selectivity and limiting capacity for cyrene in the mixture of n-octane (i) and benzene (j). The separation problem was compared with recent ionic-liquid (ILs) used by other researchers at temperature of 313.15 K. The separation problem was satisfactory in terms of its selectivity. This implies that cyrene is capable to separate aliphatic from aromatics. However, lower capacity values were observed for solvents, accept for [bmPY][NTf2], which was above a unit, and this gives a clear insight that [bmPY][NTf2] outperforms cyrene for the separation of paraffin from aromatics.

Table 5-14: A comparison of the selectivity and capacity of solvents for n-Octane (***i***) and benzene (***j***) separation mixture at the temperature of 313.15 K and p = (101.3 ± 2) kPa.

	Selectivity $S^{\infty}_{ij.s}$	**Capacity $k^{\infty}_{j.s}$**
Solvent	**n-octane(i)/benzene(j)**	**Benzene(j)**
Cyrene[a]	10.51	0.188
[4C1NCl] + [Hdiol][b]	12.00	0.102
[bmPY][NTf2][c]	34.84[†]	1.407[†]
[EMIM][SCN][d]	177.3[†]	0.289[†]
[EMIM][TfO][e]	74.97	0.450
[BMIM][SbF6][f]	33.48	0.787

[a]This work; [b](Nkosi 2018); [c](Domańska and Marciniak 2009); [d](Domanska and Marciniak 2008); [e][f](Tumba 2009); [i]interpolated value.

5.7.4 Selectivity and limiting capacity of cyrene for acetone (i) and ethanol (j)

Table 5-15, presents the selectivity and capacity of cyrene for acetone (i) and ethanol (j) at, 313.15 K. Comparing ionic-liquids and conventional solvent NDBF, cyrene's selectivity is the best performing solvent for the separation of ketones from alcohols. However, lower values of capacity are observed, which indicates that more of the solvent is needed, resulting in more energy required for pumping the solvent into the system which becomes cost effective.

Table 5-15: A comparison of the selectivity and capacity of solvents for acetone (***i***) and ethanol (***j***) separation mixture at the temperature of 313.15 K and p = (101.3 ± 2) kPa.

	Selectivity $S_{ij.s}^{\infty}$	Capacity $k_{j.s}^{\infty}$
Solvent	**Acetone(i)/ethanol(j)**	**ethanol(j)**
Cyrene[a]	37.4	0.67
[[BDMiM] + EG][b]	0.50	0.19
[EMIM Cl_4Al] [DEG] [1:4][c]	4.37	0.23
[[EMPYR] Br + 1,5-PDO][d]	5.95	0.17
[[EMPyr][Cl] + EG] [1:2][e]	1.92	0.33
[ChCl + 1,5-PDO][f]	4.78	0.21
Sulfolane[g]	0.530[†]	0.336[†]
NDBF[h]	1.273[†]	1.199[†]

[a]This work;[b](Manyoni, Kabane and Redhi 2022), [c](Kabane et al. 2023),[d](Manyoni and Redhi 2023) [e](Manyoni, Kabane and Redhi 2022),[f](Li et al. 2022),[g][h](Möllmann and Gmehling 1997); [†]inteporlation.

5.7.5 Selectivity and limiting capacity of cyrene for cyclohexane (*i*) and ethanol (*j*)

Table 5-16, presents the selectivity and limiting capacity of cyrene for cyclohexane (***i***) and ethanol (***j***) mixture. The performance of cyrene solvent for this mixture was satisfactory since its selectivity is above a unit. This indicates that it has potential to separate a mixture of cycloalkanes from alcohols. However, a lower capacity value is observed for cyrene, this indicates that more solvent will be required to achieve the desired separation, and more energy will be required to pump the solvent into the system which is costly since separation is based on a reboiler.

Table 5-16: A comparison of the selectivity and capacity of solvents for n-cyclohexane (***i***) and ethanol (***j***) separation mixture at the temperature of 313.15 K and p = (101.3 ± 2) kPa.

	Selectivity $S_{ij.s}^{\infty}$	Capacity $k_{j.s}^{\infty}$
	Cyclohexane(i)/ethanol(j)	**Ethanol(j)**
Cyrene[a]	4.570	0.229
Ethaline[b]	0.65	0.01
Sulfolane[c]	7.749[†]	0.330[†]
4C1NCl + 1,6-Hdiol [1:2][d]	19.61	0.569
[[TMAmim][1,6-HD] [1:1][e]	19.60	0.580
[[EMPYR] Br + 1,6-HDO][f]	2.22	0.45
[EMIM][SCN][g]	102.6[†]	1.040[†]
[BDMIM] Cl + DEG][h]	13.5	0.07

[a]This work; [b](Lindokuhle and Redhi 2023),[c] (Möllmann and Gmehling 1997); [d](Nkosi 2018); [e] (Nkosi, Tumba and Ramsuroop 2019); [f](Manyoni and Redhi 2023);[g](Domanska and Marciniak 2008); [h](Manyoni, Kabane and Redhi 2022); [†]interpolated.

5.7.6 Selectivity and limiting capacity of cyrene for n-octane (i) and pyridine (j)

Table 5-17, presents the selectivity and limiting capacity of cyrene for n-octane (i) and pyridine (j) mixture at temperature 313.15 K. For this separation problem, it is observed that cyrene has the potential to separate paraffin from heterocyclic. However, low capacity value is observed for cyrene, which implies that more of the solvent is required into the separation process, and more energy will be required to pump the solvent into the system, since the separation is based on the reboiler. In addition, the ionic-liquid [4C1NCl] + [Hdiol] outperforms cyrene in terms of its selectivity and capacity values this shows that it is the best solvent for this separation problem.

Table 5-17: A comparison of the selectivity and capacity of solvents for n-octane (i) and pyridine (j) separation mixture at the temperature of 313.15 K and p = (101.3 ± 2) kPa.

	Selectivity $S_{ij.s}^{\infty}$	Capacity $k_{j.s}^{\infty}$
Solvent	**n-octane(i)/pyridine(j)**	**Pyridine(j)**
Cyrene[a]	37.418	0.669
[4C1NCl] + [Gly][b]	342.810	1.618
[4C1NCl] + [Hdiol][b]	556.290	4.717
Limonene[c]	2.48	0.01

[a]This work; [b](Nkosi 2018);[c](Mbatha 2021)

5.8 Observation of binary mixtures:

In relation to some of the findings in this study, includes the separation challenges of binary mixtures into individual components for common industrial separation problems. For this work, the analysis of selectivity (S_{ij}^{∞}) and capacity (k_j^{∞}) at infinite dilution were obtained for different chemical mixtures. This would then provide a clear insight on the suitability of the cyrene solvent. The following observations in this study were as follows:

- **n-hexane (1) – benzene (2) system:** The properties of cyrene solvent showed favorable results in terms of its selectivity since it was above a unit. However, low capacity values was observed for this separation mixture, which implies that more of the solvent is required into the system. The best selectivity and limiting capacity was obtained for the ionic liquid [DDA][BF_4].

- **n-hexane (1) – hex-1-ene (2) system:** For this separation mixture, the investigated solvent showed a fair selectivity with very low limiting capacity. Thus, the best selectivity was showed by the ionic-liquid [$4C_1$NCl + Gly: [1:2]] and [EMIM][SCN] with also low limiting capacity. In conclusion, the separation costs for this mixture will be taken into consideration due to very low limiting capacities.

- **n-octane (1) – benzene (2) system:** Comparing the investigated solvent with that of the ionic liquids reported by other researchers. The ionic liquid [bmPY][NTf2] was found to be the best performing extracting agent for this separation mixture on the basis of both the selectivity and limiting capacity values. Furthermore, cyrene also showed promising results in terms of its selectivity, however its performing index was found to be very low, which requires more solvent into the system and this is cost effective. Therefore the properties of the selected solvent has to be taken into consideration.

- **acetone (1) – ethanol (2) system:** The separation of acetone over ethanol was possible for the investigated solvent. This was supported with a high selectivity value, however a very low capacity value was also observed. This indicated that more solvent and more heat is required into the system to achieve this separation, and this will be cost effective since separation is based on the reboiler. In addition, higher values of selectivity and limiting capacity were observed for the conventional solvents which are to be phased away due to their toxicity.

- **cyclohexane (1) – ethanol (2) system:** The separation performance for the mixture of cyclohexane and ethanol showed promising results in terms of its selectivity, however, the performance index was found to be very low for cyrene solvent. The ionic liquids used in previous study shows very low performance index when compared with that of the current study, except for ionic liquid [EMIM][SCN], it shows a high selectivity and limiting capacity values.

- **n-octane (1) – pyridine (2) system:** For this separation problem, the selectivity was within acceptable limits, but lower capacity value was observed. Furthermore, the cyrene solvent was not comparable with the previously investigated ionic liquids due to their higher values of both selectivity and limiting capacity for this separation mixture.

CHAPTER SIX

CONCLUSSIONS AND RECOMMENDATIONS

Chapter overview

The primary objective of this study was to assess the impact of molecular structure as well as the effect of temperature on the solute-solvent interaction for the separation of organic mixtures. It was therefore necessary to measure the thermophysical properties of cyrene, such as its density, viscosity and refractive index to understand its characteristics. Therefore to assess the performance of cyrene as a separating agent, selectivity and capacity were computed from the experimental measurements of the activity coefficient at infinite dilution by gas liquid chromatograph.

The GLC method for this research was found to be the most efficient technique due to its high sensitivity, high accuracy, and precision with very small amounts of analyte. Therefore a test system was conducted to verify the experimental configuration as well as the experimental procedures for the accuracy of the equipment before the actual measurements were conducted for the new system. The obtained results on the selected solutes for the hexadecane test system showed a good correlation literature values. It is worth noting that the study of cyrene for the measurement of infinite dilution activity coefficient γ_{13}^{∞} data for the new system is crucial, since there is no data available in the literature for benchmarking. This was then verified by developing predictive thermodynamic model.

On the basis of the results attained, this study provides a clear understanding on how a chemical structure and temperature influences the activity coefficient at infinite dilution in terms of molecular interaction. Additionally, the reported predictive thermodynamic models, such as the COSMO-RS and SRK-EOS were also incorporated for the prediction of activity coefficients at infinite dilution and were found to be inconsistent for almost all the organic solutes except for acetone, butan-2-one, pentan-2-one, ethanol and water, which was giving medium range values that were slightly closer to the experimental values.

6.2. Recommendations

This section includes recommendations for additional research. Suggestions were informed by research findings and observations. As a result, the following suggestions have been made:

- More separation problems should be investigated on cyrene for future work.
- More experimental measurements such as vapor-liquid equilibrium (VLE) and liquid-liquid equilibrium technique (LLE).
- Developing of thermodynamic models should also be considered to provide valuable and useful data.

REFERENCES

Abbott, M. M. 1986. Low-pressure phase equilibria: Measurement of VLE. *Fluid Phase Equilibria*, 29: 193-207.

Alessi, P., Fermeglia, M. and Kikic, I. 1991. Significance of dilute regions. *Fluid Phase Equilibria*, 70 (2-3): 239-250.

Ali, H. and Khan, E. 2017. Environmental chemistry in the twenty-first century. *Environmental Chemistry Letters*, 15 (2): 329-346.

Anastas, P. T. and Kirchhoff, M. M. 2002. Origins, current status, and future challenges of green chemistry. *Accounts of chemical research*, 35 (9): 686-694.

Anastas, P. T. and Warner, J. C. 1998. Principles of green chemistry. *Green chemistry: Theory and practice*, 29: 14821-14842.

Bahadur, I., Govender, B. B., Osman, K., Williams-Wynn, M. D., Nelson, W. M., Naidoo, P. and Ramjugernath, D. 2014. Measurement of activity coefficients at infinite dilution of organic solutes in the ionic liquid 1-ethyl-3-methylimidazolium 2-(2-methoxyethoxy) ethylsulfate at T=(308.15, 313.15, 323.15 and 333.15) K using gas+ liquid chromatography. *The Journal of Chemical Thermodynamics*, 70: 245-252.

Baird, Z. S., Uusi-Kyyny, P., Pokki, J.-P., Pedegert, E. and Alopaeus, V. 2019. Vapor pressures, densities, and PC-SAFT parameters for 11 bio-compounds. *International Journal of Thermophysics*, 40 (11): 102.

Berthod, A. and Carda-Broch, S. 2004. Determination of liquid–liquid partition coefficients by separation methods. *Journal of chromatography A*, 1037 (1-2): 3-14.

Brouwer, T. and Schuur, B. 2019. Model performances evaluated for infinite dilution activity coefficients prediction at 298.15 K. *Industrial & Engineering Chemistry Research*, 58 (20): 8903-8914.

Brouwer, T. and Schuur, B. 2020. Bio-based solvents as entrainers for extractive distillation in aromatic/aliphatic and olefin/paraffin separation. *Green Chemistry*, 22 (16): 5369-5375.

Camp, J. E. 2018. Bio-available solvent Cyrene: synthesis, derivatization, and applications. *ChemSusChem*, 11 (18): 3048-3055.

Castells, R. C., Arancibia, E. L., Nardillo, A. M. and Castells, C. 1990. Thermodynamics of hydrocarbon solutions using glc n-Hexane, n-heptane, benzene, and toluene as solutes each at

infinite dilution in n-hexadecane, in n-octadecane, and in n-eicosane. *The Journal of Chemical Thermodynamics*, 22 (10): 969-977.

Chien, C., Kopecni, M., Laub, R. and Smith, C. 1981. Solute liquid-gas activity and partition coefficients with mixtures of n-hexadecane and n-octadecane with N, N-dibutyl-2-ethylhexylamide solvents. *The Journal of Physical Chemistry*, 85 (13): 1864-1871.

Clark, J. H., Macquarrie, D. J. and Sherwood, J. 2013. The combined role of catalysis and solvent effects on the Biginelli reaction: improving efficiency and sustainability. *Chemistry–A European Journal*, 19 (16): 5174-5182.

Conder, J. R. and Young, C. L. 1979. *Physicochemical measurement by gas chromatography*. John Wiley & Sons.

Cruickshank, A., Windsor, M. and Young, C. 1966. The use of gas-liquid chromatography to determine activity coefficients and second virial coefficients of mixtures I. Theory and verification of method of data analysis. *Proceedings of the Royal Society of London. Series A. Mathematical and Physical Sciences*, 295 (1442): 259-270.

Deenadayalu, N., Letcher, T. M. and Reddy, P. 2005. Determination of activity coefficients at infinite dilution of polar and nonpolar solutes in the ionic liquid 1-ethyl-3-methyl-imidazolium bis (trifluoromethylsulfonyl) imidate using gas− liquid chromatography at the temperature 303.15 K or 318.15 K. *Journal of Chemical & Engineering Data*, 50 (1): 105-108.

Doble, M., Rollins, K. and Kumar, A. 2010. *Green chemistry and engineering*. Academic Press.

Dohnal, V. and Horáková, I. 1991. A new variant of the Rayleigh distillation method for the determination of limiting activity coefficients. *Fluid Phase Equilibria*, 68: 173-185.

Dohrn, R. and Pfohl, O. 2002. Thermophysical properties—Industrial directions. *Fluid Phase Equilibria*, 194: 15-29.

Domanska, U. and Marciniak, A. 2008. Activity coefficients at infinite dilution measurements for organic solutes and water in the ionic liquid 1-butyl-3-methylimidazolium trifluoromethanesulfonate. *The Journal of Physical Chemistry B*, 112 (35): 11100-11105.

Domańska, U. and Marciniak, A. 2009. Activity coefficients at infinite dilution measurements for organic solutes and water in the ionic liquid triethylsulphonium bis (trifluoromethylsulfonyl) imide. *The Journal of Chemical Thermodynamics*, 41 (6): 754-758.

Domańska, U., Zawadzki, M., Królikowska, M., Tshibangu, M. M., Ramjugernath, D. and Letcher, T. M. 2011. Measurements of activity coefficients at infinite dilution of organic

compounds and water in isoquinolinium-based ionic liquid [C8iQuin][NTf2] using GLC. *The Journal of Chemical Thermodynamics*, 43 (3): 499-504.

Doyle, A. C., Weir, R. and de Loos, T. W. 2005. EMMERICH WILHELM. *Measurement of the Thermodynamic Properties of Multiple Phases*, Article ID: 137.

Everett, D. 1965. Effect of gas imperfection on GLC measurements: a refined method for determining activity coefficients and second virial coefficients. *Transactions of the Faraday Society*, 61: 1637-1645.

Fowlis, I. and Scott, R. P. W. 1963. A vapour dilution system for detector calibration. *Journal of Chromatography A*, 11: 1-10.

Fredenslund, A. 2012. *Vapor-liquid equilibria using UNIFAC: a group-contribution method*. Elsevier.

Gao, G., Daridon, J.-L., Saint-Guirons, H., Xans, P. and Montel, F. 1992. A simple correlation to evaluate binary interaction parameters of the Peng-Robinson equation of state: binary light hydrocarbon systems. *Fluid phase equilibria*, 74: 85-93.

Gautreaux Jr, M. and Coates, J. 1955. Activity coefficients at infinite dilution. *AIChE Journal*, 1 (4): 496-500.

Gibbs, R. E. and Van Ness, H. C. 1972. Vapor-liquid equilibria from total-pressure measurements. A new apparatus. *Industrial & Engineering Chemistry Fundamentals*, 11 (3): 410-413.

Gu, Y. and Jerome, F. 2013. Bio-based solvents: an emerging generation of fluids for the design of eco-efficient processes in catalysis and organic chemistry. *Chemical Society Reviews*, 42 (24): 9550-9570.

Harris, R. A. 2000. Monoethanolamine: suitability as an extractive solvent. Article ID.

Haynes, W. M. 2014. *CRC handbook of chemistry and physics*. CRC press.

Heintz, A., Kulikov, D. V. and Verevkin, S. P. 2001. Thermodynamic properties of mixtures containing ionic liquids. 1. Activity coefficients at infinite dilution of alkanes, alkenes, and alkylbenzenes in 4-methyl-n-butylpyridinium tetrafluoroborate using gas− liquid chromatography. *Journal of Chemical & Engineering Data*, 46 (6): 1526-1529.

Hicks, C. and Young, C. 1968. Activity coefficients of C 4–C 8 n-alkanes in C 16–C 32 n-alkanes. *Transactions of the Faraday Society*, 64: 2675-2682.

Holste, J., Young, J., Eubank, P. and Hall, K. 1982. Interaction second virial coefficients and binary interaction parameters for the CO2 C2H6 systems between 250 and 300 K. *AIChE Journal*, 28 (5): 807-812.

Hudson, G. and McCoubrey, J. 1960. Intermolecular forces between unlike molecules. A more complete form of the combining rules. *Transactions of the Faraday Society*, 56: 761-766.

Hussam, A. and Carr, P. W. 1985. Rapid and precise method for the measurement of vapor/liquid equilibria by headspace gas chromatography. *Analytical Chemistry*, 57 (4): 793-801.

Jeřábek, V. c., Štejfa, V. c., Klajmon, M. and Řehák, K. 2023. Thermodynamic Properties and Phase Equilibria of Dihydrolevoglucosenone and Its Mixtures with Hydrocarbons. *Journal of Chemical & Engineering Data*, 68 (12): 3361-3376.

Kabane, B., de P Soares, R., Deenadayalu, N. and Bahadur, I. 2023. Pre-screening of 1-ethyl-3-methylimidazolium tetrachloroaluminate and influence of diethylene glycol on the ionic liquid in separation of molecular solutes: Activity coefficients at infinite dilution and COSMO-SAC modelling. *Fluid Phase Equilibria*, 571: 113808.

Kabane, B., Molefi, R., Matshetshe, K., Deenadayalu, N. and Bahadur, I. Pre-Screening of an Eco-Friendly Deep Eutectic Solvent for Separating Industrial Mixtures: A Useful Tool for Solvent Selection. *Available at SSRN 4710041*, Article ID.

Klamt, A. 1995. Conductor-like screening model for real solvents: a new approach to the quantitative calculation of solvation phenomena. *The Journal of Physical Chemistry*, 99 (7): 2224-2235.

Kolb, B. and Ettre, L. S. 2006. *Static headspace-gas chromatography: theory and practice*. John Wiley & Sons.

Krummen, M., Wasserscheid, P. and Gmehling, J. 2002. Measurement of activity coefficients at infinite dilution in ionic liquids using the dilutor technique. *Journal of Chemical & Engineering Data*, 47 (6): 1411-1417.

Laub, R. J. and Pecsok, R. L. 1978. *Physicochemical applications of gas chromatography*. Wiley.

Lei, Z., Li, C. and Chen, B. 2003. Extractive distillation: a review. *Separation & Purification Reviews*, 32 (2): 121-213.

Lerol, J.-C., Masson, J.-C., Renon, H., Fabries, J.-F. and Sannier, H. 1977. Accurate measurement of activity coefficient at infinite dilution by inert gas stripping and gas

chromatography. *Industrial & Engineering Chemistry Process Design and Development*, 16 (1): 139-144.

Letcher, T. and Jerman, P. 1976. The thermodynamics of mixing for the systems, benzene, cyclohexane, and n-hexane with n-alkanes, at infinite dilution. *South African Journal of Chemistry*, 29 (1): 55-62.

Letcher, T. M. 1980. Activity coefficients at infinite dilution from gas–liquid chromatography. In: Proceedings of *Faraday Symposia of the Chemical Society*. Royal Society of Chemistry, 103-112.

Letcher, T. M., Marciniak, A., Marciniak, M. and Domańska, U. 2005. Determination of activity coefficients at infinite dilution of solutes in the ionic liquid 1-butyl-3-methylimidazolium octyl sulfate using gas− liquid chromatography at a temperature of 298.15 K, 313.15 K, or 328.15 K. *Journal of Chemical & Engineering Data*, 50 (4): 1294-1298.

Li, Y., Wang, W., Wang, Q., Yalikun, N. and Tang, J. 2022. Thermodynamic parameters and infinite dilution activity coefficients for organic solutes in deep eutectic solvent: Choline Chloride+ 1, 5-Pentanediol. *The Journal of Chemical Thermodynamics*, 170: 106784.

Lindokuhle, M. and Redhi, G. 2023. Separation Performance of Ethaline: Infinite Dilution Activity Coefficients and the Excess Thermodynamic Properties. *Journal of Chemical & Engineering Data*, 68 (11): 2924-2933.

Lobien, G. M. and Prausnitz, J. M. 1982. Infinite-dilution activity coefficients from differential ebulliometry. *Industrial & Engineering Chemistry Fundamentals*, 21 (2): 109-113.

Manyoni, L., Kabane, B. and Redhi, G. G. 2022. Deep eutectic solvent as a possible entrainer for industrial separation problems: Pre-screening tool for solvent selection. *Fluid Phase Equilibria*, 553: 113266.

Manyoni, L. and Redhi, G. 2022a. 1.6-Hexanediol based deep eutectic solvent and their excess data at infinite dilution. *Chemical Thermodynamics and Thermal Analysis*, 8: 100088.

Manyoni, L. and Redhi, G. 2023. Separation potential of 1, 5-pentanediol-based deep eutectic solvent: Infinite dilution activity coefficients and excess thermodynamic data. *Heliyon*, 9 (11).

Manyoni, L. and Redhi, G. G. 2022b. Measurements of infinite dilution activity coefficient for aromatic and aliphatic hydrocarbons in Deep Eutectic Solvent, 1-ethyl-1-methylpyrrolidinium bromide+ ethylene glycol at different temperatures and a stated molar ratio. *Chemical Thermodynamics and Thermal Analysis*, 7: 100057.

Mbatha, B. P. 2021. Infinite dilution activity coefficient measurements for limonene as a green solvent for separation. Article ID.

Mbatha, B. P., Ngema, P. T., Nkosi, N. and Ramsuroop, S. 2022. Infinite dilution activity coefficient measurements for 1-Methyl-4-(1-methylethenyl)-cyclohexene as a green solvent for separation. *Journal of Chemical & Engineering Data*, 67 (4): 966-974.

McGlashan, M. and Potter, D. 1962. An apparatus for the measurement of the second virial coefficients of vapours; the second virial coefficients of some n-alkanes and of some mixtures of n-alkanes. *Proceedings of the Royal Society of London. Series A. Mathematical and Physical Sciences*, 267 (1331): 478-500.

Meng, X., Pu, Y., Li, M. and Ragauskas, A. J. 2020. A biomass pretreatment using cellulose-derived solvent Cyrene. *Green Chemistry*, 22 (9): 2862-2872.

Milescu, R. A. 2021. Applications of the novel bio-derived solvent Cyrene™ in polymer chemistry. Article IDUniversity of York.

Milescu, R. A., Segatto, M. L., Stahl, A., McElroy, C. R., Farmer, T. J., Clark, J. H. and Zuin, V. G. 2020. Sustainable single-stage solid–liquid extraction of hesperidin and rutin from agro-products using cyrene. *ACS Sustainable Chemistry & Engineering*, 8 (49): 18245-18257.

Möllmann, C. and Gmehling, J. 1997. Measurement of activity coefficients at infinite dilution using Gas− Liquid chromatography. 5. Results for N-methylacetamide, N, N-dimethylacetamide, N, N-dibutylformamide, and sulfolane as stationary phases. *Journal of Chemical & Engineering Data*, 42 (1): 35-40.

Moollan, W. C. 1995. The determination of activity coefficients at infinite dilution. Article IDUniversity of Natal.

Ngema, P. T. 2010. Separation processes for high purity ethanol production. Article ID.

Nkosi, N. 2018. Infinite dilution activity coefficient measurements of organic solutes in selected deep eutectic solvents by gas-liquid chromatography. Article ID.

Nkosi, N., Tumba, K. and Ramsuroop, S. 2019. Activity coefficients at infinite dilution of various organic solutes in the deep eutectic solvent (tetramethylammonium chloride+ 1, 6 hexanediol in the 1: 1 molar ratio). *South African journal of chemical engineering*, 27 (1): 7-15.

Novák, J. P., Matouš, J. and Pick, J. 1987. *Liquid-liquid equilibria*. Elsevier Science Limited.

Oklu, N. K., Matsinha, L. C. and Makhubela, B. C. 2019. Bio-solvents: synthesis, industrial production and applications. *Solvents, Ionic Liquids and Solvent Effects*, Article ID: 1-24.

Paolo, A., Maurizio, F. and Ireneo, K. 1986. A differential static apparatus for the investigation of the infinitely diluted region. *Fluid Phase Equilibria*, 29: 249-256.

Perrone, S., Messa, F. and Salomone, A. 2023. Towards Green Reductions in Bio-Derived Solvents. *European Journal of Organic Chemistry*, 26 (14): e202201494.

Poling, B. E., Prausnitz, J. M. and O'connell, J. P. 2001. *Properties of gases and liquids*. McGraw-Hill Education.

Porter, P., Deal, C. and Stross, F. 1956. The determination of partition coefficients from gas-liquid partition chromatography. *Journal of the American Chemical Society*, 78 (13): 2999-3006.

Prieto, M. G., Williams-Wynn, M. D., Bahadur, I., Sánchez, F. A., Mohammadi, A. H., Pereda, S. and Ramjugernath, D. 2017. Activity coefficients at infinite dilution of hydrocarbons in glycols: Experimental data and thermodynamic modeling with the GCA-EoS. *The Journal of Chemical Thermodynamics*, 105: 226-237.

Qian, L., Xu, F., Liu, S., Lv, G., Jiang, L., Su, T., Wang, Y. and Zhao, Z. 2021. Selective production of levoglucosenone by catalytic pyrolysis of cellulose mixed with magnetic solid acid. *Cellulose*, 28: 7579-7592.

Raal, J. and Muhlbauer, A. 1998. *Phase Equilibria: Measurement and*: Ž.

Rackett, H. G. 1970. Equation of state for saturated liquids. *Journal of Chemical and Engineering Data*, 15 (4): 514-517.

Ram, N. 2013. Investigation and Measurement of Liquid-Liquid Phase Equilibria Using Ionic Liquids as a Solvent. *Chemical Engineering [Master's thesis], University of KwaZulu-Natal*, Article ID.

Redlich, O. and Kister, A. 1948. Algebraic representation of thermodynamic properties and the classification of solutions. *Industrial & Engineering Chemistry*, 40 (2): 345-348.

Richon, D. 2011. New equipment and new technique for measuring activity coefficients and Henry's constants at infinite dilution. *Review of Scientific Instruments*, 82 (2): 025108.

Richon, D., Sorrentino, F. and Voilley, A. 1985. Infinite dilution activity coefficients by the inert gas stripping method: extension to the study of viscous and foaming mixtures. *Industrial & Engineering Chemistry Process Design and Development*, 24 (4): 1160-1165.

Ricles, J. M., Sause, R. and Green, P. S. 1998. High-strength steel: implications of material and geometric characteristics on inelastic flexural behavior. *Engineering Structures*, 20 (4-6): 323-335.

Sandler, S. 1996. Infinite dilution activity coefficients in chemical, environmental and biochemical engineering. *Fluid Phase Equilibria*, 116 (1-2): 343-353.

Sarafraz-Yazdi, A. and Amiri, A. 2010. Liquid-phase microextraction. *TrAC Trends in Analytical Chemistry*, 29 (1): 1-14.

Seader, J. D., Henley, E. J. and Roper, D. K. 2016. *Separation process principles: With applications using process simulators*. John Wiley & Sons.

Singh, S. 2017. Thermo-physical properties and activity coefficients at infinite dilution for ionic liquid systems at several temperatures. Article ID.

Sithersingh, M. 2018. Determination of polar solvents by static headspace extraction–gas chromatography (SHE-GC). Article ID.

Smith, J. M., Van Ness, H. C. and Abbott, M. M. 2001. *Solutions manual to accompany Introduction to chemical engineering thermodynamics*. McGraw-Hill.

Snyder, P. S. and Thomas, J. F. 1968. Solute activity coefficients at infinite dilution via gas-liquid chromatography. *Journal of Chemical & Engineering Data*, 13 (4): 527-529.

Soni, M. 2003. Vapour-liquid equilibria and infinite dilution activity coefficient measurements of systems involving diketones. Article ID.

Taylor, B. N. and Kuyatt, C. E. 1994. *Guidelines for evaluating and expressing the uncertainty of NIST measurement results*. US Department of Commerce, Technology Administration, National Institute of ….

Trampe, D. B. and Eckert, C. A. 1993. A dew point technique for limiting activity coefficients in nonionic solutions. *AIChE Journal*, 39 (6): 1045-1050.

Tsonopoulos, C., Dymond, J. H. and Szafranski, A. 1989. Second virial coefficients of normal alkanes, linear 1-alkanols and their binaries. *Pure and applied chemistry*, 61 (8): 1387-1394.

Tumba, A. K. 2009. Infinite dilution activity coefficient measurements of organic solutes in fluorinated ionic liquids by gas-liquid chromatography and the inert gas stripping method. Article ID.

Wardencki, W., Curyło, J. and Namieśnik, J. 2005. Green Chemistry--Current and Future Issues. *Polish Journal of Environmental Studies*, 14 (4).

Whitehead, P. G. 1996. Part 1: The determination of activity coefficients at infinite dilution; Part 2: Investigations into the colour components of raw sugar. Article ID.

Williams-Wynn, M. D., Letcher, T. M., Naidoo, P. and Ramjugernath, D. 2013. Activity coefficients at infinite dilution of organic solutes in diethylene glycol and triethylene glycol from gas–liquid chromatography. *The Journal of Chemical Thermodynamics*, 65: 120-130.

Wilson, K. L., Murray, J., Jamieson, C. and Watson, A. J. 2018. Cyrene as a bio-based solvent for the Suzuki–Miyaura cross-coupling. *Synlett*, 29 (05): 650-654.

Wittig, R., Lohmann, J. and Gmehling, J. 2003. Vapor− liquid equilibria by UNIFAC group contribution. 6. Revision and extension. *Industrial & engineering chemistry research*, 42 (1): 183-188.

Yaws, C. L. 2015. *The Yaws handbook of vapor pressure: Antoine coefficients*. Gulf Professional Publishing.

Zhang, M., He, Z.-Z., Kang, R.-X. and Ge, M.-L. 2019. Thermodynamics and activity coefficients at infinite dilution for organic compounds in the ionic liquid 1-hexyl-3-methylimidazolium chloride. *The Journal of Chemical Thermodynamics*, 128: 187-194.

Ziemblińska-Bernart, J., Bielecki, P. and Wasiak, W. 2019. Measurements of activity coefficients at infinite dilution for organic solutes in two quaternary ammonium-based ionic liquids [DDA][ClO4] and [DDA][BF4]. *Fluid Phase Equilibria*, 482: 99-107.

APPENDIX A: SUPPLIER AND PURITY OF CHEMICALS

Table A-1: The sources and mass fraction purities of organic solutes used.[a]

Chemical	Supplier	Purity (Mass fraction)[a]	CAS No.
n-hexane	Merck	≥ 0.99	110-54-3
n-heptane	Sigma-Aldrich	≥ 0.99	142-82-5
n-octane	Fluka	≥ 0.999	111-65-9
n-nonane	Merck	≥ 0.99	111-84-2
hex-1-ene	Sigma-Aldrich	≥ 0.98	592-41-6
hept-1-ene	Flucka	≥ 0.98	592-76-7
dec-1-ene	Capital lab	≥ 0.98	872-05-9
hex-1-yne	Sigma-Aldrich	≥ 0.97	693-02-7
oct-1-yne	Fluka	≥ 0.98	629-05-0
cyclopentane	Fluka	≥ 0.985	287-92-3
cyclohexane	ACE	≥ 0.99	110-82-7
cycloheptane	ACE	≥ 0.999	291-64-5
cyclooctane	Sigma-Aldrich	≥ 0.995	292-64-8
ethanol	Sigma-Aldrich	≥ 0.999	64-17-5
methanol	Macron	≥ 0.999	67-56-1
propan-1-ol	Lab scan	≥ 0.995	71-23-8
propan-2-ol	Lab scan	≥ 0.995	67-63-0
benzene	Sigma-Aldrich	≥ 0.999	71-43-2
toluene	Sigma-Aldrich	≥ 0.999	108-88-3
ethylbenzene	ACE	≥ 0.999	100-41-4
m-xylene	Sigma-Aldrich	≥ 0.999	108-38-3
o-xylene	Fluka	> 0.99	95-47-6
p-xylene	Fluka	> 0.99	106-42-3
acetone	Sigma-Aldrich	≥ 0.999	67-64-1
butan-2-one	Sigma-Aldrich	≥ 0.997	78-93-3
pentan-2-one	Sigma-Aldrich	≥ 0.99	107-87-9
methyl acetate	Capital lab	≥ 0.98	79-20-9
ethyl acetate	ACE	≥ 0.995	141-78-6
acetonitrile	Sigma-Aldrich	≥ 0.997	75-05-8
water	Lab purified	≥ 0.999	7732-18-5
thiophene	Sigma-Aldrich	≥ 0.999	110-02-1
pyridine	Sigma-Aldrich	≥ 0.999	110-86-1
hexadecane	Sigma-Aldrich	≥ 0.999	544-76-3
helium	Afrox-SA	≥ 0.999[†]	7440-59-7
cyrene	Sigma-Aldrich	≥ 0.999	53716-82-8
dichloromethane	Sigma-Aldrich	≥ 0.999	75-09-2

[†] Mole fraction; [a] No additional purification was done

A-2. Antoine Equation Constants

Table A-2: Antoine Constants for all solutes used in this study

Compound	A	B	C	Ref
n-hexane	4.00139	1170.875	224.317	†
n-heptane	4.02023	1263.909	216.432	†
n-octane	4.05075	1356.36	209.635	†
n-nonane	4.07356	1438.03	202.694	†
cyclopentane	4.06783	1152.574	234.51	†
cyclohexane	3.93002	1182.774	220.618	†
cycloheptane	3.9633	1322.22	215.297	†
cyclooctane	3.98125	1434.67	209.712	†
hex-1-ene	3.9826	1148.62	225.34	†
hept-1-ene	4.02677	1258.34	219.3	†
dec-1-ene	7.315	1694.625	215.316	*
hex-1-yne	6.24468	918.34	173.473	†
oct-1-yne	6.93838	1352.05	206.916	†
ethanol	5.33675	1648.22	230.918	†
methanol	5.2027	1580.08	239.5	†
propan-1-ol	4.99991	1512.94	205.807	†
propan-2-ol	5.24268	1580.92	219.61	†
butan-1-ol	7.301	1285.023	173.247	*
pentan-1-ol	7.215	1333.46	169.781	*
benzene	3.98523	1184.24	217.572	†
toluene	4.05043	1327.62	217.625	†
ethylbenzene	4.06861	1415.77	212.3	†
acetone	4.2184	1197.01	228.06	†
butan-2-one	4.1386	1232.63	218.69	†
pentan-2-one	7.374	1553.014	243.751	*
methyl acetate	4.18621	1156.43	219.69	†
ethyl cetate	4.13361	1195.13	212.47	†
m-xylene	7.181	1573.024	226.671	*
water	8.10765	1750.286	235	*
helium	1.6836	8.1548	273.71	†
pyridine	4.16749	1373.021	214.69	†
thiophene	4.08416	1246.02	221.35	†

†(Poling, Prausnitz and O'connell 2001),(Yaws 2015)*

The vapour pressure of pure component i at the system was calculated from Antione equation (A-1) given by (Poling, Prausnitz and O'connell 2001):

$$logP^{sat}(kPa) = A - \frac{B}{C + T(℃)} \quad \text{(A-1)}$$

where: A. B. and C are constants for component i

$T =$ Temperature of a system in ℃

Table A-3: Critical volume, V_c critical temperature,T_c ionization energies, I_c of the solutes critical pressure, P_c acentric factor, ω and helium gas used for the calculation of viral coefficients. (Reference: CRC Handbook of Chemistry and Physics).

Compound	Tc/K	Pc/bar	Vc/cm^3.mol^{-1}	ω	Ic/kJ.mol^{-1}
helium	5.19	2.27	57.3	-0.39	2373
n-pentane	469.70	33.70	310.0	0.252	998.6
n-hexane	507.50	30.10	370.0	0.299	977.4
n-heptane	540.20	27.40	428.0	0.350	957.1
n-octane	568.70	24.90	492.0	0.399	947.5
n-nonane	594.60	22.90	555.0	0.445	937.8
cyclopentane	512.60	80.97	118.0	0.224	1046.9
cyclohexane	553.80	40.70	308.0	0.212	951.3
cycloheptane	604.20	38.20	353.0	0.237	962.0
cyclooctane	647.20	35.60	410.0	0.236	941.7
hex-1-ene	504.00	31.43	355.1	0.281	910.8
hept-1-ene	537.10	29.20	409.0	0.358	910.8
dec-1-ene	616.40	21.10	584.0	0.478	908.9
hex-1-yne	539.30	331.00	376.2	0.146	960.0
oct-1-yne	598.50	31.01	441.0	0.262	960.0
ethanol	513.90	61.48	167.0	0.649	1010.2
methanol	512.60	80.97	118.0	0.565	1046.9
propan-1-ol	536.80	51.75	219.0	0.629	982.2
propan-2-ol	508.30	47.62	220.0	0.665	981.3
benzene	562.20	48.95	256.0	0.212	892.2
toluene	591.80	41.08	316.0	0.263	851.0
ethylbenzene	617.20	36.09	374.0	0.304	846.2
acetone	508.10	47.00	209.0	0.307	935.9
butan-2-one	536.80	24.10	267.0	0.322	918.5
pentan-2-one	561.08	37.10	301.0	0.345	895.4
methyl acetate	506.80	46.90	228.0	0.326	989.0
ethyl acetate	523.20	38.30	286.0	0.362	966.0
m-xylene	617.10	35.40	376.0	0.259	825.9
acetonitrile	545.00	48.30	173.0	0.327	1177.3
thiophene	580.00	219.00	56.6	0.252	0.2
pyridine	620.00	254.00	56.7	0.267	0.2
Water	647.3	221.2	57.1	0.344	951.3

[a]*(Haynes 2014)*

Physical properties of cyrene

Table A-4: Dynamic viscosity (η), density (ρ) and refractive index (RI) at different temperatures for Cyrene in the Present Work and Literature at p = (101.3 ± 2) kPa .[a]

T/K	ρ/g.cm^{-3}			μ/mPa.s			RI [b]		
	Exp.	Lit.[b]	R.S.D.%	Exp.	Lit. [b]	R.S.D.%	Exp.	Lit. [a]	R.S.D.%
293.15	1.2518	1.2522	0.03	14.00	13.70	2.20	1.4721	1.4732	0.10
298.15	1.2474	1.2473†	0.01	11.70	11.50†	1.74	1.4714	1.4712†	0.01
303.15	1.2425	1.2424	0.01	9.470	9.680	2.17	1.4706	1.4691	0.10
308.15	1.2380	1.2375†	0.04	8.110	8.270†	1.94	1.4683	1.4670†	0.09
313.15	1.2327	1.2326	0.01	6.760	7.130	5.19	1.4659	1.4651	0.05
318.15	1.2258	1.2277†	0.15	5.890	6.210†	5.15	1.4639	1.4630†	0.06
323.15	1.2229	1.2228	0.01	5.020	5.450	7.90	1.4618	1.4611	0.05
328.15	1.2164	1.2179†	0.12	4.970	4.810†	3.33	1.4596	1.4592†	0.03
333.15	1.2131	1.2131	0.00	4.920	4.290	0.00	1.4573	1.4571	0.01

[a] Standard uncertainties u (0.68 level of confidence) are $u(\rho)$ = 5.2×10^{-3} g/cm^3, $u(RI)$ = 2.5×10^{-4}, $u(T)$ = 0.01 K and u(p) = 2.0 kPa. Relative standard uncertainty $u_r(\eta)$ = 12.3% of measured values. [b] Wavelength (λ) = 589.3 nm.

†Interpolated.

[a](Baird *et al.* 2019)

[b](Jeřábek *et al.* 2023)

APPENDIX B: SAMPLE OF CALCULATIONS

B.1 Calculations of activity coefficients at infinite dilution

The sample of calculation for activity coefficient at infinite dilution for hexane using 27% loading as a basis of calculation at T= 313.15 K.

$$J_3^2 = \left(\frac{2}{3}\right)\left[\frac{\left(\frac{P_1}{P_O}\right)^3 - 1}{\left(\frac{P_i}{P_O}\right)^3 - 1}\right] \quad \text{(B-1)}$$

$$J_3^2 = \left(\frac{2}{3}\right)\left[\frac{\left(\frac{11580}{102600}\right)^3 - 1}{\left(\frac{11580}{102600}\right)^3 - 1}\right]$$

$$J_3^2 = 1.0656$$

$$U_O = U\left(1 - \frac{P_w}{P_o}\right)\frac{T}{T_f} \quad \text{(B-2)}$$

$$U_O = 3.4722 \times 10^{-7}\left(1 - \frac{7280.5}{102600}\right)\frac{313.15}{297.25}$$

$$U_O = 3.3983\times 10^{-7}\ m^3.s^{-1}$$

Net retention volume

$$V_N = (J_2^3)^{-1} U_O (t_r - t_G) \quad (2\text{-}5)$$
$$= (1.07)^{-1}(3.3983 \times 10^{-7})(86.16 - 23.28)$$
$$= 2.0053 \times 10^{-5}$$

Second viral coefficient of the solute

$$B/V_c = 0.43 - 0.886\left(\frac{T_c}{T}\right) - 0.694\left(\frac{T_c}{T}\right)^2 - 0.0375(n-1)\left(\frac{T_c}{T}\right)^{4.5} \quad (B\text{-}4)$$

$$B/V_c = 0.43 - 0.886\left(\frac{507.5}{313.15}\right) - 0.694\left(\frac{507.5}{313.15}\right)^2 - 0.0375(5-1)\left(\frac{507.5}{313.15}\right)^{4.5}$$

$$B_{11} = -0.001655819 \times V_c$$

$$B_{11} = -0.001655819 \times 0.0003700$$

$$B_{11} = -6.12653 \times 10^{-7}$$

Solute molar volume

$$v_i^* = V_c(0.29056 - 0.08775\omega)e^{\left[1-\frac{T}{T_c}\right]^{\frac{2}{7}}} \quad (B\text{-}5)$$

$$v_i^* = (0.0003700)(0.29056 - 0.08775 \times 0.299)e^{\left(1-\frac{313.15}{507.50}\right)^{\frac{2}{7}}}$$
$$= 0.0001434$$

Mixed critical properties

$$I_{C12} = (I_{C11} + I_{C12})^{0.5}\left(V_{C11}^{1/3} + V_{C12}^{1/3}\right)^6 \quad \text{(B-6)}$$

$$I_{C12} = (977400 + 2372600) \times 10^3 \left[(370 \times 10^{-6})^{\frac{1}{3}} + (57.3 \times 10^{-6})^{\frac{1}{3}}\right]^6$$

$$= 6.0466\, J.mol^{-1}$$

$$= 6.0466\, J.mol^{-1}$$

$$V_{C12} = \frac{1}{8}\left(V_{C11}^{1/3} + V_{C12}^{1/3}\right)^3 \quad \text{(B-7)}$$

$$= \frac{1}{8}\left[(370 \times 10^{-6})^{\frac{1}{3}} + (57.3 \times 10^{-6})^{\frac{1}{3}}\right]^3$$

$$= 0.0001679\, m^3$$

$$T_c = 128(T_{C11}.T_{C22})^{0.5}(I_{C11}.I_{C22})^{0.5}\left({}^{V_{C11}.V_{C22}}/_{I_{C12}}\right) \quad \text{(B-8)}$$

$$T_c = 128(507.5 \times 5.19)^{0.5}(977.4 \times 2372.6 \times 10^3)^{0.5}\left(\frac{370 \times 57.3 \times 10^{-6}}{6.0466}\right)$$

$$= 35.0755\ \text{K}$$

Cross second viral coefficient of the solute and carrier gas

$${}^{B}/_{V_c} = 0.43 - 0.886\left(\frac{T_c}{T}\right) - 0.694\left(\frac{T_c}{T}\right)^2 - 0.0375(n-1)\left(\frac{T_c}{T}\right)^{4.5} \quad \text{(B-9)}$$

$${}^{B}/_{V_c} = 0.43 - 0.886\left(\frac{35.0755}{313.15}\right) - 0.694\left(\frac{35.0755}{313.15}\right)^2 - 0.0375(5-1)\left(\frac{35.0755}{313.15}\right)^{4.5} \times 0.0001679$$

$$B_{12} = 0.000053\, m^3.mol^{-1}$$

Infinite dilution activity coefficient

The IDAC equation is broken down into three terms

$$\ln \gamma_{13}^{\infty} = \left(\frac{n_3 RT}{V_N P_i^*}\right) - \frac{(B_{11} - v_1^*)P_i^*}{RT} + \frac{(2B_{12} - v_i^{\infty})J_2^3 P_o}{RT} \quad \text{(B-10)}$$

Term 1:

$$ln\gamma_{13}^{\infty} = ln\left(\frac{n_3 RT}{V_N P_i^*}\right)$$

$$ln\gamma_{13}^{\infty} = ln\left(\frac{0.0088 \times 8.314 \times 313.15}{2.0053 \times 10^{-5} \times 36217.3352}\right)$$

$$\gamma_{13}^{\infty} = \left(\frac{22.91105608}{0.7262662228}\right)$$

$$\gamma_{13}^{\infty} = 31.642$$

Term 2:

$$\ln \gamma_{13}^{\infty} = -\frac{(B_{11} - v_1^*)P_i^*}{RT}$$

$$\ln \gamma_{13}^{\infty} = \frac{(-0.00165 - 0.0001434) \times 36217.3352}{8.314 \times 313.15}$$

$$\gamma_{13}^{\infty} = \frac{-64.95216}{2620.1571}$$

$$\gamma_{13}^{\infty} = 0.9755$$

Term 3:

$$\ln \gamma_{13}^{\infty} = \frac{(2B_{12} - v_i^{\infty})J_2^3 P_o}{RT}$$

$$\ln \gamma_{13}^{\infty} = \frac{(2 \times 0.000053 - 0.0001434) \times 1.0656 \times 36217.3352}{8.314 \times 313.15}$$

$$\gamma_{13}^{\infty} = 0.9994$$

$$\gamma_{13}^{\infty} = Term\ 1 + Term\ 2 + Term\ 3$$

$$\gamma_{13}^{\infty} = 31.642 + 0.9755 + 0.9994$$

$$\gamma_{13}^{\infty} = 33.62$$

Estimation of experimental uncertainty

In this study, the estimation of the combined uncertainty for the infinite dilution activity coefficient can be obtained by adding the square of the uncertainties due to the experimental repeatability measurements. The combined was calculated using the Equation (B-11).

$$u(\gamma_{13}^{\infty}) = \sqrt{\left[u_{rep}(\gamma_{13}^{\infty})\right]^2 + [u_{eve}(\gamma_{13}^{\infty})]^2} \qquad \text{(B-11)}$$

The highest number uncertainty value for the infinite dilution activity coefficient for this study, was found to be $\pm$ 25.78 % for n-hept-1-ene at the temperature 333.15 K, and the lowest uncertainty was found at $\pm$ 0.015 % for n-hexane at a temperature of 303.15 K.

APPENDIX C: PREDICTED ACTIVITY COEFFICIENTS

Table C-1: Predicted activity coefficients at infinite dilution for various organic solutes at T = (303.15, 313.15, 323.15 and 333.15) K using Aspen Plus for PC-Saft model.

	T/K			
Solute	303.15	313.15	323.15	333.15
n-hexane	1.658	1.616	1.579	1.514
n-heptane	1.601	1.558	1.519	1.470
n-octane	1.502	1.459	1.421	1.381
n-nonane	1.427	1.384	1.345	1.294
hex-1-ene	1.616	1.582	1.549	1.507
hept-1-ene	1.480	1.447	1.417	1.387
dec-1-ene	1.310	1.270	1.235	1.186
hex-1-yne	-	-	-	-
oct-1-yne	-	-	-	-
cyclopentane	1.138	1.131	1.125	1.116
cyclohexane	1.053	1.048	1.044	1.038
cycloheptane	-	-	-	-
cyclooctane	-	-	-	-
benzene	0.974	0.975	0.976	0.976
toluene	0.954	0.955	0.956	0.957
ethylbenzene	0.908	0.909	0.910	0.911
m-xylene	0.926	0.927	0.928	0.928
acetone	3.074	2.856	2.669	2.551
butan-2-one	2.539	2.386	2.254	2.143
pentan-2-one	2.302	2.177	2.068	2.013
methanol	55.68	50.43	45.40	40.39
ethanol	31.37	27.92	24.69	21.11
propan-1-ol	10.49	8.927	7.631	6.878
propan-2-ol	13.12	11.28	9.708	8.558
methyl acetate	4.990	4.510	4.111	4.012
ethyl acetate	5.286	4.767	4.337	4.183
pyridine	1.006	1.005	1.004	1.004
thiophene	0.959	0.960	0.961	0.961
acetonitrile	0.993	0.995	0.998	0.999
water	83.95	69.98	58.16	34.37

Table C-2: Predicted activity coefficients at infinite dilution for various organic solutes at T = (303.15, 313.15, 323.15 and 333.15) K using Aspen Plus for Lee Plock model.

	T/K			
Solute	303.15	313.15	323.15	333.15
n-hexane	24.48	21.23	19.78	17.37
n-heptane	18.19	15.93	14.97	13.26
n-octane	9.197	8.284	7.904	7.182
n-nonane	4.875	4.506	4.358	4.054
hex-1-ene	23.62	20.53	19.11	16.81
hept-1-ene	15.56	13.74	12.94	11.55
dec-1-ene	3.15	2.97	2.89	2.74
hex-1-yne	11.66	10.48	9.930	9.008
oct-1-yne	7.215	6.589	6.316	5.812
cyclopentane	17.36	15.23	14.17	12.58
cyclohexane	9.644	8.678	8.193	7.443
cycloheptane	5.746	5.287	4.888	4.538
cyclooctane	3.080	2.913	2.838	2.698
benzene	5.926	5.454	5.202	4.823
toluene	4.669	4.343	4.179	3.913
ethylbenzene	4.781	4.437	4.276	3.995
m-xylene	4.639	4.311	4.159	3.890
acetone	3.995	3.777	3.655	3.470
butan-2-one	6.259	5.778	5.539	5.147
pentan-2-one	5.795	5.356	5.145	4.787
methanol	0.460	0.483	0.497	0.518
ethanol	0.304	0.327	0.343	0.366
propan-1-ol	0.576	0.600	0.616	0.638
propan-2-ol	0.238	0.270	0.276	0.299
methyl acetate	4.502	4.237	4.098	3.875
ethyl acetate	7.145	6.577	6.307	5.844
pyridine	2.192	2.110	2.064	1.994
thiophene	3.999	3.743	3.600	3.389
acetonitrile	1.505	1.485	1.468	1.449
water	0.001	0.002	0.002	0.002

Table C-3: Predicted activity coefficients at infinite dilution for various organic solutes at T = (303.15, 313.15, 323.15 and 333.15) K using Aspen Plus for Peng Robinson model.

	T/K			
Solute	303.15	313.15	323.15	333.15
n-hexane	8.548	7.654	6.911	6.532
n-heptane	12.31	10.73	9.449	8.843
n-octane	19.76	16.68	14.26	13.23
n-nonane	31.98	26.13	21.66	19.95
hex-1-ene	6.338	5.772	5.295	5.043
hept-1-ene	8.485	7.562	6.798	6.420
dec-1-ene	34.84	28.21	23.19	21.40
hex-1-yne	3.260	3.084	2.931	2.848
oct-1-yne	6.726	6.055	5.493	5.226
cyclopentane	2.046	1.975	1.906	1.875
cyclohexane	2.491	2.363	2.250	2.180
cycloheptane	2.677	2.511	2.366	2.241
cyclooctane	3.138	2.895	2.688	2.563
benzene	1.477	1.445	1.416	1.397
toluene	2.103	2.007	1.923	1.870
ethylbenzene	2.752	2.578	2.427	2.337
m-xylene	2.788	2.612	2.460	2.372
acetone	1.548	1.525	1.505	1.495
butan-2-one	1.917	1.860	1.809	1.781
pentan-2-one	2.168	2.082	2.006	1.962
methanol	1.075	1.060	1.050	1.041
ethanol	1.006	1.007	1.009	1.012
propan-1-ol	1.053	1.057	1.061	1.065
propan-2-ol	1.246	1.248	1.251	1.257
methyl acetate	1.591	1.567	1.545	1.535
ethyl acetate	2.362	2.276	2.199	2.158
pyridine	1.096	1.089	1.082	1.077
thiophene	1.171	1.160	1.150	1.143
acetonitrile	1.347	1.332	1.318	1.311
water	7.974	6.976	6.156	5.476

Table C-4: Predicted activity coefficients at infinite dilution for various organic solutes at T = (303.15, 313.15, 323.15 and 333.15) K using Amsterdam Modelling Suite for COSMO-SAC model.

	T/K			
Solute	303.15	313.15	323.15	333.15
n-hexane	9.701	9.284	8.880	8.492
n-heptane	12.63	12.01	11.42	10.85
n-octane	16.90	15.97	15.08	14.24
n-nonane	21.50	20.19	18.95	17.78
hex-1-ene	4.354	4.260	4.164	4.068
hept-1-ene	5.752	5.596	5.439	5.282
dec-1-ene	12.43	11.88	11.34	10.82
hex-1-yne	1.484	1.500	1.514	1.525
oct-1-yne	2.306	2.315	2.319	2.318
cyclopentane	5.895	5.692	5.494	5.302
cyclohexane	8.191	7.842	7.506	7.185
cycloheptane	10.38	9.889	9.415	8.964
cyclooctane	12.09	11.49	10.92	10.37
benzene	1.592	1.606	1.618	1.626
toluene	1.968	1.977	1.981	1.983
ethylbenzene	2.554	2.551	2.542	2.530
m-xylene	2.522	2.519	2.512	2.501
acetone	1.004	1.003	1.001	1.000
butan-2-one	1.213	1.209	1.205	1.200
pentan-2-one	1.468	1.459	1.450	1.440
methanol	3.083	2.941	2.812	2.695
ethanol	3.883	3.678	3.494	3.328
propan-1-ol	4.072	3.861	3.670	3.497
propan-2-ol	3.980	3.776	3.591	3.424
methyl acetate	1.049	1.049	1.048	1.047
ethyl acetate	1.260	1.256	1.252	1.247
pyridine	1.369	1.367	1.365	1.362
thiophene	0.927	0.956	0.983	1.008
acetonitrile	0.968	0.966	0.965	0.963
water	15.04	14.00	13.07	12.24

APPENDIX D: JOURNAL ABSTRACT

Infinite Dilution Activity Coefficients Measurements for Cyrene as a Potential Natural Green Solvent for Chemical Separation Applications

Malusi Danisa[a], Banzi P. Mbatha[a,], Peterson T. Ngema[a,*], Suresh Ramsuroop[b], Lindokuhle Manyoni[a] and Nkululeko Nkosi[c,*]

[a] Department of Chemical Engineering, Green Engineering Group: Chemical Engineering Thermodynamics, Durban University of Technology, Steve Biko Campus, Durban, 4001, South Africa

[b] Cape Peninsula University of Technology, Department of Chemical Engineering, Bellville Campus, Bellville 7535, South Africa

[c] Department of Chemical Engineering, Thermodynamics, Materials and Separations Research Group (TMSRG), Mangosuthu University of Technology, uMlazi, Durban, 4031, South Africa

***Corresponding authors:** nkullenkosi@gmail.com (N. Nkosi) and ngemat@dut.ac.za (P.T. Ngema)

Abstract

In this present study, a bio-derived solvent, namely, cyrene, was investigated as an alternative to conventional solvents that are currently used for separation processes. It is a sustainable solvent that is produced from the pyrolysis of cellulose waste. The bio-derived alternative was discovered in response to the need for solvents to meet stricter regulation requirements for both industry and environmental sustainability. The activity coefficients at infinite dilution γ_{13}^{∞} of 32 organic solutes, which include alkane, alkene, alcohol, cycloalkane, ketone, aromatic, heterocyclic, nitrile, ester and water. Cyrene was used for extraction of binary mixtures using a gas-liquid chromatography (GLC) at temperature of (303.15 to 333.15) K. The selectivity (S_{ij}^{∞}) and limiting capacity (k_j^{∞}) at infinite dilution were calculated for the evaluation of cyrene's separation potential. This was also taken further by calculating the partial excess molar enthalpies ($\Delta H_1^{E,\infty}$, $T_{ref}\,\Delta S_i^{E,\infty}$, $\Delta G_i^{E,\infty}$) at infinite dilution which rely solely on the solute-solvent interaction. Also, it became difficult to build thermodynamic models in conjunction with the experimental data, since cyrene is still a new bio-derived solvent with not enough available data on activity coefficients at infinite dilution.

Keywords: Cyrene; Green Solvent; Separation factors, COSMO-RS, SRK-EOS, Excess Thermodynamic properties; Intermolecular interactions.